# Selenocysteine tRNA methylation promotes oxidative stress resistance in melanoma metastasis

Leona A. Nease[1,5], Kellsey P. Church[1], Ines Delclaux[1], Shino Murakami[5], Maider A. Amiama[6], Marwa Zerhouni[1], Graciela Cascio[1], Riley O. Hughes[1,5], Kelsey N. Aguirre[1], Paul Zumbo[6], Lukas E. Dow[1,3,4], Samie Jaffrey[5], Doron Betel[6], and Elena Piskounova[1,2,3*]

[1]Sandra and Edward Meyer Cancer Center, Weill Cornell Medicine, New York, NY; [2]Department of Dermatology, Weill Cornell Medicine, New York, NY, [3]Department of Biochemistry, Weill Cornell Medicine, New York NY, [4]Department of Medicine, Weill Cornell Medicine, New York NY, [5]Department of Pharmacology, Weill Cornell Medicine, New York, NY, [6]Institute of Computational Biomedicine, Weill Cornell Medicine, New York, NY #Equal contribution, *Corresponding author: Elena Piskounova, PhD, elp2025@med.cornell.edu

## Abstract

**Selenocysteine-containing proteins play a central role in redox homeostasis. Their translation is a highly regulated process dependent on two tRNA$^{Sec}$ isodecoders differing by a single 2'-O-ribose methylation, called Um34. We characterized FTSJ1 as the Um34 methyltransferase and show that its activity is required for efficient selenocysteine insertion at the UGA stop codon during translation. Specifically, Loss of Um34 leads to ribosomal stalling and decreased UGA recoding. FTSJ1-deficient cells are more sensitive to oxidative stress and have decreased metastatic colonization in xenograft models of melanoma metastasis. Our findings uncover a role for tRNA$^{Sec}$ Um34 modification in oxidative stress resistance and highlight FTSJ1 as a potential therapeutic target specific for metastatic disease.**

## Introduction

Dynamic changes in protein translation enable cells to rapidly adapt to environmental cues and survive under various stress conditions. tRNA modifications have recently been recognized as a novel regulatory mechanism with diverse consequences on translation[1,2]. Specifically, modifications on the tRNA anticodon loop have been shown to affect translational efficiency and fidelity[3,4]. Selenocysteine-containing proteins play a central role in oxidative stress and ER homeostasis and are particularly unique as their translation is regulated by two distinct isodecoders of the Sec tRNA that differ by a single methyl group at the wobble position ($U_{34}$) of the anticodon loop[5].

Selenocysteine (Sec), the 21st amino acid, is coded for by the UGA stop codon. Synthesis of selenoproteins is energetically costly to the cell and therefore must be tightly regulated to maintain ER and redox homeostasis while preventing depletion of selenium. Biosynthesis of Sec occurs on its tRNA rather than as a small molecule, and co-translational incorporation of selenocysteine in the polypeptide chain depends on several unique features. A conserved hairpin structure in the 3' UTR called the Selenocysteine Incorporation Sequence (SECIS) is recognized by a complex of proteins including a Sec-specific elongation factor, EEFSEC, SECIS binding protein 2 (SECISBP2) and SECp43. This complex positions the Sec tRNA for loading onto the ribosome and allows for UGA readthrough rather than a stop in translation[6-9] (Figure 1A).

Sec tRNA is unusual as it is longer than all other tRNAs with 90 nucleotides and it is hypomodified at only 4 positions. Two of the modifications on Sec tRNA (pseudoU55 and $m^1$A58) are involved in proper folding, while $i^6$A37 and $mcm^5$U(m)34 on the anticodon loop are essential for regulating selenoprotein translation.[10] Sec tRNA exists in two major forms, one that contains $mcm^5$U, catalyzed by ALKBH8[11,12] while the other contains a further 2'O-ribose methylation, generating $mcm^5$Um (Um34) – a modification unique to the Sec tRNA. Um34 is the final step in Sec tRNA maturation and affects the tertiary structure of the tRNA. Additionally, Um34 is highly responsive to selenium availability, and has been proposed to increase efficiency of Sec insertion[13,14]. Previous work has suggested that these two isodecoders act as a mechanism to regulate the translation of a hierarchy of Sec-containing proteins[15]. This ensures that only essential selenoproteins are synthesized when selenium is limiting, or conversely, non-essential or stress-related selenoproteins are translated when Um34 is increased.

There are 25 known selenoproteins, and 11 of which have been directly implicated in the cellular antioxidant response. Glutathione peroxidases (GPX1-4, GPX6) detoxify ROS by utilizing glutathione (GSH) as a reducing agent, and GPX4 has specifically been identified to inhibit ferroptosis[16-18]. Thioredoxin reductases (TXNRD1-3) are key to maintaining a reductive environment through reduction of oxidized cysteine residues[19,20]. MSRB1 mediates reduction of oxidized methionine[21] while SELENOH is a nuclear oxidoreductase able to regulate p53 in response to oxidative stress[22]. SELENOO is an AMPylase localized to the mitochondria and is necessary for cellular response to oxidative stress[23]. Other selenoproteins have been implicated in ER homeostasis (SELENOF, K, M, N, S and T) and use their oxidative functions in aiding protein folding[24]. Enzymes DIO1-3 are essential for thyroid hormone metabolism[25] and SELENOP is a selenium chaperone required for distribution of selenium throughout the body[26]. Due to the low pKa of Sec, these enzymes are highly reactive and resistant to permanent oxidative damage[27,28].

As selenoproteins are a necessary component of the cell's antioxidant response, it has been suggested that Um34 regulates translation of stress-related proteins while housekeeping selenoproteins do not require Um34[15]. Previous work has focused on understanding the mechanistic role of Um34 in selenoprotein translation, using a mutant $tRNA^{Sec}$ i6A37G, lacking the i6A modification which is the prerequisite for Um34 formation[29,30]. However, this approach does not allow uncoupling of the Um34 role from that of i6A and no functional studies on the specific function of Um34 have been done. Recent work has proposed FTSJ1 to be the Um34 methyltransferase[31]. Intriguingly, there were no clear selenoprotein translational effects in the FTSJ1 KO adult mouse brain[32], leaving the role of Um34 in selenoprotein translation unresolved.

We have addressed the question of Um34 function in the context of oxidative stress, given the central role for selenoproteins in oxidative stress resistance. We have found that levels of Um34 increase with oxidative stress even in the absence of selenium. This correlates with a translational increase in selenoproteins and an increased readthrough of UGA as a selenocysteine under oxidative stress. We characterized the proposed Um34 methyltransferase, FTSJ1 as a component of the selenocysteine translation machinery that assembles on the SECIS. Loss of FTSJ1 leads to decreased readthrough of UGA as a selenocysteine and affects translation of primarily antioxidant selenoproteins, pointing to the hierarchy of Sec translation. We found that loss of FTSJ1 sensitizes melanoma cells to oxidative stress, while overexpression of FTSJ1 has a protective effect but only in the presence of selenium, emphasizing that this oxidative stress resistance is mediated by selenoproteins. A defining feature of metastasizing cancer cells are high levels of oxidative stress and increased dependence on antioxidant pathways[33]. Our data show that loss of FTSJ1 in melanoma cells has no impact on primary tumor growth however it decreases metastatic colonization in distant organs. Overexpression of FTSJ1 similarly has no effect on primary tumor growth but promotes metastatic colonization presumably by increasing oxidative stress resistance. Our work discovered oxidative stress as a specific context for Um34-mediated selenoprotein translation consistent with previous models in which Um34 drives stress-related selenoproteins. Most importantly, our work identifies metastasis as a pathophysiological context in which Um34 plays an important role and highlights FTSJ1 as the Um34 methyltransferase and a potential therapeutic target specific to metastatic disease.

## RESULTS

*Selenoprotein translation and Sec tRNA methylation increase under oxidative stress*

To measure levels of Um34, Sec tRNA was isolated using a biotinylated oligo probe coupled with LC-MS/MS analysis of Um34 levels (Figure 1B and Extended Figure 1A). To establish the effect of extracellular selenium on Sec tRNA methylation in melanoma cells, A375 cells were depleted of selenium in serum-free DMEM/F12 media. Increasing

amounts of extracellular selenium increased levels of the Um34 Sec tRNA modification and decreased levels of $mcm^5U$ modification, showing that selenium concentration regulates Um34 biosynthesis and shifts the ratio between the two Sec tRNA isodecoders in melanoma cells (Figure 1C). Selenoproteins GPX1, GPX4 and SELENOW increased under selenium supplementation, while housekeeping selenoproteins TXNRD1 and SEPHS2 did not increase consistently in A375, SK-MEL2 and HeLa cell lines (Extended Figure 1B and 1C). The cooresponding mRNA levels did not increase with selenium supplementation suggesting this effect is mediated through translation (Figure 1G).

$H_2O_2$ treatment has been shown to increase Um34 modification in MEFs[34] as well as translation of a subset of antioxidant selenoproteins in HEK293T cells[35]. We asked whether oxidative stress has a similar effect in cancer cells, which have elevated ROS levels and antioxidant capacity compared to nontransformed cells. We treated A375 melanoma cells with $H_2O_2$ or a global prooxidant, pyocyanin, which increases intracellular levels of $H_2O_2$ and superoxide[36], a species of ROS produced by mitochondria complex I and III and released by tumor-infiltrating macrophages and neutrophils[37]. Both $H_2O_2$ and pyocyanin treatment increased Um34 levels. In fact, pyocyanin without selenium supplementation increased Um34 to similar levels as selenium supplementation alone (Figure 1D), indicating that oxidative stress drives Um34 biosynthesis independent of selenium status. Consistent with the role of Um34 in selenoprotein translation, oxidative stress increased translation of endogenous selenoproteins involved in the redox regulation (GPX1, GPX4, MSRB1, TXNRD1) in melanoma cell lines (Figure 1E and F) without significant effect on mRNA levels (Figure 1G). Several selenoproteins (SELENOK, SELENOF and SELENOP) were upregulated at the mRNA level suggesting there may be additional transcriptional regulation in response to oxidative stress. Components of the selenocysteine machinery such as SECISBP2 and SEPSECS were not affected by either selenium or oxidative stress, consistent with our observation that increased Um34 modification likely drives the upregulation of some selenoproteins after selenium supplementation or oxidative stress.

To test the effect of oxidative stress on recoding of the UGA stop codon as a selenocysteine, we established a GFP-Reporter Of Selenocysteine Insertion (gROSI), in which a cysteine at position 71 in the GFP was replaced with the UGA stop codon coupled with the GPX4 Selenocysteine Insertion Sequence (SECIS) required for UGA readthrough as a selenocysteine[38] (Figure 1H). In these reporters, expression of GFP is dependent on successful insertion of selenocysteine by readthrough of the UGA stop codon. This reporter was responsive to extracellular selenium (Figure 1I). More importantly, gROSI with either GPX1 or GPX4 3' UTR SECIS was responsive to oxidative stress induction in the absence of selenium (Figure 1J). The combination of selenium and oxidative stress had an additive effect on UGA readthrough as a selenocysteine.

*FTSJ1 is the Um34 selenocysteine-tRNA modifying methyltransferase.*

The Um34 methyltransferase has been a long-standing unknown in the field of selenocysteine biology, and previous work that has attempted to address the role of Um34 has relied on a mutant form of Sec tRNA, i6A37G, that is missing the i6A modification required for Um34 methylation[29]. To specifically address the role of Um34 in selenoprotein translation independent of i6A modification and to identify the Um34 methyltransferase we performed a proteomic analysis of proteins interacting with selenocysteine-specific elongation factor EEFSEC in A375 melanoma cells. Out of 15 RNA-modifying enzymes interacting with EEFSEC, we identified FTSJ1 as the only tRNA methyltransferase that has previously been shown to methylate the 2'O-ribose at the wobble position of tRNAs (Figure 2A and Extended Figure 2A)[31,39]. To confirm the interaction of FTSJ1 with selenocysteine translation machinery we performed co-immunoprecipitation of FLAG-tagged FTSJ1 with HA-tagged EEFSEC and SECp43 from A375 melanoma cells and demonstrated that FTSJ1 specifically interacts with both EEFSEC and SECp43 (Figure 2B, Extended Figure 2B).

To test whether FTSJ1 is able to bind $tRNA^{Sec}$, we performed RNA-immunoprecipitation from A375 melanoma cells, using either wild type or a catalytically dead A26P mutant of FTSJ1 (found in some patients with X-linked intellectual disability) as well as known $tRNA^{Sec}$-interacting proteins, ALKBH8 and EEFSEC as positive controls (Figure 2C). We saw significant enrichment in the binding of wild type FTSJ1 to $tRNA^{Sec}$, which was not observed in the catalytically dead mutant A26P (Figure 2D). WDR6, the RNA-adapting partner of FTJS1 also showed enrichment for $tRNA^{Sec}$ binding (Figure 2E). FTSJ1 did bind its known substrate $tRNA^{Phe(GAA)}$ but did not show enrichment in binding to other tRNAs such as $tRNA^{Lys(UUU)}$ and $tRNA^{Glu(CUC)}$ (Extended Figure 2C and D).

To functionally validate FTSJ1 as the Um34 methyltransferase, we generated FTSJ1-knockout (FTSJ1-KO) cell lines in A375, SK-MEL28 and SK-MEL2 melanoma cell lines. Knockout of FTSJ1 lead to a reduction of downstream selenocysteine protein GPX1, indicating that FTSJ1 activity directly affects selenocysteine protein levels (Figure 2F). Nucleoside digestion and LC/MS-MS analysis of $tRNA^{Sec}$ from control and FTSJ1-KO cell lines showed near-complete loss of Um34 on $tRNA^{Sec}$ in the knockout cells (Figure 2G and Extended Figure 2E and F). Conversely, overexpression of wild type FTJS1 lead to an increase in the levels of another known selenocysteine protein, GPX4, while catalytically inactive mutant A26P had no effect (Figure 2H). Overexpression of wildtype FTSJ1 also lead to an increase of Um34 on $tRNA^{Sec}$, while mutant A26P FTSJ1 had a dominant negative effect, causing a decrease in Um34 levels (Figure 2I and Extended Figure 2G). Overexpression of wildtype FTSJ1 in the knockout cell lines rescued the loss of Um34 levels while overexpression of mutant A26P had no effect (Extended Figure 2H and I). Finally, extracellular selenium had no effect on Um34 levels in the absence of FTSJ1 demonstrating that FTSJ1 Um34 methyltransferase activity is the limiting step of Um34 Sec tRNA isoform generation (Figure 2J). In fact, there was a marked increase in $mcm^5U$

levels, suggesting a compensatory mechanism by ALKBH8 which generates the $mcm^5U$ Sec tRNA modification. To definitively show that FTSJ1 is the $tRNA^{Sec}$ Um34 methyltransferase, we performed an *in vitro* methyltransferase assay with FTSJ1 and WDR6 on $tRNA^{Sec}$ from FTSJ1-KO cells. Um34 levels were only detectable in the presence of both FTSJ1 and WDR6 (Figure 2K and Extended Figure 2I and J). These data directly establish FTSJ1 as the $tRNA^{Sec}$ Um34 methyltransferase, demonstrating that FTSJ1 activity is necessary and sufficient for $tRNA^{Sec}$ Um34 modification and that changes in Um34 modification levels affect selenoprotein levels in melanoma cells.

*Loss of Um34 affects translation of a subset of selenoproteins*

To systematically assess changes in protein translation in FTSJ1-KO cells, we used ribosomal profiling to quantify ribosome-protected fragments (RPFs) across the transcriptome. The density of RPFs positioned at a specific codons indicates the average ribosomal dwelling time and reflects the relative ribosome translation speed across each codon[40]. Given that FTSJ1 is known to modify other tRNAs (Phe $tRNA^{GAA}$ and Trp $tRNA^{CCA}$) in addition to Sec tRNA, we first investigated whether loss of FTSJ1 affects translation of individual codons. We compared ribosomal P-site occupancy in FTSJ1-KO and Control A375 melanoma cells in the presence of selenium (30nM) and saw that there was no significant difference in codon usage across the global transcriptome especially for codons coding for Phe(GAA) and Trp(CCA), known to be modified by FTSJ1 (Extended Figure 3A). This confirms that while FTSJ1 may lead to loss of modifications on other tRNAs, this does not lead to global defects in translational readthrough in melanoma cells.

If $tRNA^{Sec}$ levels are low and/or the ability to decode UGA is impaired (for instance in FTSJ1-KO cells), then ribosomes will accumulate upstream of the UGA or translation will terminate and ribosomes will be depleted downstream of the UGA. UGA recoding efficiency is defined by the ratio of RPF 3' to 5' of the Sec UGA. First, we compared UGA recoding efficiency in WT A375 melanoma cells in the presence vs absence of selenium (30nM NaSe) (Figure 3A). We saw a significant decrease in UGA recoding efficiency in cells in the absence of selenium as expected. Next, we compared UGA recoding efficiency in WT and FTSJ1 KO A375 melanoma cells in the presence of selenium (30nM NaSe) (Figure 3B). We saw the same decrease in UGA recoding efficiency in FTJS1 KO cells. As a control we compared FTSJ1 KO cells in the presence and absence of selenium (Figure 3C), and observed no difference between these two conditions, indicating that FTSJ1-mediated Um34 modification regulates UGA recoding efficiency independent of selenium availability. To quantify the differences in UGA recoding efficiency, we plotted changes in the z-score of UGA recoding efficiency comparing WT A375 in the presence and absence of selenium with FTJS1 KO cells (Figure 3H). We observed a similar decrease in UGA recoding efficiency in WT A375 melanoma cells without selenium and FTSJ1 KO cells. This highlights the role of Um34 modification in UGA readthrough.

To more precisely determine how ribosome occupancy differed between Control and FTSJ1 KO cells with and without selenium supplementation, we plotted the Cumulative Fraction of RPFs across each transcript to determine ribosomal accumulation across the transcript. First, we compared WT A375 melanoma cells in the presence and absence of selenium (30nM NaSe). We found that a subset of selenoproteins was affected by absence of selenium and showed a significant increase in accumulation of ribosomes 5' of the UGA Sec-coding codon (Extended Figure 4A). Next we compared WT and FTSJ1 KO A375 melanoma cells and showed that FTSJ1 KO cells showed a similar accumulation of ribosomes 5' of the UGA Sec-coding codon in this subset of proteins (Extended Figure 4B). Interestingly, SELENOK was not affected by the absence of selenium in WT A375 melanoma cells but showed significant ribosomal accumulation in FTSJ1 KO cells. The opposite was true for SELENON, which showed some accumulation of ribosomes in WT A375 melanoma cells in the absence of selenium but was not affected by FTSJ1 KO. We also found that not all selenoproteins were affected by either absence of selenium or FTSJ1 loss (Extended Figure 5A and B). Taken together, these data show that loss of Um34 leads to a decrease in UGA-recoding as a selenocysteine and an increase in ribosome accumulation and stalling 5' to the Sec UGA likely due to inefficient readthrough of UGA as selenocysteine in a subset of selenocysteine-containing proteins.

*FTSJ1 regulates selenocysteine insertion independent of selenium*

To determine the effect of impaired UGA-readthrough on endogenous selenoproteins, we assessed selenoprotein levels in two different FTSJ1-KO melanoma cell lines, A375 and SK-MEL2. Strikingly most selenoproteins were decreased in both A375 and SK-MEL2 FTSJ1-KO melanoma cell lines (Figure 3E), especially those involved in the antioxidant response (GPX1, GPX4, MSRB1 and SELENOH). SELENOS was only decreased in A375 melanoma cells and SELENOM was only decreased in SK-MEL2 cells suggesting there may be a difference in how selenoprotein translation is regulated depending on the genetic background of the cells. Other proteins such as SELENOK, SELENON, SELENOO, TNXRD1 and SEPHS2 were not significantly affected by FTSJ1 loss in either cell line, although SELENOK and SELENON did show a smaller isoform in SK-MEL2 cells which could indicate a truncated protein where the Sec-coding UGA is read as a stop codon. Importantly, these changes were not observed at the mRNA level (Extended Figure 3B) emphasizing that loss of Um34 leads to a translational defect of a specific subset of selenoproteins, involved in the antioxidant response. Strikingly, upon loss of FTSJ1 we also saw a decrease in SECISBP2, a SECIS-binding protein essential for selenocysteine translation. This suggests that FTSJ1 may be involved in stabilizing the SECIS-binding protein complex to promote selenoprotein translation, however this finding warrants further study.

To address whether FTSJ1 is sufficient to drive translation of endogenous selenoproteins when selenium is limiting, we established a system to decrease selenium levels in cells without complete depletion. Due to the variable presence of selenium in serum albumin (150-300nM)[41], A375 and SK-MEL2 melanoma cells were cultured in either normal (10%) or reduced (2%) FBS levels, with or without selenium supplementation (30nM NaSe). In normal growth conditions (10% FBS, no NaSe), cells had basal levels of known selenoproteins GPX1, GPX4 and TXNRD1 (Extended Figure 3C). Growth in 2% FBS, and therefore reduced selenium levels, led to a significant decrease in selenoproteins. Supplementation with selenium increased selenoprotein levels in both conditions. This effect on selenoproteins was also seen in HEK-293T cells (Extended Figure 3C). Unlike their proteins, TXNRD1 and GPX4 mRNAs did not change when levels of selenium were varied, suggesting that levels of selenium affect translation but not transcription of selenoproteins in melanoma cells (Extended Fig 3D). GPX1 mRNA, which is known to be regulated through nonsense mediated decay[29] showed a modest reduction with reduced FBS but did not increase with selenium supplementation. Compared to control cells, FTSJ1-overexpressing cells showed significantly higher expression of antioxidant response selenoproteins GPX1 and GPX4 both in high and low levels of selenium, whereas housekeeping selenoproteins TXNRD1 and SEPHS2 were not affected by FTSJ1 overexpression (Figure 3F). Other components of the selenocysteine machinery such as SEPSECS were also unaffected.

To confirm the role of Um34 in selenoprotein translation we measured UGA readthrough in FTSJ1-knockout cells using the gROSI reporter (Figure 1H). Analysis of GFP fluorescence revealed that translation of the seleno-GFP was increased in the presence of selenium, but this increase was abolished in FTSJ1-knockout cells (Figure 3G). Conversely, overexpression of FTSJ1 caused a significant increase in translation of gROSI independent of selenium levels, indicating that Um34 modification is sufficient for efficient readthrough of UGA as a selenocysteine (Figure 3H).

To specifically assess the role of FTSJ1 and Um34 in selenocysteine-insertion into selenoproteins, we adapted a previously published method for selenocysteine-specific labeling and enrichment[42,43]. Selenocysteine-containing proteins are specifically labelled with a biotinylated probe at low pH, while cysteines are blocked from non-specific labelling at high pH, followed by avidin-immunoprecipitation of the selenocysteine-containing proteins (Sec-IP). As proof of concept we used this method to specifically isolate and enrich for known selenocysteine proteins such as GPX4, SELENOS, SEPHS2 and TXNRD1, in the presence of biotin and selenium, with the non-selenocysteine containing protien SECISBP2 as a negative control. (Extended Figure 3E). Next, we performed Sec-IP on Control and FTSJ1-KO A375 melanoma cells and found that some selenoproteins, such as GPX1, GPX4, SELENOK, SELENOS were pulled down less in the absence of FSTJ1 (Extended Figure 3F). This data supports the model in which FTSJ1-

mediated Um34 modification promotes efficient readthrough of UGA as a selenocysteine especially in a subset of selenoproteins involved in the antioxidant response.

To confirm that the increase in selenoprotein levels upon FTSJ1 overexpression is specifically due to increased in UGA readthrough as a selenocysteine, we performed Sec-IP of control and FTSJ1-overexpressing A375 melanoma cells in the absence and presence of selenium. Even without selenium, FTSJ1-overexpressing cells exhibit as much insertion of Sec into known antioxidant selenoproteins such as GPX4 and SELENOS as control cells with selenium supplementation (Extended Figure 3G). TXNRD1, which is considered a housekeeping selenoprotein not regulated by Um34 modification, did not respond to FTSJ1 overexpression, suggesting that FTSJ1 activity and Um34 modification drives selenocysteine insertion into a specific subset of selenoproteins. These data demonstrate that FTSJ1 is both necessary and sufficient for recoding of the stop codon UGA as selenocysteine in a subset of selenoproteins. These data also highlight the Um34-regulated translational hierarchy that exists among different selenocysteine proteins and suggests that selenoproteins specifically involved in the antioxidant response are translationally regulated by the Um34 modification.

*Um34-mediated translation of selenoproteins protects cancer cells from oxidative stress.*

Because Um34 is increased in response to oxidative stress and that Um34 is required for translation of several selenoproteins involved in the antioxidant response, we hypothesized that Um34 and FTSJ1 will be required for the oxidative stress response. Surprisingly, we did not detect a significant increase in oxidative stress levels under normal growth conditions in FTSJ1-deficient melanoma cell lines, and only SK-MEL2 showed an increase in lipid peroxidation (Extended Figure 6A-C). However, when we treated FTSJ1-KO A375 and SK-MEL2 melanoma cells with pro-oxidant Pyocyanin and measured cell survival, FTSJ1-deficient cells were more sensitive to Pyocyanin both with and without selenium supplementation. However, sensitivity to Pyocyanin greatly increased in both control and FTSJ1-KO cells in the absence of selenium, suggesting a crucial role for selenoproteins in the antioxidant response (Figure 4A-D). FTSJ1-deficient cells were also sensitive to ferroptosis, a form of cell death caused by lipid peroxidation, when treated with RSL3 (Extended Figure 6D and E). To test whether increased Um34 levels can protect against oxidative stress, we treated A375 and SK-MEL2 melanoma cells overexpressing either control Renilla luciferase or FTSJ1 with increasing concentrations of prooxidant Pyocyanin in the presence or absence of selenium. Overexpression of FTSJ1 protected cells from oxidative stress in the presence of selenium (Figure 4E and F). In the absence of selenium, overexpression of FTSJ1 had no effect, supporting that FTSJ1-driven antioxidant response is dependent on selenium and therefore occurs through Um34-mediated translation of antioxidant selenoproteins (Figure 4G and H). To demonstrate that the sensitivity to oxidative stress was FTSJ1-dependent, we performed rescue experiments and

observed that overexpressing FTSJ1 can partially rescue sensitivity to oxidative stress both in the presence and absence of selenium (Figure 4I and J, Extended Figure 7A and B). FTSJ1 can similarly partially rescue sensitivity of FTSJ1-KO cells to ferroptosis induced by RSL3 treatment (Extended Figure 6F and G). Partial rescue is likely due to the fact that FTSJ1 requires its binding partner WDR6 for its enzymatic activity as well as a sufficient level of charged $tRNA^{Sec}$, both of which are likely limiting for the reaction. In support of this, overexpression of wild type $tRNA^{Sec}$ increased cell survival under oxidative stress in the absence of selenium (Figure 4K and L and Extended Figure 6H and I), supporting the fact that $tRNA^{Sec}$ may be limiting especially in the absence of selenium. In addition to testing the effect of wild type Sec tRNA on oxidative stress resistance, we also overexpressed a mutant Sec tRNA containing the C65G mutation. This is a known patient mutation which was originally shown to specifically affect translation of stress-related selenoproteins due to loss of Um34[44], however has subsequently been shown to have a more widespread effect on modifications within the anticodon loop[45]. Our data show that the C65G mutant Sec tRNA is unable to rescue oxidative stress sensitivity. Consistent with this data, we found that overexpression of wild type Sec tRNA leads to an increase in Um34 levels on $tRNA^{Sec}$ while overexpression of C65G mutant Sec tRNA had no significant effect on Um34 levels (Extended Figure 6J). Finally, to demonstrate that oxidative stress sensitivity was not dependent on other tRNAs that are modified by FTSJ1, we overexpressed either $Phe^{GAA}$ or $Trp^{CCA}$, known substrates of FTSJ1. Neither had any effect on oxidative stress resistance with or without selenium (Extended Figure 6K-N, Extended Figure 7C-F). These data demonstrate that FTSJ1 is both necessary and sufficient for oxidative stress resistance including ferroptosis and that this resistance is specific to $tRNA^{Sec}$ rather than other tRNAs modified by FTSJ1.

*Micrometastases experience high levels of oxidative stress and increase selenocysteine biosynthesis.*

Given the central role of oxidative stress in metastatic colonization, we explored the role of selenoprotein translation in oxidative stress resistance in metastasis. We used a patient-derived xenograft (PDX) model of melanoma metastasis, in which patient melanomas transplanted into NSG mice recapitulate metastatic behavior of the tumor observed in patients[46]. Using two patient tumors with different driver mutations, M481 (BRAF V600E) and M405 (NRAS Q61R), we measured levels of both cytoplasmic and mitochondrial oxidative stress levels in micrometastatic (<0.2mm), macrometastatic (>0.2mm) and primary subcutaneous tumors. Micrometastases had significantly higher levels of oxidative stress in both of the subcellular compartments compared to macrometastases or primary tumors (Figure 5A). Increase in oxidative stress in micro and macrometastatic lesions was mirrored by a significant increase in the mRNAs for major components of selenocysteine biosynthesis machinery such as PSTK, SEPSECS, ALKBH8, SECISBP2 and SECp43 (Figure 5B). In contrast, we did not see significant transcriptional differences in selenoprotein mRNA levels between micrometastases, macrometastases and primary subcutaneous tumors (Extended Figure 8A).

However, we did observe significant upregulation of certain selenoproteins in metastatic nodules compared to the primary tumors (Figure 5C and D), consistent with our model that selenoprotein translation increases as a protective mechanism against oxidative stress. We performed Ribosomal profiling comparing primary tumors and metastatic nodules from our patient derived xenograft model of melanoma metastasis and quantified the UGA recoding efficiency of detected selenoproteins (Extended Figure 8B). A subset of selenoproteins including GPX4, SELENOF, SELENOH, SELENOI, SELENOS, SELENOT and SELENOW had higher UGA recoding efficiency in metastases, while other selenoproteins such as GPX1, MSRB1, SELENON and SEPHS2 had higher UGA recoding efficiency in the primary tumor. Overall our data suggest a translational mechanism for the upregulation of selenoproteins during metastasis. Levels of precursor $tRNA^{Sec}$ were not changing, however levels of mature $tRNA^{Sec}$ were slightly elevated in metastases compared to the primary tumor, similarly suggesting a translational mechanism of selenoprotein upregulation (Extended Figure 8C and D). Levels of FTSJ1 were also elevated in metastases, increasing more in micrometastases compared to macrometastases (Figure 5C and 5E-F). Consistent with FTSJ1 increase, levels of Um34 modification on $tRNA^{Sec}$ were also elevated in metastatic nodules compared to the primary tumor (Figure 5G).

To confirm translational upregulation of selenoproteins in metastasizing melanoma cells, we transplanted A375 melanoma cells expressing the gROSI reporter with no UTR, GPX1 SECIS or GPX4 SECIS. We showed by quantifying GFP signal in metastatic nodules compared to primary tumors that metastases had significantly more seleno-GFP with either GPX1 SECIS and GPX4 SECIS, demonstrating an increase in UGA readthrough as a selenocysteine in metastasizing melanoma cells (Extended Figure 8 E and F). Overall, these data indicate that metastatic lesions experience higher levels of oxidative stress and have increase selenocysteine biosynthesis, UGA readthrough, and translation of some selenocysteine proteins.

*Um34 is a driver of metastasis in vivo.*

To determine if FTSJ1 and therefore $tRNA^{Sec}$ Um34 modification are necessary for metastasis, we transplanted FTJS1 KO A375 melanoma cells that co-expressed luciferase subcutaneously into immunocompromised mice and measured both primary tumor growth as well as overall metastatic burden in the organs of the mice at the endpoint. Loss of FTSJ1 lead to significant decrease in metastasis without any impact on the growth of the primary tumor (Figure 6A and B, Extended Figure 9A). MeWo melanoma cells expressing FTSJ1-targeting shRNAs exhibited the same phenotype when transplanted *in vivo* with knockdown of FTSJ1 causing a decrease in metastatic burden without impacting the growth of the primary tumor (Figure 6C and D, Extended Figure 9B-D). Depleting FTSJ1 using shRNAs in two different PDX melanoma tumors, M405 and M481, also lead to no change in primary tumor growth but significantly decreased metastatic spread into the organs (Figure 6E-H, Extended Figure 9E and F). To address

352 whether FTSJ1 activity was sufficient to drive metastasis, we overexpressed FTSJ1 in A375 melanoma cells and
353 transplanted them *in vivo*. FTSJ1 overexpression had no effect on primary tumor growth but it increased the
354 metastatic burden in the organs of the mice (Figure 6I – J, Extended Figure 9G). The same phenotype was observed
355 when FTSJ1 was overexpressed in a PDX tumor, M481 (Figure 6K-L, Extended Figure 9H). The second PDX tumor,
356 M405, also showed a trend towards an increase in metastasis (Extended Figure 9I - J). To assess whether FTSJ1 had
357 an effect specifically on metastatic colonization, we injected FTSJ1 KO cells intravenously. There was a trend towards
358 a decrease in metastasis (Extended Figure 9K). Similarly, when we transplanted FTSJ1 overexpressing cells
359 intravenously, there was a trend towards an increase in metastasis (Extended Figure 9L). We assessed whether levels
360 of lipid peroxidation were specifically affected in either FTSJ1-depleted cells or FTSJ-overexpressing cells *in vivo*. In
361 either case lipid peroxidation markers did not significantly change in the primary tumor (Extended Figure 9M and N).
362 These data demonstrate that FTSJ1 is both necessary and sufficient for metastatic colonization *in vivo*.
363

364 **DISCUSSION**

365 Our findings reveal that a single modification of the anticodon loop on the selenocysteine tRNA, Um34, can mediate
366 translation of selenoproteins, promoting oxidative stress resistance and metastasis. It has been previously shown
367 that Um34 levels respond to extracellular selenium. We specifically identify oxidative stress as an inducer of Um34
368 and selenoprotein translation independent of selenium. Previous work that has tried to address the functional role
369 of Um34 has relied on a mutant form of Sec tRNA, $i^6$A37G, which is missing the $i^6$A modification at position 37 that is
370 a pre-requisite for the Um34 modification. No study has directly uncoupled the function of $i^6$A from that of Um34. It
371 has been impossible to directly study the role of Um34 since the identity of the Um34 methyltransferase has been
372 unknown. Recently, loss of FTSJ1 has been correlated to loss of Um34 on Sec tRNA. We directly characterized FTSJ1
373 as the Um34 methyltransferase by showing its direct interaction with Sec tRNA as well as selenocysteine translational
374 machinery. We demonstrate its Um34 methyltranferase activity *in vitro* and show that its activity is required for UGA
375 readthrough as a selenocysteine. By characterizing FTSJ1 as the Um34 methyltransferase, we were able to
376 specifically functionally test the role of Um34 in selenoprotein translation. Using ribosomal profiling we were able to
377 show that loss of Um34 specifically impacts UGA readthrough efficiency and causes ribosomal stalling on
378 selenoprotein transcripts. We speculate that Um34 modification may promote interaction of Sec tRNA with the
379 ribosome during UGA readthrough and therefore promote Sec insertion at the UGA, but further studies are required
380 to establish the exact mechanism by which Um34 regulates selenoprotein translation at the molecular level. Although
381 FTSJ1 has been knocked out in the mouse, the only defects observed were in the brain and were linked to Phe GAA
382 translation. Ftsj1 KO mouse brains showed no changes in selenoprotein translation[32]. Currently there are no functional
383 examples of a physiological context for Um34-mediated selenoprotein regulated translation. In contrast, we have

been able to establish a functional role for Um34-mediated translation of selenoproteins in oxidative stress resistance and specifically showed that Um34 modification is a *bona fide* metastatic driver in xenograft models of melanoma. Importantly, loss of Um34 specifically impacted metastatic colonization likely by increasing oxidative stress resistance but is dispensable for proliferation of cancer cells in the primary tumor. Overall, our results reveal the molecular and functional mechanisms of $tRNA^{Sec}$ Um34 modification in oxidative stress resistance and melanoma metastasis and highlight the potential role of FTSJ1 as a therapeutic target specific to metastatic disease.

Interestingly, FTSJ1 is known to modify several other tRNAs, mainly $tRNA^{Phe}$ and $tRNA^{Trp}$ and its pathogenesis has been implicated in X-linked intellectual disability in patients[47,48]. Previous studies show that constitutive knockout of FTSJ1 in mice leads to loss of anticodon modifications on 11 tRNAs and aberrant brain function but otherwise normal tissue development in the body. Similarly, patients with mutations in FTSJ1 manifest intellectual and behavioral symptoms that result in non-syndromic X-linked intellectual disability but show no dysmorphism. This work emphasized that PheGAA tRNA was most significantly affected in the KO mouse brain which correlated with impaired translation at Phe codons and neurological phenotypes but was unaffected in other adult tissues[31]. Our data also does not show significant changes in Phe GAA codon readthrough in FTSJ1 KO melanoma cells, suggesting FTSJ1 activity has phenotypic tissue specificity. Given the role of FTSJ1 in brain development it would be interesting to explore whether selenoprotein translation is affected at different stages of embryonic and specifically, brain development.

Given that redox dysregulation is a hallmark to cancer it is possible that effects of Um34 loss are more pronounced in cancer cells. Most importantly, metastasis may represent a unique process, highly sensitive to perturbation in oxidative stress, and therefore highly dependent on the antioxidant selenoproteome regulated by Um34 for metastatic colonization. Out work highlights Um34 as a regulatory node that specifically controls the antioxidant response through translation of selenoproteins. It will be particularly important to explore the molecular synergy between how selenium levels and oxidative stress regulate Um34-driven translation. We observe an increase in FTSJ1 protein expression in response to oxidative stress and selenium supplementation as well as in metastatic nodules. ALKBH8, which generates the Um34-precursor, $mcm^5U$, is also induced upon oxidation[34]. It is possible that together these Sec tRNA modifying enzymes coordinate the selenium and oxidation status of the cell to promote specific translation of selenoproteins. We propose that these enzymes have the potential to be potent therapeutic targets for metastatic disease. Although previous reports have identified other tRNAs as drivers of metastasis[49], these code for common amino acids that are also required by normal tissues and are difficult to drug. In contrast, tRNA modifying enzymes such as FTSJ1 and ALKBH8 may represent effective drug targets with minimal toxicity to normal

tissues, since their function seems to be confined to brain development.

Finally, while we have found that FTSJ1 specifically regulates metastasis, further studies are needed to explore other physiological contexts in which $tRNA^{Sec}$ Um34 maybe required, including thyroid hormone regulation, inflammation and neurodegenerative pathologies that are also associated with oxidative stress dysregulation.

## METHODS

### Reagents and Equipment

Commercially available reagents were used without further purification.

### Cell lines and culture conditions

A-375 (CRL-1619), SK-MEL-2 (HTB-68), SK-MEL-28 (HTB-72), MeWo (HTB-65), HeLa (ATCC CCL-2) and HEK-293T (ATCC CRL-3216) cell lines were purchased from ATCC. All cells were maintained in DMEM containing 4.5g/L glucose and L-glutamine without sodium pyruvate (Corning 10-017-CV). All media was supplemented with 10% Fetal Bovine Serum (Thermo Fisher Scientific) and 1% Penicillin Streptomycin (Corning). All cell lines were grown at 37°C with 5% CO2 and tested for mycoplasma.

### Plasmid Construction

miR-E shRNA knockdown constructs were generated by the splashRNA program and ordered from Invitrogen as oligos. Hairpins were ligated (T4 Ligase, NEB) into SiREP lentiviral plasmid behind an SFFV promoter and EGFP fluorescent protein using XhoI and EcoRI sites. For overexpression constructs, the coding sequences of specific proteins were ordered as gene fragments (IDT) with an N-terminus Kozack sequence and 3xFLAG or 3xHA tag. (C-terminus tag: FTSJ1, SECp43, N-terminus tag: SBP2, EEFSEC, WDR6). Constructs were ligated (In-Fusion HD, Takara) into pLenti vector behind an EFS promoter using BamHI and NsiI sites. A cleavable P2A site links the protein expression to a fluorescent protein tag. CRISPR knockout sgRNA sequences were generated using Geneious cloning software and ordered as single stranded oligos from IDT. Vector backbones were kindly provided by Lukas Dow, and all plasmids were sequence verified.

### Lentiviral transduction and generation of stable cell lines

For virus production, 0.9µg of plasmid was combined with 1µg of packaging plasmids (0.4µg pMD2G and 0.6µg psPAX2) and transfected into HEK 293T cells using Polyjet (SignaGen) according to manufacturer's instructions.

448 Fresh media was added the following day and viral supernatants were collected 72hr after transfection and filtered
449 through a 0.45µM filter. Approximately 1 million cells were infected with viral supernatant and 10µg/mL polybrene
450 (Sigma-Aldrich). Cells then underwent antibiotic selection with puromycin, hygromycin or blasticidin (Inviogen)
451 depending on the antibiotic resistance of each plasmid. For CRISPR knockout, cells stably-expressing Cas9 were
452 infected with the gRNA construct. To generate single clones, cells were diluted and plated into a 10cm dish. Glass
453 rings were used to isolate single cells and grow colonies. All single clones were verified by western blot analysis and
454 Synthego genomic DNA sequencing.
455
456 **Selenium supplementation and depletion in cell culture**
457 Sodium selenite (VWR) was used to supplement selenium in cell culture. "Full media" constitutes DMEM media with
458 10% FBS – which contains trace levels of selenium bound to albumin. 2% FBS in DMEM was used to lower selenium
459 levels in media without depleting cells of FBS. To achieve 0nM Se, DMEM was combined with Ham's F12 nutrient mix
460 (Thermo Scientific) at a 1:1 ratio with no FBS present. 30nM sodium selenite was then added for selenium
461 supplementation in DMEM/F12 media.
462
463 **tRNA biotin enrichment**
464 Small RNA was extracted from cells or tissue using RNAzol RT (Molecular Research Center) according to
465 manufacturer's instructions. tRNA enrichment was performed as previously described[12]. Briefly, M270 magnetic
466 Streptavidin beads were washed then incubated with a biotin-labelled oligo specific to the 3' end of the tRNA for
467 30min at RT with gentle shaking. Beads were then washed to remove excess oligo and resuspended in in 6xSSC
468 buffer (Fisher Scientific). 40-60µg small RNA was also resuspended in 6xSSC buffer. The beads and RNA were
469 incubated separately for 5 min at 75°C and then combined for an additional 5 min incubation. The combined beads
470 and small RNA were then incubated for 40 min at RT with gentle shaking. Beads were then washed three times with
471 3x SSC, two times with 1x SSC, and several times with 0.1x SSC until the absorbance at 260nm of the wash
472 supernatant was 0. tRNA was eluted in 0.1x SSC by incubating the beads with buffer at 65°C for 3-4 min. tRNA was
473 then precipitated by adding 1µL glycogen (Sigma-Aldrich) and 300mM NaOAc to the tRNA elution followed by the
474 addition of 4x volume 100% ethanol. Samples were then stored at -80°C overnight.
475
476 **Analysis of nucleoside modification by LCMS**
477 Ethanol-precipitated tRNA was pelleted by centrifugation for 15min at 10,000rpm. After washing with 70% ethanol,
478 the pellet was resuspended in 20µL $H_2O$. tRNA samples were enzymatically hydrolyzed to nucleosides as previously
479 described[50]. Briefly, tRNA was then boiled at 100°C for three minutes and then immediately placed in an ice water

bath to cool. Two units Nuclease P1 (NEB) were added with 1/10 volume 0.1M ammonium acetate pH 5.3 for two hours at 45°C. 0.002 units of venom phosphodiesterase (Sigma Aldridge) were added with 1/10 volume 1M ammonium bicarbonate and incubated for 2 hours at 37°C. 0.5 units alkaline phosphatase (NEB) was then added and incubated for one hour. Once digestion was complete, the full volume was transferred to a 10kDa centrifugal filter (Pall Nanosep OD010C34) to remove enzymes. Columns were centrifuged for 8 min at 14,000xg at 4°C. Digested nucleosides were then used directly for LC-MS analysis on an Agilent ZORBAX SB-C18, 2.1 X 150mm, 3.5µm column. Chromatography and Mass Spectrometry methods were performed exactly as described in Songe-Moller et al, 2009 on an Agilent HPLC 1290 connected to an Agilent QQQ (#).

**Analysis of GFP selenocysteine reporter by flow cytometry**

The selenocysteine insertion reporter consists of a destabilized-GFP (d2GFP) as described by Corish et al[51] and a selenocysteine insertion element (SECIS) from GPX1 or GPX4. This is followed by an IRES – iRFP in order to normalize GFP signal to active translation levels in the cell. Both cysteines in GFP were either replaced with UGA, UAA or UAG codons to mimic a UGA-selenoprotein or act as an alternate stop codon control. Cells were transduced with lentiviral constructs containing the reporter and cells were then selected with hygromycin (Invivogen) for one week. GFP and iRFP levels were quantified by flow cytometry on an Attune NxT (Invitrogen). Analysis was completed with FlowJo software and GFP signal was normalized to iRFP signal.

**Real- Time PCR Quantification of tRNA and mRNA**

tRNA and mRNA were extracted using a classic Trizol-chloroform RNA extraction. Reverse transcription was performed using iScript cDNA synthesis kit (Rio-Rad) as described by manufacturer. cDNA was then diluted and used for qPCR analysis with SYBR Green PCR master mix (Thermo Fisher). IDT online primer design tool was used to generate qPCR primers and UCSC In-Silico PCR database was then used to verify human-specificity of primers. qPCR analysis was performed on an Applied Biosystems QuantStudio 6 Real-Time PCR System. All targets were normalized to Actin or U6 snRNA in a standard ΔΔCt analysis.

**Immunoprecipitation of protein complexes**

Cell lines overexpressing 3xFLAG or 3xHA- tagged proteins were grown in 10cm dishes and protein lysates were made with 1% Triton X-100 lysis buffer with DTT and PMSF added. Cell debris and insoluble fraction was removed by centrifugation. Anti-FLAG M2 (Sigma-Aldrich) or Anti-HA (Thermo Fisher) agarose beads were washed with PBS and added to the cell lysates for an overnight incubation on a rotator at 4°C. The following day, the beads were pelleted

511 by centrifugation at 1000xg at 4°C and washed 3 times with BC100 wash buffer (0.5M Tris HCl pH 7.6, 250mM EDTA,
512 100mM KCl, 10% glycerol). Protein complexes were eluted with 3x-FLAG peptide (Sigma-Aldrich) or HA peptide
513 (Thermo Fisher) diluted to 1mg/mL in TBS. Protein eluates were then submitted for proteomic analysis or run on 4-
514 20% Tris-Glycine polyacrylamide gels for western blot analysis.
515
516 **RNA-immunoprecipitation**
517 Cells were lysed in Triton-X as described above, with the addition of 5µL ribonuclease inhibitor, RNaseOUT
518 (invitrogen) per sample to the lysis buffer. Anti-FLAG M2 agarose beads were added to the lysate for overnight
519 enrichment. The following day, beads were washed as described above and protein/RNA complexes were eluted
520 with 1mg/mL 3xFLAG peptide diluted in TBS. Proteinase K (VWR) was used to digest the protein in the eluate and
521 RNA was extracted. Briefly, PK Buffer (100mM Tris-HCl pH 7.5, 50mM NaCl, 10mM EDTA) was incubated with
522 Proteinase K at 37°C for 20 min to digest any potential RNAses present. FLAG bead supernatant was combined with
523 100µL Proteinase K solution and incubated for 20 min at 37°C. 100µL 7M Urea buffer (7M Urea, 100mM Tris-HCl pH
524 7.5, 50mM NaCl, 10mM EDTA) was added to the reaction and incubated for an additional 20 min at 37°C. All 37°C
525 incubations were performed on a thermomixer with gentle mixing. For small RNA extraction, 700µL RNAzol RT was
526 added to the reaction and incubated for an additional 20 min at 37°C. Small RNA was extracted as described by
527 manufacturer's instructions. Small RNA was precipitated with 20µg glycogen using 1M NaOAC/Ethanol extraction.
528 cDNA was synthesized using iScript cDNA Synthesis Kit (Bio-Rad) and RNA bound to protein complexes was analyzed
529 by qPCR.
530
531 **Recombinant protein expression and purification**
532 FTSJ1 (C-6xHis) and WDR6 (N-6xHis) coding sequences were codon-optimized for e.coli bacteria and cloned
533 separately into petDuet-1 (purchased from Addgene) using the NcoI site downstream of the first T7 promoter.
534 Plasmids were transformed into One Shot BL21 (DE3) E. coli (ThermoFisher). Colonies were grown in 6mL LB ampicillin
535 overnight. The following day, cells were expanded to 1 L LB and grown until OD = 0.5-0.6. IPTG was added to 0.1mM
536 and cells were shaken overnight at 18°C and 225 RPM to allow for induction of recombinant protein. The following
537 day, cells were pelleted, washed with PBS and resuspended in lysis buffer (1% Triton X-100, 5mM imidazole in PBS)
538 and sonicated 4x 15 sec at 30% duty cycle output 3 with 1 minute on ice between sonication. Lysates were centrifuged
539 to remove insoluble fraction. NaCl was added to supernatant to raise salt to 500mM. 1mL/sample Ni-NTA resin
540 (Qiagen) was first washed with lysis buffer with 500mM NaCl then beads were added to supernatant and incubated
541 with rotation for 40 min at 4°C. Resin was washed first with 40mL high salt wash buffer (10mM Tris pH 7.8, 1% Triton

542 X-100, 50mM imidazole, 1M NaCl) then 20mL low salt wash buffer (0.5M Tris-HCl pH 7.6, 250mM EDTA, 50mM
543 imidazole, 70mM KCl, 10% glycerol). Recombinant proteins were eluted 4 times with 1mL elution buffer (0.5M Tris-HCl
544 pH 7.6, 250mM EDTA, 250mM imidazole, 70mM KCl, 10% glycerol). Protein was concentrated using Amicon 10K
545 centrifugal filters (Millipore). PMSF was added to all buffers including PBS and DTT was also added to the elution
546 buffer. Purification was validated using Coomassie staining and western blot analysis.
547

548 ***in vitro* tRNA methyltransferase assay**

549 *in vitro* assays of FTSJ1/WDR6 2'-O-methylation of Sec tRNA was performed as previously described[39], however Sec
550 tRNA was extracted from mammalian FTSJ1 KO cells to provide a tRNA substrate with $mcm^5U_{34}$ precursor. Reactions
551 were carried out at 37°C for 2hr in a 100µL reaction mixture containing 50mM Tris-HCl pH 7.5, 200mM NaCl, 10mM
552 $MgCl_2$, 100µg/mL BSA, 5mM DTT, 5µM Sec tRNA, 100µM SAM with 1µM FTSJ1 and 0.2µM WDR6. tRNAs were
553 extracted with phenol/chloroform and ethanol precipitated. tRNAs were digested as described above with Nuclease
554 P1, venom phosphodiesterase and alkaline phosphatase then analyzed using HPLC-MS/MS analysis as described
555 above.
556

557 **Selenocysteine-specific protein enrichment**

558 Utilizing the differential pKa values of Sec (5.2) and Cys (8.5), we are able to specifically label Sec residues and block
559 Cys residues in both cell lines and tissues[42,52].Cell or tissue were lysed in MES lysis buffer pH 5.6 (50mM MES (Sigma
560 Aldrich), 150mM NaCl, 1mM EDTA, 1% Triton X-100) in the presence of protease inhibitors and 0.1mM Iodoacetyl PEG2
561 biotin (IodoAPB, Fisher Scientific). Protein was quantified and 2mg input was used for protein enrichment by rotating
562 for 1hr at RT to in 0.1mM IodoAPB to selectively label deprotonated selenocysteine residues. Protein was then
563 precipitated with methanol and the pellet was washed a couple times to remove any remaining IodoAPB. Protein
564 pellets were then resuspended in buffered 8M Urea. 5M iodoacetamide (Sigma-Aldrich) was added for 1hr at RT to
565 selectively block deprotonated cysteines. Proteins in urea were added directly to streptavidin agarose beads
566 (Invitrogen) in PBS, 0.1% SDS and rotated overnight at 4°C. The following day, beads were washed three times with
567 2M Urea in PBS, 0.1% SDS and then three additional times in 2M Urea in PBS without SDS. For western blot analysis,
568 beads were boiled in 1x protein loading buffer at 95°C for 5 minutes.
569

570 **Ribosomal Sequencing**

571 The Ribo-seq libraries were generated as previously described with following modifications (McGlincy et al.). Cells
572 were snap-frozen and allowed to thaw on ice, then lysed in lysis buffer [50 mM Tris-HCl (pH 7.4), 150 mM NaCl, 5 mM
573 $MgCl_2$, 1 mM DTT, 1% Triton X-100, 100 µg/mL cycloheximide, 100 µg/mL tigecycline, 15 U/mL DNaseI (ThermoFisher,

574 89836)]. RNA was quantified using Qubit Broad range RNA kit (ThermoFisher, Q10211). Ribosome footprint was
575 generated using 15 U RNase I (Biosearch Technologies, N6901K) to 300 ug RNA in 200 µL reaction volume at room
576 temperature for 45 min. The ribosome was collected by ultracentrifugation and ribosome footprint was purified using
577 TRIzol (ThermoFisher, 15596018). RNA was then dephosphorylated and subjected to size selection from 17-40 nt
578 range from 15% polyacrylamide TBE-Urea gel. Ribosome footprint was extracted from the gel in the extraction buffer
579 [50 mM Tris-HCl (pH 7.0), 300 mM NaCl, 1 mM EDTA, 0.25 % SDS] and subjected to rRNA depletion using
580 Human/Mouse/Rat riboPOOL kit (Galen Molecular, dp-K024-000050) by following the manufacture's instruction.
581 rRNA-depleted ribosome footprint was precipitated in 80% ethanol at -20 °C overnight. rRNA-depleted ribosome
582 footprint was then ligated to a pre-adenylated linker (rApp-WWAGATCGGAAGAGCACACGTC-3ddC). The footprint
583 was reverse transcribed by SuperScript III reverse transcriptase (ThermoFisher, 18080044) with a 5' phosphorylated
584 primer that contains eight-nucleotide unique molecular identifiers and two spacer residues (Phos-
585 NNNNNNNNAGATCGGAAGAGCGTCGTGTA-iSp18-AA-iSp18-TAGACGTGTGCTC). cDNA was run on 10% non-
586 denaturing gel to remove the non-ligated linker and the reverse transcription primer. cDNA was the circularized
587 using CircLigase I in the presence of 1 mM ATP. The library was PCR amplified using KAPA HiFi HotStart ReadyMix
588 (FisherScientific, 50-196-5217) and NEBNext® Multiplex Oligos for Illumina® Dual Index Primers Set 1 (NEB, E7600S).
589 The library was purified twice using 1x AMPure XP Bead (BeckmanCoulter, A63881). The library was sequenced for
590 single-end 100 cycles on Illumina NextSeq 2000 or paired-end 100 cycles on Illumina NovaSeq 6000.
591

592 **RNA-sequencing**

593 RNA-seq library was prepared from the lysate prepared for Ribo-seq. Cells were snap-frozen and allowed to thaw
594 on ice, then lysed in lysis buffer [50 mM Tris-HCl (pH 7.4), 150 mM NaCl, 5 mM $MgCl_2$, 1 mM DTT, 1% Triton X-100, 100
595 µg/mL cycloheximide, 100 µg/mL tigecycline, 15 U/mL DNaseI (ThermoFisher, 89836)]. RNA was purified from the
596 lysate using TRIzo (ThermoFisher, 15596018) and quantified on NanoDrop. RNA library was generated using 1 µg
597 total RNA. Ribosomal RNA was removed using NEBNext® rRNA Depletion Kit (Human/Mouse/Rat; NEB, E6310X).
598 rRNA-depleted RNA was converted to a library using NEBNext® Ultra™ II Directional RNA Library Prep Kit (NEB,
599 E7760L) by following manufacture's protocol. cDNA library was PCR amplified using KAPA HiFi HotStart ReadyMix
600 (FisherScientific, 50-196-5217) and NEBNext® Multiplex Oligos for Illumina® Dual Index Primers Set 1 (NEB, E7600S).
601 The library was purified twice using 1x AMPure XP Bead (BeckmanCoulter, A63881). The library was sequenced for
602 single-end 100 cycles on Illumina NextSeq 2000.
603

604 **Ribo-Seq Analysis**

605 Bulk RNA-seq and RIBO-seq libraries from cell lines were analyzed in a similar way. Reads were trimmed using Trim

606 Galore v0.6.10 (https://github.com/FelixKrueger/TrimGalore/tree/master) to remove nucleotides with low quality and
607 adaptor contamination. For RIBO-seq data, duplicated reads created by PCR amplification were removed using the
608 UMI reads and running fastq2collapse.pl and stripBarcode.pl scripts from CTK tool kit (PMID: 27797762). For both
609 types of libraries, non-coding RNA was removed using a custom reference genome composed by miRNA, rRNA,
610 tRNA and lncRNA sequences. miRNA sequences were downloaded from RNAcentral database (https://rnacentral.org)
611 , tRNA sequences were obtained from GtRNAdb (http://gtrnadb.ucsc.edu/index.html) using High confidence
612 GRCH38/hg38 tRNA sequences, lncRNA were downloaded from LNCipedia (PMCID: PMC3531107) and rRNA
613 reference sequence was built using U13369.1, NR_145819.1, NR_146144.1, NR_146151.1, NR_146117.1, X12811.1,
614 NR_003287.4, NR_023379.1, NR_003285.3 and NR_003286.4. Mapping was performed using STAR v2.7.9a
615 (PMCID: PMC3530905) with default parameters and reads that mapped to the custom reference were removed.
616 FastQC v0.11.8 was used for quality control of the remaining reads. STAR v2.7.9a was used for a second mapping
617 step to the full human reference genome, with –alignEndsType EndToEnd and –quantMode TranscriptomeSAM,
618 using GRCh38 primary assembly genome and MANE v1.2 annotation file to obtain transcriptome and genome
619 mapping coordinates. Using bam files of the mapped RNA-seq reads to the whole genome gene counts quantification
620 of CDS regions was calculated using featureCounts v 2.0.1 (PMID: 24227677).
621
622 For RIBO-seq profiling, aligned bam files originated from mapping to the transcriptome were used as input for
623 riboWaltz package (https://doi.org/10.1371/journal.pcbi.1006169). Nucleotide base in-frame p-sites coverage were
624 calculated to determinate stalling based on downstream cumulative distribution function (CDF), to identify
625 readthrough by 5' and 3' footprints, to calculate p-site codon usage and finally, for gene quantification to use in
626 translation efficiency (TE) analysis. For in-frame p-site coverage quantification, reads longer than 25 pb and shorter
627 than 45 pb were kept and p-offsites were calculated for each read length using psite function in riboWaltz with default
628 arguments. Once, p-site position of each read was identified, only in-frame p-sites were kept for further analysis.
629 Mean values and cumulative fractions in the different conditions were calculated using the in-frame p-site coverage
630 in selenoproteins. Differences in CDF values between KO and WT (Met and Primary tumor) were calculated using
631 fixed size windows (Figure X). Windows sizes were set by dividing the CDS 5' end to the first UGA codon to five
632 equal-length bins and similarly dividing the sequence from UGA to the CDS 3' end to five segments. Therefore, each
633 fraction account for the 20% length of 5' or 3' to Sec codon. Maximum of cumulative fraction for each bin was
634 calculated for KO and WT (Met and Primary tumor) conditions and their difference were used for plotting.
635
636 In a similar way, ribosome readthrough was determined based on the obtained CDS p-site coverage values from the
637 RIBO-seq libraries (Figure X). 5' and 3' coverages were calculated on fixed -X and +X bases relative to the Sec codon.

638 Since we were using only CDS p-site values and for some of the selenoproteins the distance between Sec and stop
639 codon was short, these fixed bins were different between selenoproteins (refer to GitHub code to identify the number
640 of bases used for each selenoprotein). To determine significant differences between KO and WT conditions in
641 footprints ratios, unpaired two-sided Student t-test from rstatix package was applied with a $p < 0.05$ cutoff
642 (https://github.com/kassambara/rstatix). Codon usage of p-site was calculated using codon_usage_psite function
643 from riboWaltz (Figure X). Lastly, gene quantification for TE analysis was based on CDS in-frame p-site for every gene.
644 For Xenograft data, in addition to the steps described above, mouse reads were removed in two different ways. Prior
645 to non-coding RNA removal, bbsplit.sh from BBMap v38.90 (https://escholarship.org/uc/item/1h3515gn) was used to
646 remove mouse reads using ambiguous2=="toss" using gencode GRCh38 human and GRCm39 mouse references.
647 Only reads that mapped unambiguously to human reference were used for the second filtering step. In the second
648 step, a mouse reference using healthy liver RIBO-seq data was created and reads that didn't align to this reference
649 (=Human reads) using STAR were kept for subsequent steps. Unless otherwise stated, plots involving high-
650 throughput sequencing data were created using R version 4.2.1 (R Core Team, 2017). Script used in this analysis are
651 available at https://github.com/abcwcm/piskounova_ribo.
652

653 **Analysis of cell survival under prooxidant treatment**

654 Cells were plated at 10,000 cells/well in a white TC-treated 96 well plate (Corning). The following day, DMEM/F12
655 media with 0nM or 30nM selenium was added. After 24 hours of selenium depletion or supplementation, cells were
656 then treated with prooxidant pyocyanin (Cayman), $H_2O_2$ (Sigma-Aldrich) or translation inhibitor tunicamycin (Tocris).
657 After 24 or 48 hours of treatment, CellTiter-Glo 2.0 (Promega) was used according to manufacturers instructions to
658 quantify cell viability.
659

660 **Lentiviral transduction of human melanoma cells**

661 A lentiviral construct with luciferase and dsRed (luc P2A dsRed) was used to label patient-derived melanoma cells as
662 described in Piskounova et al. Nature (2015). Virus was produced as described above. For lentiviral transduction,
663 500,000 freshly dissociated melanoma cells were infected with viral supernatant and supplemented with 10 µg/mL
664 polybrene (Sigma). The following day, the media was replaced and 48hrs post-infection cells were either injected
665 subcutaneously into mice as bulk tumors or FACS sorted for positive infection.
666

667 **Cell labeling and sorting**

668 All melanoma cells in this study stably express dsRed and luciferase so that melanoma cells could be distinguished
669 by flow cytometry or bioluminescent imaging. When preparing cells for sorting by flow cytometry, cells were stained

with antibodies against mouse CD45 (30-F11-VioletFluor, Tonbo), mouse CD31 (390-VioletFluor, eBiosciences), Ter119 (Ter-119-VioletFluor, Tonbo) and human HLA-A, -B, -C (BD Biosciences) to select live human melanoma cells and exclude mouse endothelial and hematopoietic cells. Antibody labelling was performed for 20 min on ice, followed by washing and centrifugation. Before sorting, cells were resuspended in staining medium (L15 medium containing bovine serum albumin (1 mg/mL), 1% penicillin/streptomycin, and 10mM HEPES, pH 7.4) containing 4'6-diamidino-2-phenylindole (DAPI; 5µg/mL; Sigma) to eliminate dead cells from sorting. Live human melanoma cells were isolated by flow cytometry by sorting cells that were positive for dsRed and HLA and negative for mouse CD45, CD31, Ter-119 and DAPI.

**Transplantation of melanoma cells**

After sorting, cells were counted and resuspended in DMEM media with 50% high-protein Matrigel (product 354248, Corning). For a standard metastasis assay, 100 cells were injected subcutaneously into the right flank of the mice. Tumor formation was evaluated by regular palpitation of the injection site and tumors were measured weekly until any tumor in the mouse cohort reached 2.5cm in its largest diameter. Mice were monitored daily for signs of distress according to a standard body condition score or within 24hr of their tumors reaching 2.5 cm in diameter – whichever came first. These experiments were performed according to protocols approved by the Institutional Animal Care and Use Committee at Weill Cornell Medicine (protocol 2017-0033). For intravenous transplantation, 1000 A375 melanoma cells were injected in 100ul of PBS. Mice were imaged weekly by bioluminescence until signal was saturated.

**Bioluminescence imaging**

Mice injected subcutaneously with melanoma cells expressing luciferase were monitored until tumors reached 2.5cm in diameter. For bioluminescent imaging, mice were injected intraperitoneally with 100µL of DPBS containing D-luciferin monopotassium salt (40µg/mL, Goldbio) 5 min before imaging, followed by general anesthesia with isoflurane 2 min before imaging. IVIS Imaging System 200 Series (Caliper Life Sciences) with Living Image Software was used with the exposure time set to 10 seconds. After imaging the whole body, mice were euthanized and individual organs were dissected and imaged. The bioluminescent signal was quantified with 'region of interest' measurement tools in Living Image (Perkin Elmer) software. After imaging, tumors and organs were fixed in paraformaldehyde for histopathology.

**Circulating tumor cell analysis**

During imaging described above, once mice were euthanized for organ dissection, blood was also collected by

cardiac puncture with a syringe pretreated with citrate-dextrose solution (Sigma). Red blood cells were precipitated by Ficoll sedimentation according to manufacturer's instructions (Ficoll Paque Plus, GE Healthcare). Remaining cells were washed with HBSS (Invitrogen) before antibody staining as described above and flow cytometric analysis.

**Immunofluorescence staining of tissue sections**

Tissues were fixed in 4% paraformaldehyde for 12 h at 4 uC, embedded in paraffin, and then sectioned. Sections (10 mm) were deparaffinized and then subjected to antigen retrieval for 10 minutes at 121 uC at 15 PSI in 2.94 g/L sodium citrate (pH 6; Sigma Aldrich, 61332-04-3). Sections were permeabilized in PBS with 0.4% Triton X-100 (PBT) and 1% bovine serum, for 10 min, and blocked in 5% bovine serum in PBT for 45 min at room temperature. Sections were then stained with primary antibodies overnight at 4uC: FTSJ1 (A7967, ABclonal; 1:250), GPX1 (A11166, ABclonal; 1:250), GPX4 (52455S, Cell Signaling; 1:250), MSRB1 (A6737, ABclonal; 1:250), Seleno F (SEP15) (A7967, Abcam; 1:250), SELENOH (HPA048362, Atlas Antibodies; 1:250), SELENOK (HPA008196, Atlas Antibodies; 1:250), SELENO S (VIMP-1) (15160S, Cell Signaling Technology; 1:250), TXNRD1 (15140S, Cell Signaling Technology; 1:250), GFP (13970, abcam, 1:1000) in PBS with 0.1% Triton X-100 and 1% bovine serum. The next day, sections were washed in PBS with 0.1% Triton X-100 and 1% bovine serum and stained with secondary, either goat anti-rabbit antibody (A-21244, Invitrogen; 1:500) or goat anti-chicken (ab150169, abcam; 1:1000), for 1 hour in the dark at room temperature. Sections were washed with PBS with 0.1% Triton X-100 and 1% bovine serum with DAPI (1:1500) for four minutes in the dark at room temperature and mounted for imaging. Fluorescent signal was analyzed and quantified using QuPath v0.4.3 software.

**Statistical methods**

No statistical methods were used to predetermine sample size. The data in most figure panels reflect several independent experiments as indicated in figure legends. Variation is always indicated using standard deviation. For analysis of statistical significance, when only two conditions were compared a two-sided unpaired t-test was used, unless otherwise indicated. For comparison of multiple conditions, one-way ANOVA was used for multiple comparisons, unless otherwise indicated. P value of $<0.05$ was considered statistically significant. All in vivo experiments were randomized to each experimental cohort. The number of mice used is indicated in figure legends. Any mice that died before the end of the experiment due to opportunistic infection, the data from these mice were excluded. No blinding was used in any experiment.

**ACKNOWLEDGEMENTS**

This work was supported by American Cancer Society, Elsa U. Pardee Foundation Grant and Feldstein Medical Research Foundation Award. LN is supported by Ruth L. Kirschstein Predoctoral Individual National Research Service Award.

**AUTHOR CONTRIBUTIONS**

LN designed and performed experiments, analyzed data, and wrote the paper. KC, ID, MZ, GC, RH and KA performed experiments and analyzed data. LED supervised CRISPR/Cas9 experiments and provided reagents. SM and SJ designed, performed and supervised Ribo-Seq experiments. MAA, PZ and DB designed, performed and supervised Ribo-Seq data analysis. EP designed, performed, and supervised experiments, analyzed data, supervised data analysis, and wrote the paper.

**CONFLICTS OF INTEREST**

LED is an advisor and holds equity in Mirimus Inc. and is a consultant for Volastra Therapeutics and Frazier Healthcare Partners. The other authors have no conflicts to disclose.

**REFERENCES**

1 Chan, C., Pham, P., Dedon, P. C. & Begley, T. J. Lifestyle modifications: coordinating the tRNA epitranscriptome with codon bias to adapt translation during stress responses. *Genome Biol* **19**, 228 (2018). https://doi.org:10.1186/s13059-018-1611-1

2 Suzuki, T. The expanding world of tRNA modifications and their disease relevance. *Nat Rev Mol Cell Biol* **22**, 375-392 (2021). https://doi.org:10.1038/s41580-021-00342-0

3 Agris, P. F., Narendran, A., Sarachan, K., Vare, V. Y. P. & Eruysal, E. The Importance of Being Modified: The Role of RNA Modifications in Translational Fidelity. *Enzymes* **41**, 1-50 (2017). https://doi.org:10.1016/bs.enz.2017.03.005

4 Endres, L., Dedon, P. C. & Begley, T. J. Codon-biased translation can be regulated by wobble-base tRNA modification systems during cellular stress responses. *RNA Biol* **12**, 603-614 (2015). https://doi.org:10.1080/15476286.2015.1031947

5 Hatfield, D. L., Tsuji, P. A., Carlson, B. A. & Gladyshev, V. N. Selenium and selenocysteine: roles in cancer, health, and development. *Trends Biochem Sci* **39**, 112-120 (2014). https://doi.org:10.1016/j.tibs.2013.12.007

6 Fradejas-Villar, N. *et al.* The RNA-binding protein Secisbp2 differentially modulates UGA codon reassignment and RNA decay. *Nucleic Acids Res* **45**, 4094-4107 (2017). https://doi.org:10.1093/nar/gkw1255

7 Small-Howard, A. *et al.* Supramolecular complexes mediate selenocysteine incorporation in vivo. *Mol Cell Biol* **26**, 2337-2346 (2006). https://doi.org:10.1128/MCB.26.6.2337-2346.2006

8 Xu, X. M. *et al.* Evidence for direct roles of two additional factors, SECp43 and soluble liver antigen, in the selenoprotein synthesis machinery. *J Biol Chem* **280**, 41568-41575 (2005). https://doi.org:10.1074/jbc.M506696200

9 Hatfield, D. L., Carlson, B. A., Xu, X. M., Mix, H. & Gladyshev, V. N. Selenocysteine incorporation machinery and the role of selenoproteins in development and health. *Prog Nucleic Acid Res Mol Biol* **81**, 97-142 (2006). https://doi.org:10.1016/S0079-6603(06)81003-2

10 Kim, L. K. *et al.* Methylation of the ribosyl moiety at position 34 of selenocysteine tRNA[Ser]Sec is governed by both primary and tertiary structure. *RNA* **6**, 1306-1315 (2000). https://doi.org:10.1017/s1355838200000388

11 van den Born, E. *et al.* ALKBH8-mediated formation of a novel diastereomeric pair of wobble nucleosides in mammalian tRNA. *Nat Commun* **2**, 172 (2011). https://doi.org:10.1038/ncomms1173

12 Songe-Moller, L. *et al.* Mammalian ALKBH8 possesses tRNA methyltransferase activity required for the biogenesis of multiple wobble uridine modifications implicated in translational decoding. *Mol Cell Biol* **30**, 1814-1827 (2010). https://doi.org:10.1128/MCB.01602-09

13 Diamond, A. M. *et al.* Dietary selenium affects methylation of the wobble nucleoside in the anticodon of selenocysteine tRNA([Ser]Sec). *J Biol Chem* **268**, 14215-14223 (1993).

14 Howard, M. T., Carlson, B. A., Anderson, C. B. & Hatfield, D. L. Translational redefinition of UGA codons is regulated by selenium availability. *J Biol Chem* **288**, 19401-19413 (2013). https://doi.org:10.1074/jbc.M113.481051

15 Carlson, B. A. *et al.* Selective restoration of the selenoprotein population in a mouse hepatocyte selenoproteinless background with different mutant selenocysteine tRNAs lacking Um34. *J Biol Chem* **282**, 32591-32602 (2007). https://doi.org:10.1074/jbc.M707036200

16 Li, Z. *et al.* Ribosome stalling during selenoprotein translation exposes a ferroptosis vulnerability. *Nat Chem Biol* **18**, 751-761 (2022). https://doi.org:10.1038/s41589-022-01033-3

17 Yant, L. J. *et al.* The selenoprotein GPX4 is essential for mouse development and protects from radiation and oxidative damage insults. *Free Radic Biol Med* **34**, 496-502 (2003). https://doi.org:10.1016/s0891-5849(02)01360-6

18 Ingold, I. *et al.* Selenium Utilization by GPX4 Is Required to Prevent Hydroperoxide-Induced Ferroptosis. *Cell* **172**, 409-422 e421 (2018). https://doi.org:10.1016/j.cell.2017.11.048

19 Jakupoglu, C. *et al.* Cytoplasmic thioredoxin reductase is essential for embryogenesis but dispensable for cardiac development. *Mol Cell Biol* **25**, 1980-1988 (2005). https://doi.org:10.1128/MCB.25.5.1980-1988.2005

20 Conrad, M. *et al.* Essential role for mitochondrial thioredoxin reductase in hematopoiesis, heart development, and heart function. *Mol Cell Biol* **24**, 9414-9423 (2004). https://doi.org:10.1128/MCB.24.21.9414-9423.2004

21 Tarrago, L. *et al.* The selenoprotein methionine sulfoxide reductase B1 (MSRB1). *Free Radic Biol Med* **191**, 228-240 (2022). https://doi.org:10.1016/j.freeradbiomed.2022.08.043

22 Cox, A. G. *et al.* Selenoprotein H is an essential regulator of redox homeostasis that cooperates with p53 in development and tumorigenesis. *Proc Natl Acad Sci U S A* **113**, E5562-5571 (2016). https://doi.org:10.1073/pnas.1600204113

23 Sreelatha, A. *et al.* Protein AMPylation by an Evolutionarily Conserved Pseudokinase. *Cell* **175**, 809-821 e819 (2018). https://doi.org:10.1016/j.cell.2018.08.046

24 Addinsall, A. B., Wright, C. R., Andrikopoulos, S., van der Poel, C. & Stupka, N. Emerging roles of endoplasmic reticulum-resident selenoproteins in the regulation of cellular stress responses and the implications for metabolic disease. *Biochem J* **475**, 1037-1057 (2018). https://doi.org:10.1042/BCJ20170920

25 Kohrle, J. Thyroid hormone deiodinases--a selenoenzyme family acting as gate keepers to thyroid hormone action. *Acta Med Austriaca* **23**, 17-30 (1996).

26 Shetty, S. P. & Copeland, P. R. The Selenium Transport Protein, Selenoprotein P, Requires Coding Sequence Determinants to Promote Efficient Selenocysteine Incorporation. *J Mol Biol* **430**, 5217-5232 (2018). https://doi.org:10.1016/j.jmb.2018.09.005

27 Reich, H. J. & Hondal, R. J. Why Nature Chose Selenium. *ACS Chem Biol* **11**, 821-841 (2016). https://doi.org:10.1021/acschembio.6b00031

28 Brigelius-Flohe, R. & Flohe, L. Selenium and redox signaling. *Arch Biochem Biophys* **617**, 48-59 (2017). https://doi.org:10.1016/j.abb.2016.08.003

29 Carlson, B. A., Xu, X. M., Gladyshev, V. N. & Hatfield, D. L. Selective rescue of selenoprotein expression in mice lacking a highly specialized methyl group in selenocysteine tRNA. *J Biol Chem* **280**, 5542-5548 (2005). https://doi.org:10.1074/jbc.M411725200

30 Moustafa, M. E. *et al.* Selective inhibition of selenocysteine tRNA maturation and selenoprotein synthesis in transgenic mice expressing isopentenyladenosine-deficient selenocysteine tRNA. *Mol Cell Biol* **21**, 3840-3852 (2001). https://doi.org:10.1128/MCB.21.11.3840-3852.2001

31 Nagayoshi, Y. *et al.* Loss of Ftsj1 perturbs codon-specific translation efficiency in the brain and is associated with X-linked intellectual disability. *Sci Adv* **7** (2021). https://doi.org:10.1126/sciadv.abf3072

32 Fradejas-Villar, N. *et al.* The Effect of tRNA([Ser]Sec) Isopentenylation on Selenoprotein Expression. *Int J Mol Sci* **22** (2021). https://doi.org:10.3390/ijms222111454

33 Piskounova, E. *et al.* Oxidative stress inhibits distant metastasis by human melanoma cells. *Nature* **527**, 186-191 (2015). https://doi.org:10.1038/nature15726

34 Endres, L. *et al.* Alkbh8 Regulates Selenocysteine-Protein Expression to Protect against Reactive Oxygen Species Damage. *PLoS One* **10**, e0131335 (2015). https://doi.org:10.1371/journal.pone.0131335

35 Touat-Hamici, Z., Legrain, Y., Bulteau, A. L. & Chavatte, L. Selective up-regulation of human selenoproteins in response to oxidative stress. *J Biol Chem* **289**, 14750-14761 (2014). https://doi.org:10.1074/jbc.M114.551994

36 Hall, S. *et al.* Cellular Effects of Pyocyanin, a Secreted Virulence Factor of Pseudomonas aeruginosa. *Toxins (Basel)* **8** (2016). https://doi.org:10.3390/toxins8080236

37 Zhu, Z., Guo, R., Li, Y., Li, S. & Tu, P. Comparison of three analytical methods for superoxide produced by activated immune cells. *J Pharmacol Toxicol Methods* **101**, 106637 (2020). https://doi.org:10.1016/j.vascn.2019.106637

38 Mistry, H. D. *et al.* Differential expression and distribution of placental glutathione peroxidases 1, 3 and 4 in normal and preeclamptic pregnancy. *Placenta* **31**, 401-408 (2010). https://doi.org:10.1016/j.placenta.2010.02.011

39 Li, J. *et al.* Intellectual disability-associated gene ftsj1 is responsible for 2'-O-methylation of specific tRNAs. *EMBO Rep* **21**, e50095 (2020). https://doi.org:10.15252/embr.202050095

40 Ingolia, N. T. Ribosome Footprint Profiling of Translation throughout the Genome. *Cell* **165**, 22-33 (2016). https://doi.org:10.1016/j.cell.2016.02.066

41 Karlenius, T. C. *et al.* The selenium content of cell culture serum influences redox-regulated gene expression. *Biotechniques* **50**, 295-301 (2011). https://doi.org:10.2144/000113666

42 Guo, L. *et al.* Selenocysteine-Specific Mass Spectrometry Reveals Tissue-Distinct Selenoproteomes and Candidate Selenoproteins. *Cell Chem Biol* **25**, 1380-1388 e1384 (2018). https://doi.org:10.1016/j.chembiol.2018.08.006

43 Bak, D. W., Gao, J., Wang, C. & Weerapana, E. A Quantitative Chemoproteomic Platform to Monitor Selenocysteine Reactivity within a Complex Proteome. *Cell Chem Biol* **25**, 1157-1167 e1154 (2018). https://doi.org:10.1016/j.chembiol.2018.05.017

44 Schoenmakers, E. *et al.* Mutation in human selenocysteine transfer RNA selectively disrupts selenoprotein synthesis. *J Clin Invest* **126**, 992-996 (2016). https://doi.org:10.1172/JCI84747

45 Vindry, C. *et al.* A homozygous mutation in the human selenocysteine tRNA gene impairs UGA recoding activity and selenoproteome regulation by selenium. *Nucleic Acids Res* (2023). https://doi.org:10.1093/nar/gkad482

46 Quintana, E. *et al.* Human melanoma metastasis in NSG mice correlates with clinical outcome in patients. *Sci Transl Med* **4**, 159ra149 (2012). https://doi.org:10.1126/scitranslmed.3004599

47 Guy, M. P. *et al.* Defects in tRNA Anticodon Loop 2'-O-Methylation Are Implicated in Nonsyndromic X-Linked Intellectual Disability due to Mutations in FTSJ1. *Hum Mutat* **36**, 1176-1187 (2015). https://doi.org:10.1002/humu.22897

48 Takano, K. *et al.* A loss-of-function mutation in the FTSJ1 gene causes nonsyndromic X-linked mental retardation in a Japanese family. *Am J Med Genet B Neuropsychiatr Genet* **147B**, 479-484 (2008). https://doi.org:10.1002/ajmg.b.30638

49 Goodarzi, H. *et al.* Modulated Expression of Specific tRNAs Drives Gene Expression and Cancer Progression. *Cell* **165**, 1416-1427 (2016). https://doi.org:10.1016/j.cell.2016.05.046

50 Crain, P. F. Preparation and enzymatic hydrolysis of DNA and RNA for mass spectrometry. *Methods Enzymol* **193**, 782-790 (1990). https://doi.org:10.1016/0076-6879(90)93450-y

51 Corish, P. & Tyler-Smith, C. Attenuation of green fluorescent protein half-life in mammalian cells. *Protein Eng* **12**, 1035-1040 (1999). https://doi.org:10.1093/protein/12.12.1035

52 Bak, D. W., Gao, J., Wang, C. & Weerapana, E. A Quantitative Chemoproteomic Platform to Monitor Selenocysteine Reactivity within a Complex Proteome. *Cell Chem Biol* (2018). https://doi.org:10.1016/j.chembiol.2018.05.017

## FIGURE LEGENDS

**Figure 1: Selenoprotein translation and tRNA$^{Sec}$ Um34 levels increase in response to oxidative stress**

(A) Schematic of selenocysteine biosynthesis and selenoprotein translation. Sec is synthesized on its tRNA. The tRNA is then modified at the wobble uridine and the Sec translation complex associated with the SECIS allows for co-translational readthrough of UGA stop codon.

898 (B) Schematic of $tRNA^{Sec}$ isolation and Um34 modification analysis
899 (C) Quantification of Um34 and $mcm^5U$ levels in A375 melanoma cells grown in DMEM/F12 medium
900 supplemented with increasing concentrations of selenium measured by LC-MS/MS. n = 2 independent
901 experiments, Mean +/- SD. Statistical significance assessed by two-way analysis of variance (ANOVAs)
902 followed by Fisher LSD test for multiple comparisons. *p<0.05, **p<0.005.
903 (D) Quantification of Um34 modification levels on $tRNA^{Sec}$ in A375 melanoma cells treated with pro-oxidant $H_2O_2$
904 (100µM) pyocyanin (10µM) in DMEM/F12 media in the presence or absence of 30nM NaSe. n = 2 independent
905 experiments, Mean +/- SD. Statistical significance assessed by one-way ANOVA followed by Fisher LSD test
906 for multiple comparisons. **p<0.005, ***p<0.0005.
907 (E) Schematic of the split-seleno-GFP reporter - GFP Reporter Of Selenocysteine Insertion (gROSI).
908 (F) Flow cytometry analysis of split-seleno-GFP reporter (gROSI) expression with different combinations of stop
909 codons UAA or UGA and with No UTR or SECIS from GPX4, in the presence or absence of selenium (30nM
910 NaSe) in A375 melanoma cells. n = 3, Mean +/- SD of 3 independent replicates; representative experiment
911 shown; two-sided unpaired t-test, ***p<0.0005
912 (G) Flow cytometry analysis of GFP fluorescence of gROSI variants without a 3'UTR, with a GPX4 SECIS and with
913 a GPX1 SECIS treated with Pyocyanin (10uM) and NaSe (30nM). n=2 independent experiment, Mean +/- SD.
914 Statistical significance measured by two-way ANOVA followed by Fisher LSD test for multiple comparisons.
915 **p<0.005, ****p<0.00005.
916 (H) Levels of selenoproteins in A375 melanoma cells and (I) SK-MEL-2 melanoma cells after treatment with NaSe
917 (30nM) and pyocyanin (10uM). Representative experiments shown.
918 (J) Transcript levels of selenoproteins in A375 melanoma cells after treatment with NaSe and pyocyanin
919 measured by qRT-PCR. n=3 independent replicates.
920
921 **Figure 2: FTSJ1 is the $mcm^5Um$ (Um34) methyltransferase for $tRNA^{Sec}$**
922 (A) Alignment schematic of FTSJ1 and its homologs, highlighting a catalytic lysine and the catalytically dead
923 A26P mutation.
924 (B) Co-immunoprecipitation assay of the interaction between HA-tagged FTSJ1 and FLAG-tagged component of
925 selenocysteine machinery, EEFSEC, compared to FLAG-tagged Scarlet-expressing control vector co-
926 expressed in A375 melanoma cells. Representative experiment shown.
927 (C) Schematic of RNA-immunoprecipitation.

928 (D) Levels of $tRNA^{Sec}$ bound to FLAG-tagged Renilla, wild type and A26P-mutant FTSJ1, ALKBH8 and EEFSEC by
929 qRT-PCR. n = 3. Mean +/- SD of 3 independent replicates. Two-sided unpaired t-test. **p<0.005,
930 ****p<0.00005
931 (E) Levels of $tRNA^{Sec}$ bound to FLAG-tagged Renilla, FTSJ1 and WDR6 by qRT-PCR. n=3. Mean +/- SD of 3
932 independent replicates. Two-sided unpaired t-test.
933 (F) Western blot analysis of FTSJ1 and selenoprotein GPX1 levels in control and FTSJ1 knockout A375 melanoma
934 cell lines.
935 (G) Quantification of Um34 modification levels on $tRNA^{Sec}$ from control and FTSJ1 knockout A375 melanoma cell
936 lines measured by LC-MS/MS. n = 3 independent experiments. One-way analysis of variance (ANOVA)
937 followed by Dunnett's tests for multiple comparisons. ****p<0.0001
938 (H) Western blot analysis of overexpression of control Renilla luciferase, wild type and mutant A26P FTSJ1 and
939 selenoprotein GPX4 in A375 melanoma cell lines.
940 (I) Quantification of Um34 modification levels on $tRNA^{Sec}$ in A375 melanoma cells overexpressing control Renilla
941 luciferase, wild type and A26P mutant FTSJ1 measured by LC-MS/MS. n = 2 independent experiments.
942 Statistical significance assessed by one-way analysis of variance (ANOVA) followed by Dunnett's tests for
943 multiple comparisons. *p<0.05
944 (J) Quantification of Um34 and $mcm^5U$ levels on $tRNA^{Sec}$ in Control and FTSJ1 knockout A375 melanoma cells
945 grown in DMEM/F12 medium with and without selenium (30nM) measured by LC-MS/MS. n=2 independent
946 experiments. Two-way analysis of variance (ANOVA) followed by Dunnett's tests for multiple comparisons.
947 *p<0.05, **<0.005, ****<0.00005.
948 (K) Quantification of Um34 levels on $tRNA^{Sec}$ in an in vitro methyltransferase assay measured by LC-MS/MS. n=2
949 independent experiments. One-way analysis of variance (ANOVA) followed by Dunnett's tests for multiple
950 comparisons. ****p<0.0001.
951
952 **Figure 3: Um34 regulates UGA recoding efficiency in a subset of selenoproteins involved in oxidative stress**
953
954 (A) Flow cytometry analysis of seleno-GFP reporter (gROSI) expression in control and FTSJ1 knockout A375
955 melanoma cells with and without selenium (30nM). Mean +/- SD of 3 independent replicates; representative
956 experiment shown; One-way analysis of variance (ANOVA) followed by Dunnett's tests for multiple
957 comparisons. **p<0.005, ****p<0.00005.
958 (B) Flow cytometry analysis of seleno-GFP reporter (gROSI) expression in control Renilla-overexpressing or
959 FTSJ1-overexpressing A375 melanoma cells. Mean +/- SD of 3 independent replicates; representative

experiment shown; One-way analysis of variance (ANOVA) followed by Dunnett's tests for multiple comparisons. ****p<0.00005.

(C) Western blot analysis of selenoprotein levels in Control and FTSJ1-KO A375 and SK-MEL-2 melanoma cells.

(D) Western blot analysis of selenoproteins in normal (10% FBS), selenium-depleted (2% FBS) and supplemented conditions (10% + 30nM NaSe and 2% + 30nM NaSe) in A375 melanoma cell line overexpressing either control Renilla or FTSJ1.

(E) UGA Recoding Efficiency (Ratio of RPF 3' to Sec UGA/RPF 5' to Sec UGA) of selenoproteins in WT A375 melanoma cells in the absence and presence of selenium (30nM NaSe).

(F) UGA Recoding Efficiency (Ratio of RPF 3' to Sec UGA/RPF 5' to Sec UGA) of selenoproteins in Control and FTSJ1 KO A375 melanoma cells in the presence of selenium (30nM NaSe).

(G) UGA Recoding Efficiency (Ratio of RPF 3' to Sec UGA/RPF 5' to Sec UGA) of selenoproteins in FTSJ1 KO A375 melanoma cells in the absence and presence of selenium (30nM NaSe).

(H) Z-score values of UGA recoding efficiency comparing WT A375 melanoma cells without selenium, Control A375 melanoma cells with selenium (30nM NaSe) and FTSJ1 KO A375 melanoma cells with selenium (30 nM NaSe).

**Figure 4: Um34 modification protects cancer cells from oxidative stress**

(A) Cell survival of Control and FTSJ1-KO A375 melanoma cells under pyocyanin treatment in selenium-supplemented conditions (30nM NaSe) as measured by Cell Titer Glo. n=3. Representative of 4 independent experiments. Statistical difference between IC50 values analyzed by Extra-Sum-of-Squares F-Test.

(B) Cell survival of Control and FTSJ1-KO SK-MEL-2 melanoma cells under pyocyanin treatment in selenium-supplemented conditions (30nM NaSe) as measured by Cell Titer Glo. n=3. Representative of 3 independent experiments. Statistical difference between IC50 values analyzed by Extra-Sum-of-Squares F-Test.

(C) Cell survival of Control and FTSJ1-KO A375 melanoma cells under pyocyanin treatment in selenium-depleted conditions as measured by Cell Titer Glo. n=3. Representative of 4 independent experiments. Statistical difference between IC50 values analyzed by Extra-Sum-of-Squares F-Test.

(D) Cell survival of Control and FTSJ1-KO SK-MEL-2 melanoma cells under pyocyanin treatment in selenium-depleted conditions as measured by Cell Titer Glo. n=3. Representative of 3 independent experiments. Statistical difference between IC50 values analyzed by Extra-Sum-of-Squares F-Test.

(E) Cell survival of Control and FTSJ1 overexpressing A375 melanoma cells under pyocyanin treatment in selenium-supplemented conditions (30nM NaSe) as measured by Cell Titer Glo. n=3. Representative of 4

992 independent experiments. Statistical difference between IC50 values analyzed by Extra-Sum-of-Squares F-
993 Test.
994 (F) Cell survival of Control and FTSJ1 overexpressing SK-MEL-2 melanoma cells under pyocyanin treatment in
995 selenium-supplemented conditions (30nM NaSe) as measured by Cell Titer Glo. n=3. Representative of 3
996 independent experiments. Statistical difference between IC50 values analyzed by Extra-Sum-of-Squares F-
997 Test.
998 (G) Cell survival of Control and FTSJ1 overexpressing A375 melanoma cells under pyocyanin treatment in
999 selenium-depleted conditions as measured by Cell Titer Glo. n=3. Representative of 4 independent
1000 experiments. Statistical difference between IC50 values analyzed by Extra-Sum-of-Squares F-Test.
1001 (H) Cell survival of Control and FTSJ1 overexpressing SK-MEL-2 melanoma cells under pyocyanin treatment in
1002 selenium-depleted conditions as measured by Cell Titer Glo. n=3. Representative of 3 independent
1003 experiments. Statistical difference between IC50 values analyzed by Extra-Sum-of-Squares F-Test.
1004 (I) Cell survival of Control and FTSJ1-KO A375 melanoma cells with and without FTSJ1-overexpression treated
1005 with 25 uM Pyocyanin in the presence of selenium (30nM NaSe) as measured by Cell Titer Glo. n=3.
1006 Representative of 3 independent experiments. One-way ANOVA followed by Tukey test for multiple
1007 comparisons.
1008 (J) Cell survival of Control and FTSJ1-KO A375 melanoma cells with and without FTSJ1-overexpression treated
1009 with 25 uM of Pyocyanin in the absence of selenium as measured by Cell Titer Glo. n=3. Representative of 3
1010 independent experiments. One-way ANOVA followed by Tukey test for multiple comparisons.
1011 (K) Cell survival of Control, WT $tRNA^{Sec}$ and C65G-mutant $tRNA^{Sec}$ overexpressing A375 melanoma cells treated
1012 with 25uM of Pyocyanin in the presence of selenium (30nM NaSe) as measured by Cell Titer Glo. n=3.
1013 Representative of 3 independent experiments. One-way ANOVA followed by Dunnett test for multiple
1014 comparisons.
1015 (L) Cell survival of Control, WT $tRNA^{Sec}$ and C65G-mutant $tRNA^{Sec}$ overexpressing A375 melanoma cells treated
1016 with 25uM of Pyocyanin in the absence of selenium as measured by Cell Titer Glo. n=3. Representative of 3
1017 independent experiments. One-way ANOVA followed by Dunnett test for multiple comparisons.
1018
1019 **Figure 5: Micrometastases experience high levels of stress and increase selenocysteine biosynthesis.**
1020
1021 (A) Levels of reactive oxygen species (ROS) in subcutaneous tumors vs micro and macrometastatic nodules from
1022 NSG mice transplanted with two different patient melanomas, M481 and M405, measured by flow cytometry
1023 with fluorescent dyes. CellROX DeepRed was used measure cytoplasmic oxidative stress and CellROX

1024 Green was used to measure mitochondrial oxidative stress levels. n = 6 - 9 mice from 2 - 3 independent
1025 experiments). Statistical significance assessed by one-way analysis of variance (ANOVAs) followed by
1026 Dunnett's tests for multiple comparisons. *p<0.05, **p<0.005, ***p<0.0005, ****p<0.00005.
1027 (B) Transcript levels of selenocysteine biosynthesis machinery in subcutaneous tumors vs micro and
1028 macrometastatic nodules from NSG mice transplanted with patient-derived melanoma, M481, measured by
1029 qRT-PCR. Mean +/- SD of 3 independent replicates; One-way analysis of variance (ANOVAs) followed by
1030 Dunnett's tests for multiple comparisons. *p<0.05, **p<0.005, ***p<0.0005, ****p<0.00005.
1031 (C) Levels of selenoproteins, FTSJ1 and WDR6 in metastases compared to primary tumor tissues from NSG mice
1032 transplanted with patient-derived melanoma, M405, measured by immunofluorescent staining.
1033 (D) Levels of selenoproteins and components of selenocysteine biosynthesis machinery in metastases
1034 compared to primary tumor from NSG mice transplanted with patient-derived melanomas, M405 and M481,
1035 as measured by western blotting.
1036 (E) Levels of FTSJ1 in subcutaneous vs micro vs macrometastatic nodules from NSG mice transplanted with
1037 Mewo melanoma cell lines, measured by immunofluorescence.
1038 (F) Quantification of data shown in (H). Two-tailed one sample t-test. **p<0.005, ****p<0.00005
1039 (G) Levels of Um34 modification in subcutaneous tumors vs metastatic nodules from NSG mice transplanted
1040 with two different patient-derived melanomas, M405 and M481, measured by LC-MS/MS analysis of modified
1041 $tRNA^{Sec}$ nucleosides. n=3 mice for each patient-derived melanoma. One-way ANOVA (Kruskal-Wallis test)
1042 followed by Dunn's test for multiple comparisons. *p<0.05.
1043
1044 **Figure 6: $tRNA^{Sec}$ Um34 modification is necessary and sufficient for metastasis *in vivo***
1045 (A) Subcutaneous tumor growth in mice transplanted with either Control or FTSJ1 KO A375 melanoma cells. Data
1046 reflect 3 independent experiments but only one representative experiment is shown.
1047 (B) Total metastatic burden in the visceral organs of mice subcutaneously transplanted with either Control of
1048 FTSJ1 KO A375 melanoma cells measured by bioluminescence after 7 weeks. n= 13-15 mice from 3
1049 independent experiments. Mann-Whitney t-test **p <0.005
1050 (C) Subcutaneous tumor growth in mice transplanted with either Control or FTSJ1 KD MeWo melanoma cells.
1051 Data reflect 3 independent experiments but only one representative experiment is shown.
1052 (D) Total metastatic burden in the visceral organs of mice subcutaneously transplanted with either Control of
1053 FTSJ1 KD MeWo melanoma cells measured by bioluminescence. n= 13-15 mice from 3 independent
1054 experiments. One-way analysis of variance (ANOVA) followed by unpaired t with Welch's correction. *p<0.05

1055 (E) Growth of subcutaneous tumors in mice transplanted with a patient-derived melanoma, M405, expressing
1056 either control shRNA or FTSJ1-targeting shRNAs. n=10 mice One-way analysis of variance (ANOVA) followed
1057 by unpaired t with Welch's correction. *p<0.05
1058 (F) Total metastatic burden in visceral organs of mice transplanted with a patient-derived melanoma, M405,
1059 expressing either control shRNA or FTSJ1-targeting shRNAs. n=10 mice. One-way analysis of variance
1060 (ANOVA) followed by unpaired t with Welch's correction. *p<0.05
1061 (H) Growth of subcutaneous tumors in mice transplanted from patient-derived melanoma, M481, expressing
1062 either Control shRNA or FTSJ1 targeting shRNAs.
1063 (I) Total metastatic burden in visceral organs of mice transplanted with patient-derived melanoma, M481,
1064 expressing either Control shRNA or FTSJ1 targeting shRNAs. n = 20 mice. One-way analysis of variance
1065 (ANOVA) followed by unpaired t with Welch's correction. *p<0.05, **p<0.005
1066 (J) Subcutaneous tumor growth in mice transplanted with either Control or FTSJ1 overexpressing A375
1067 melanoma cells. Data reflect 3 independent experiments but only on representative experiment is shown.
1068 (K) Total metastatic burden in the visceral organs of mice subcutaneously transplanted with either Control or
1069 FTSJ1 overexpressing A375 melanoma cells measured by bioluminescence after 7 weeks. n= 13-15 mice from
1070 3 independent experiments. Mann-Whitney t-test. *p <0.05
1071 (L) Growth of subcutaneous tumors in mice transplanted from patient-derived melanoma, M481, overexpressing
1072 either Renilla luciferase or FTSJ1 ORF.
1073 (M) Total metastatic burden in visceral organs of mice transplanted with patient-derived melanoma, M481,
1074 overexpressing either Renilla luciferase or FTSJ1 ORF. n = 20 mice. Mann-Whitney t-test. *p <0.05
1075

1076 **Extended Figure 1: Extracellular selenium drives translation of selenoproteins**

1077 (A) Western blot analysis of selenocysteine proteins TXNRD1, GPX1 and GPX4, in normal (10% FBS), selenium-
1078 depleted (2%) and supplemented conditions ( 10% + 30nM NaSe and 2% + 30nM NaSe) in A375 melanoma
1079 cell line, HEK293Ts and SK-MEL-2 melanoma cell line.
1080 (B) Transcript levels of TXNRD1, GPX4 and GPX1 in normal (10% FBS), selenium-depleted (2%) and
1081 supplemented conditions (10% + 30nM NaSe and 2% + 30nM NaSe) in A375 melanoma cell line by qRT-
1082 PCR. Mean +/- SD of 3 independent replicates; two-sided unpaired t-test.
1083 (C) Levels and purity of $tRNA^{Sec}$ analyzed by SDS-PAGE gel after biotinylated pull-down from increasing
1084 amounts of small RNA input fraction.
1085

1086 **Extended Figure 2: FTSJ1 is necessary and sufficient for Um34 modification on $tRNA^{Sec}$**

1087 (A) Summary of proteomic analysis of EEFSEC-interacting proteins with RNA-modifying activity in A375
1088 melanoma cells. PSM – peptide spectrum matches.
1089 (B) Co-immunoprecipitation assay of the interaction between HA-tagged FTSJ1 and FLAG-tagged component of
1090 selenocysteine machinery, SECp43, compared to empty vector control co-expressed in A375 melanoma
1091 cells. Representative experiment shown.
1092 (C) Levels of Phe tRNA bound to FLAG-tagged Renilla, wild type or A26P-mutant FTSJ1, ALKBH8 and EEFSEC
1093 measured by qRT-PCR. n = 3. Mean +/- SD of 3 independent replicates. Two-sided unpaired t-test. **p<0.005,
1094 ****p<0.00005
1095 (D) Lys UUU and Glu CUC tRNA levels bound to FLAG-tagged Renilla, wild type and A26P FTSJ1, ALKBH8 and
1096 EEFSEC by qRT-PCR. n = 3. Mean +/- SD of 3 independent replicates.
1097 (E) Quantification of Um34 levels on $tRNA^{Sec}$ in FTSJ1-KO SK-MEL-28 melanoma cells measured by LC-MS/MS.
1098 n=6 from two independent experiments, One-way analysis of variance (ANOVA) followed by Dunnett's tests
1099 for multiple comparisons. **p<0.005, ***p<0.0005
1100 (F) Quantification of Um34 levels on $tRNA^{Sec}$ in FTSJ1-KO SK-MEL-2 melanoma cells measured by LC-MS/MS.
1101 n=4 from two independent experimentd, One-way analysis of variance (ANOVA) followed by Dunnett's tests
1102 for multiple comparisons. **p<0.005, ***p<0.0005
1103 (G) Quantification of Um34 levels in SK-MEL-28 melanoma cells overexpressing wild-type FTSJ1 or A26P-mutant.
1104 n=3. One-way analysis of variance (ANOVA) followed by Dunnett's tests for multiple comparisons.
1105 (H) Quantification of Um34 modification levels on $tRNA^{Sec}$ in Control and FTSJ1 knockout A375 melanoma cells
1106 overexpressing either Renilla luciferase, WT FTSJ1 or mutant A26P FTSJ1 measured by LC-MS/MS. n = 3.
1107 Two-tailed one sample t-test.
1108 (I) Quantification of Um34 modification levels on $tRNA^{Sec}$ in Control and FTSJ1 knockout HeLa cells
1109 overexpressing Renilla luciferase, WT FTSJ1 or mutant A26P FTSJ1 measured by LC-MS/MS. n = 3. Two-tailed
1110 one sample t-test.
1111 (J) Levels of recombinant FTSJ1 from a His- tag purification assessed by Coomassie staining.
1112 (K) Levels of recombinant WDR6 from a His-tag purification assessed by Western blotting for WDR6.
1113
1114 **Extended Figure 3: FTSJ1 regulates recoding of UGA as a selenocysteine**
1115
1116 (A) Levels of selenoprotein transcripts in Control and FTSJ1-KO A375 and SK-MEL-2 melanoma cell lines as
1117 measured by qRT-PCR. Mean +/- SD from 3 independent replicates. Two-way ANOVA followed by Fisher
1118 LSD test for multiple comparisons. *p<0.05, **p<0.005.

(B) Western blot analysis of selenocysteine-containing proteins immunoprecipitated with selenocysteine-specific pulldown. SECISBP2 was used as a non-selenocysteine control protein.

(C) Western blot analysis of selenocysteine-containing proteins immunoprecipitated with selenocysteine-specific pulldown from Control and FTSJ1-KO A375 melanoma cells.

(D) Western blot analysis of selenocysteine-containing proteins immunoprecipitated with selenocysteine-specific pulldown from A375 melanoma cells overexpressing Renilla or FTSJ1.

(E) Global analysis of codon readthrough in FTSJ1 KO A375 melanoma cells compared to control A375 melanoma cells in the presence of selenium (30nM).

**Extended Figure 4: Loss of FTSJ1 causes ribosomal stalling around Sec UGA in a subset of selenoproteins**

(A) Cumulative RPF plots for affected selenoproteins in WT A375 melanoma cells in the absence and presence of selenium (30nM NaSe).

(B) Cumulative RPF plots for affected selenoproteins in Control and FTSJ1 KO melanoma cells in the presence of selenium (30nM NaSe).

**Extended Figure 5: Loss of FTSJ1 has no additional effect on selenoprotein translation in the absence of selenium**

(A) Cumulative RPF plots for unaffected selenoproteins in WT A375 melanoma cells in the absence and presence of selenium (30nM NaSe).

(B) Cumulative RPF plots for unaffected selenoproteins in Control and FTSJ1 KO melanoma cells in the presence of selenium (30nM NaSe).

**Extended Figure 6: Sensitivity to oxidative stress can not be rescued by overexpression of other FTSJ1 tRNA targets**

(A) Mitochondrial ROS levels measured by flow cytometry using CellROXGreen dye in Control and A375 melanoma cells in the presence of selenium (30nM). n=3. Representative of 2 independent experiments. Two-way ANOVA followed by Sidak's multiple comparison test. **$p<0.005$

(B) (B) Cytoplasmic ROS levels measured by flow cytometry using CellROX DeepRed in Control and A375 melanoma cells in the presence of selenium (30nM). n=3. Representative of 2 independent experiments. Two-way ANOVA followed by Sidak's multiple comparison test.***$p<0.0005$, ****$p<0.00005$

(C) Lipid peroxidation levels measured by flow cytometry using BODIPY665/676 in Control and A375 melanoma cells in the presence of selenium (30nM). n=3. Representative of 2 independent experiments. Two-way ANOVA followed by Sidak's multiple comparison test. ****$p<0.00005$

1151 (D) Cell survival of Control vs FTSJ1-KO A375 melanoma cells under increasing concentrations of RSL3 in the
1152 presence of selenium. n=3. Representative of 3 independent experiments. Statistical difference between
1153 IC50 values analyzed by Extra-Sum-of-Squares F-Test.
1154 (E) Cell survival of Control vs FTSJ1-KO A375 melanoma cells under increasing concentrations of RSL3 in the
1155 absence of selenium. n=3. Representative of 3 independent experiments. Statistical difference between
1156 IC50 values analyzed by Extra-Sum-of-Squares F-Test.
1157 (F) Cell survival of Control or FTSJ1-KO A375 melanoma cells with or without FTSJ1 overexpression under
1158 increasing concentrations of RSL3 in the presence of selenium. n=3. Representative of 2 independent
1159 experiments. Statistical difference between IC50 values analyzed by Extra-Sum-of-Squares F-Test.
1160 (G) Cell survival of Control or FTSJ1-KO A375 melanoma cells with or without FTSJ1 overexpression under
1161 increasing concentrations of RSL3 in the absence of selenium. n=3. Representative of 2 independent
1162 experiments. Statistical difference between IC50 values analyzed by Extra-Sum-of-Squares F-Test.
1163 (H) Cell survival of Control, WT $tRNA^{Sec}$ or C65G mutant $tRNA^{Sec}$ overexpressing A375 melanoma cells under
1164 increasing concentrations of pyocyanin in the presence of selenium. n=3. Representative of 3 independent
1165 experiments. Statistical difference between IC50 values analyzed by Extra-Sum-of-Squares F-Test.
1166 (I) Cell survival of Control, WT $tRNA^{Sec}$ or C65G mutant $tRNA^{Sec}$ overexpressing A375 melanoma cells under
1167 increasing concentrations of pyocyanin in the absence of selenium. n=3. Representative of 3 independent
1168 experiments. Statistical difference between IC50 values analyzed by Extra-Sum-of-Squares F-Test.
1169 (J) Quantification of Um34 modification levels on $tRNA^{Sec}$ in Control, WT $tRNA^{Sec}$ or C65G mutant $tRNA^{Sec}$
1170 overexpressing A375 melanoma cells. n=3 individual replicates
1171 (K) Cell survival of Control or FTSJ1-KO A375 melanoma cells with or without overexpression of Phe tRNA with
1172 25uM of pyocyanin in the presence of selenium (30nM NaSe). n=3. Representative of 3 independent
1173 experiments. One-way ANOVA followed by Tukey test for multiple comparisons.
1174 (L) Cell survival of Control or FTSJ1-KO A375 melanoma cells with or without overexpression of Phe tRNA with
1175 25uM of pyocyanin in the absence of selenium. n=3. Representative of 3 independent experiments. One-
1176 way ANOVA followed by Tukey test for multiple comparisons.
1177 (M) Cell survival of Control or FTSJ1-KO A375 melanoma cells with or without overexpression of Trp tRNA with
1178 25uM of pyocyanin in the presence of selenium (30nM NaSe). n=3. Representative of 3 independent
1179 experiments. One-way ANOVA followed by Tukey test for multiple comparisons.
1180 (N) Cell survival of Control or FTSJ1-KO A375 melanoma cells with or without overexpression of Trp tRNA with
1181 25uM of pyocyanin in the absence of selenium. n=3. Representative of 3 independent experiments. One-
1182 way ANOVA followed by Tukey test for multiple comparisons.

1183

1184 **Extended Figure 7: FTSJ1 overexpression can partially rescue sensitivity to oxidative stress while other tRNA**
1185 **targets of FTSJ1 can not**

1186 (A) Cell survival of Control and FTSJ1-KO A375 melanoma cells with and without FTSJ1-overexpression under
1187 increasing concentrations of pyocyanin in the presence of selenium (30nM NaSe) as measured by Cell Titer
1188 Glo. n=3. Representative of 3 independent experiments. Statistical difference between IC50 values analyzed
1189 by Extra-Sum-of-Squares F-Test.

1190 (B) Cell survival of Control and FTSJ1-KO A375 melanoma cells with and without FTSJ1-overexpression under
1191 increasing concentrations of pyocyanin in the absence of selenium as measured by Cell Titer Glo. n=3.
1192 Representative of 3 independent experiments. Statistical difference between IC50 values analyzed by Extra-
1193 Sum-of-Squares F-Test.

1194 (C) Cell survival of Control or FTSJ1-KO A375 melanoma cells with or without overexpression Phe tRNA under
1195 increasing concentrations of pyocyanin in the presence of selenium (30nM NaSe). n=3. Representative of 3
1196 independent experiments. Statistical difference between IC50 values analyzed by Extra-Sum-of-Squares F-
1197 Test.

1198 (D) Cell survival of Control or FTSJ1-KO A375 melanoma cells with or without overexpression Phe tRNA under
1199 increasing concentrations of pyocyanin in the absence of selenium. n=3. Representative of 3 independent
1200 experiments. Statistical difference between IC50 values analyzed by Extra-Sum-of-Squares F-Test.

1201 (E) Cell survival of Control or FTSJ1-KO A375 melanoma cells with or without overexpression Trp tRNA under
1202 increasing concentrations of pyocyanin in the presence of selenium(30nM NaSe). n=3. Representative of 3
1203 independent experiments. Statistical difference between IC50 values analyzed by Extra-Sum-of-Squares F-
1204 Test.

1205 (F) Cell survival of Control or FTSJ1-KO A375 melanoma cells with or without overexpression Trp tRNA under
1206 increasing concentrations of pyocyanin in the absence of selenium. n=3. Representative of 3 independent
1207 experiments. Statistical difference between IC50 values analyzed by Extra-Sum-of-Squares F-Test.

1208

1209 **Extended Figure 8: Metastases show translational upregulation of selenoproteins**

1210 (A) Transcript levels of selenoproteins in primary tumors compared to macro and micro metastatic nodules,
1211 isolated from NSG mice transplanted with patient-derived melanomas M481 and M405, as measured by RNA-
1212 sequencing, quantified as a z-score.

1213 (B) UGA recoding efficiency of detected selenoproteins in primary tumors compared to metastatic nodules from
1214 NSG mice transplanted with patient-derived melanoma, M405, as measured by ribosomal profiling.

1215 (C) Levels of precursor $tRNA^{Sec}$ in Primary, macro and micrometastatic nodules from patient-derived M405
1216 melanoma measured by qRT-PCR. Mean +/- SD from 3 independent replicates. One-way analysis of variance
1217 (ANOVAs) followed by Dunnett's tests for multiple comparisons. *p<0.05
1218 (D) Levels of mature $tRNA^{Sec}$ in Primary, macro and micrometastatic nodules from patient-derived M405
1219 melanoma measured by qRT-PCR. Mean +/- SD from 3 independent replicates. One-way analysis of variance
1220 (ANOVAs) followed by Dunnett's tests for multiple comparisons. *p<0.05
1221 (E) Levels of gROSI variant levels with No UTR, GPX1 SECIS or GPX4 SECIS in primary and metastatic nodules,
1222 formed by A375 melanoma cells transplanted into NSG mice, as measured by immunofluorescence staining
1223 for GFP expression.
1224 (F) Quantification of the GFP signal from gROSI variants shown in (E).
1225
1226 **Extended Figure 9: Loss of FTSJ1 affects metastatic colonization but has no effect on lipid peroxidation levels**
1227 (A) Western blot analysis of control and FTSJ1 KO A375 melanoma primary tumors.
1228 (B) qRT-PCR analysis of FTSJ1 targeting shRNAs in A375 melanoma cells. Mean +/- SD from 3 independent
1229 replicates. One-way analysis of variance (ANOVAs) followed by Dunnett's tests for multiple comparisons.
1230 *p<0.05
1231 (C) Western blot analysis of FTSJ1 targeting shRNAs in MeWo melanoma cells.
1232 (D) Subcutaneous tumor growth of MeWo cells transplanted into mice expressing Control or shRNA5 targeting
1233 FTSJ1. n=5 mice. Representative of 3 independent experiments.
1234 (E) Western blot analysis of M405 tumors with either control or FTSJ1-targeting shRNAs.
1235 (F) Western blot analysis of M481 tumors with either control or FTSJ1-taregting shRNAs.
1236 (G) Western blot analysis of A375 melanoma tumors overexpressing Control Renilla luciferase or FTSJ1.
1237 (H) Western blot analysis of M481 melanoma tumors overexpressing Control Renilla luciferase or FTSJ1.
1238 (I) Growth of subcutaneous tumors in mice transplanted from patient-derived melanoma, M405, overexpressing
1239 either Renilla luciferase or FTSJ1 ORF. n=5. Representative of 2 independent experiments.
1240 (J) Total metastatic burden in visceral organs of mice transplanted with patient-derived melanoma, M405,
1241 overexpressing either Renilla luciferase or FTSJ1 ORF. n = 10 mice from 2 independent experiments.
1242 Statistical significance assessed by one-way analysis of variance (ANOVAs) followed by Dunnett's tests for
1243 multiple comparisons.
1244 (K) Total metastatic burden in visceral organs of mice transplanted intravenously with either Control or FTSJ1
1245 KO A375 melanoma cells. n=9-10 mice.

1246 (L) Total metastatic burden in visceral organs of mice transplanted intravenously with either Control or FTSJ1
1247 overexpressing A375 melanoma cells. n=7-10 mice.
1248 (M) Quantification of 4-HNE immunofluorescent staining of subcutaneous tumors expressing either control
1249 shRNA or FTSJ1-targeting shRNAs. n=3 mice.
1250 (N) Flow cytometry analysis of lipid peroxidation levels in subcutaneous tumors overexpressing Control Renilla
1251 luciferase or FTSJ1, using BODIPY dye. n=10 mice.
1252
1253

# Figure 1

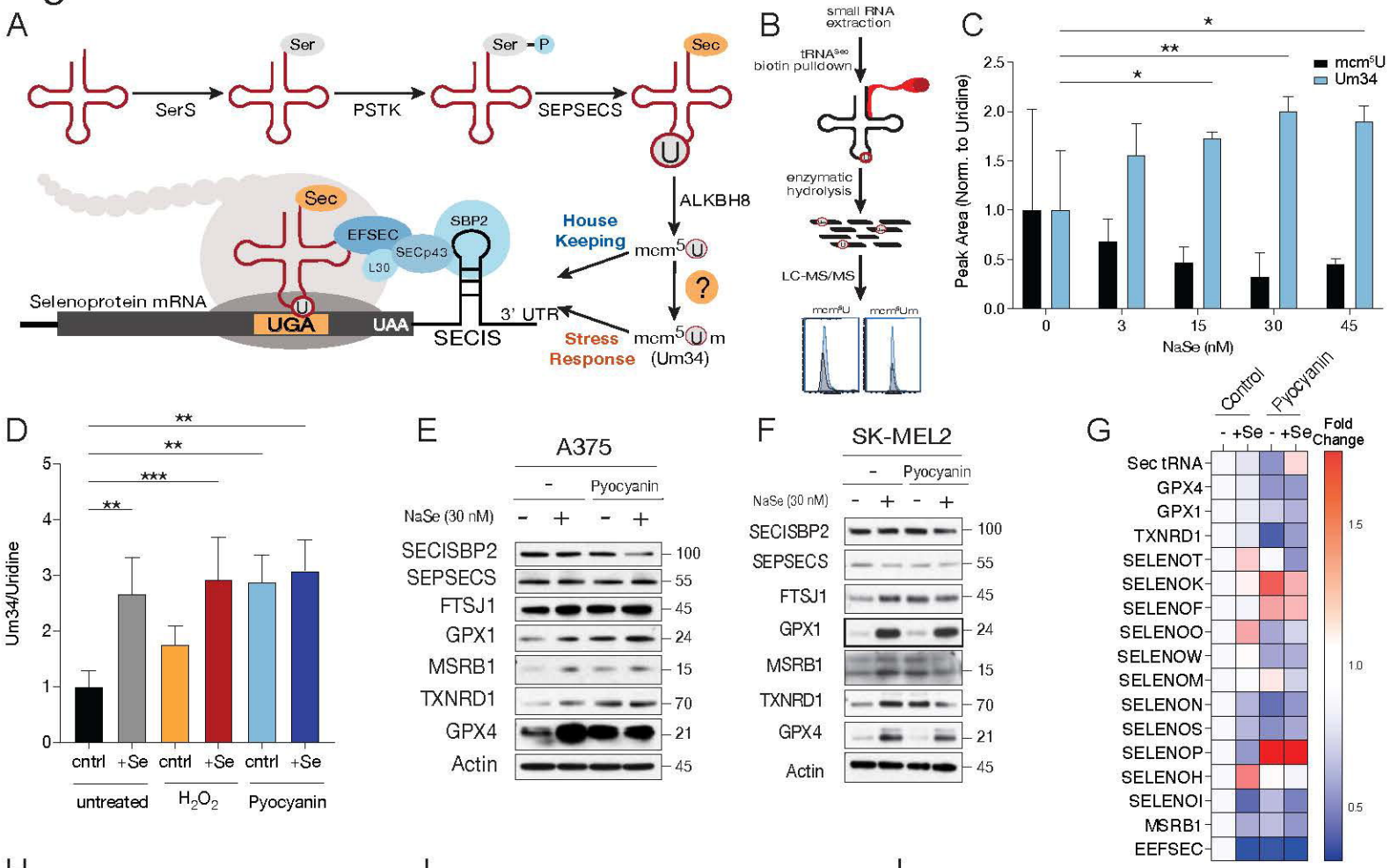


**Figure 1: Selenoprotein translation and tRNASec Um34 levels increase in response to oxidative stress**

(A) Schematic of selenocysteine biosynthesis and selenoprotein translation. Sec is synthesized on its tRNA. The tRNA is then modified at the wobble uridine and the Sec translation complex associated with the SECIS allows for co-translational readthrough of UGA stop codon.

(B) Schematic of tRNASec isolation and Um34 modification analysis

(C) Quantification of Um34 and mcm5U levels in A375 melanoma cells grown in DMEM/F12 medium supplemented with increasing concentrations of selenium measured by LC-MS/MS. n = 2 independent experiments, Mean +/- SD. Statistical significance assessed by two-way analysis of variance (ANOVAs) followed by Fisher LSD test for multiple comparisons. *p<0.05, **p<0.005.

(D) Quantification of Um34 modification levels on tRNASec in A375 melanoma cells treated with pro-oxidant H2O2 (100μM) pyocyanin (10μM) in DMEM/F12 media in the presence or absence of 30nM NaSe. n = 2 independent experiments, Mean +/- SD. Statistical significance assessed by one-way ANOVA followed by Fisher LSD test for multiple comparisons. **p<0.005, ***p<0.0005.

(E) Levels of selenoproteins in A375 melanoma cells and (F) SK-MEL-2 melanoma cells after treatment with NaSe (30nM) and pyocyanin (10uM). Representative experiments shown.

(G) Transcript levels of selenoproteins in A375 melanoma cells after treatment with NaSe and pyocyanin measured by qRT-PCR. n=3 independent replicates.

(H) Schematic of the split-seleno-GFP reporter - GFP Reporter Of Selenocysteine Insertion (gROSI).

(I) Flow cytometry analysis of split-seleno-GFP reporter (gROSI) expression with different combinations of stop codons UAA or UGA and with No UTR or SECIS from GPX4, in the presence or absence of selenium (30nM NaSe) in A375 melanoma cells. n = 3, Mean +/- SD of 3 independent replicates; representative experiment shown; two-sided unpaired t-test, ***p<0.0005

(J) Flow cytometry analysis of GFP fluorescence of gROSI variants without a 3'UTR, with a GPX4 SECIS and with a GPX1 SECIS treated with Pyocyanin (10uM) and NaSe (30nM). n=2 independent experiment, Mean +/- SD. Statistical significance measured by two-way ANOVA followed by Fisher LSD test for multiple comparisons. **p<0.005, ****p<0.00005.

# Figure 2

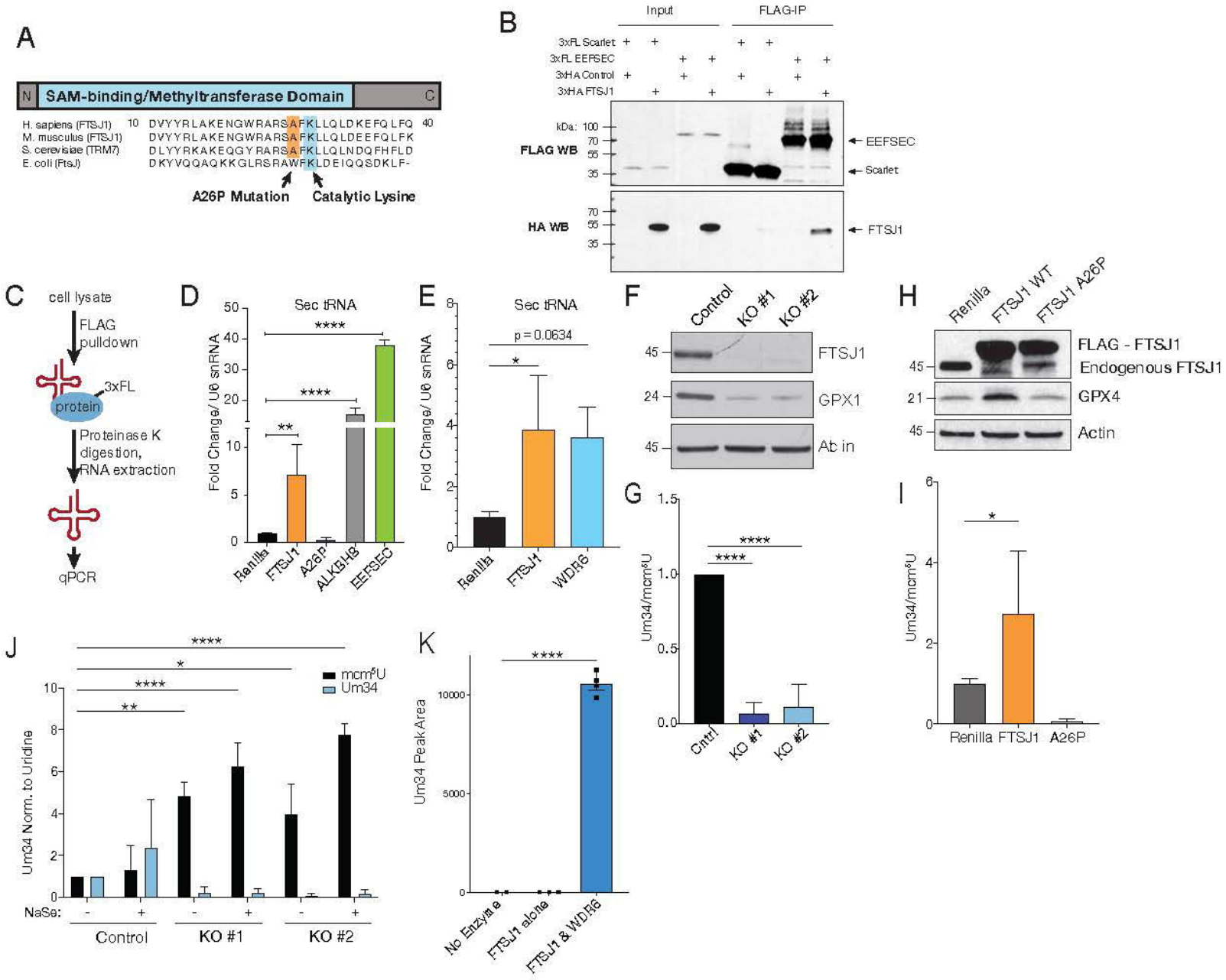


**Figure 2: FTSJ1 is the mcm$^5$Um (Um34) methyltransferase for tRNA$^{Sec}$**

(A) Alignment schematic of FTSJ1 and its homologs, highlighting a catalytic lysine and the catalytically dead A26P mutation.
(B) Co-immunoprecipitation assay of the interaction between HA-tagged FTSJ1 and FLAG-tagged component of selenocysteine machinery, EEFSEC, compared to FLAG-tagged Scarlet-expressing control vector co-expressed in A375 melanoma cells. Representative experiment shown.
(C) Schematic of RNA-immunoprecipitation.
(D) Levels of tRNA$^{Sec}$ bound to FLAG-tagged Renilla, wild type and A26P-mutant FTSJ1, ALKBH8 and EEFSEC by qRT-PCR. n = 3. Mean +/- SD of 3 independent replicates. Two-sided unpaired t-test. **p<0.005, ****p<0.00005
(E) Levels of tRNASec bound to FLAG-tagged Renilla, FTSJ1 and WDR6 by qRT-PCR. n=3. Mean +/- SD of 3 independent replicates. Two-sided unpaired t-test.
(F) Western blot analysis of FTSJ1 and selenoprotein GPX1 levels in control and FTSJ1 knockout A375 melanoma cell lines.
(G) Quantification of Um34 modification levels on tRNASec from control and FTSJ1 knockout A375 melanoma cell lines measured by LC-MS/MS. n = 3 independent experiments. One-way analysis of variance (ANOVA) followed by Dunnett's tests for multiple comparisons. ****p<0.0001
(H) Western blot analysis of overexpression of control Renilla luciferase, wild type and mutant A26P FTSJ1 and selenoprotein GPX4 in A375 melanoma cell lines.
(I) Quantification of Um34 modification levels on tRNASec in A375 melanoma cells overexpressing control Renilla luciferase, wild type and A26P mutant FTSJ1 measured by LC-MS/MS. n = 2 independent experiments. Statistical significance assessed by one-way analysis of variance (ANOVA) followed by Dunnett's tests for multiple comparisons. *p<0.05
(J) Quantification of Um34 and mcm5U levels on tRNASec in Control and FTSJ1 knockout A375 melanoma cells grown in DMEM/F12 medium with and without selenium (30nM) measured by LC-MS/MS. n=2 independent experiments. Two-way analysis of variance (ANOVA) followed by Dunnett's tests for multiple comparisons. *p<0.05, **<0.005, ****<0.00005.
(K) Quantification of Um34 levels on tRNASec in an in vitro methyltransferase assay measured by LC-MS/MS. n=2 independent experiments. One-way analysis of variance (ANOVA) followed by Dunnett's tests for multiple comparisons. ****p<0.0001.

# Figure 3

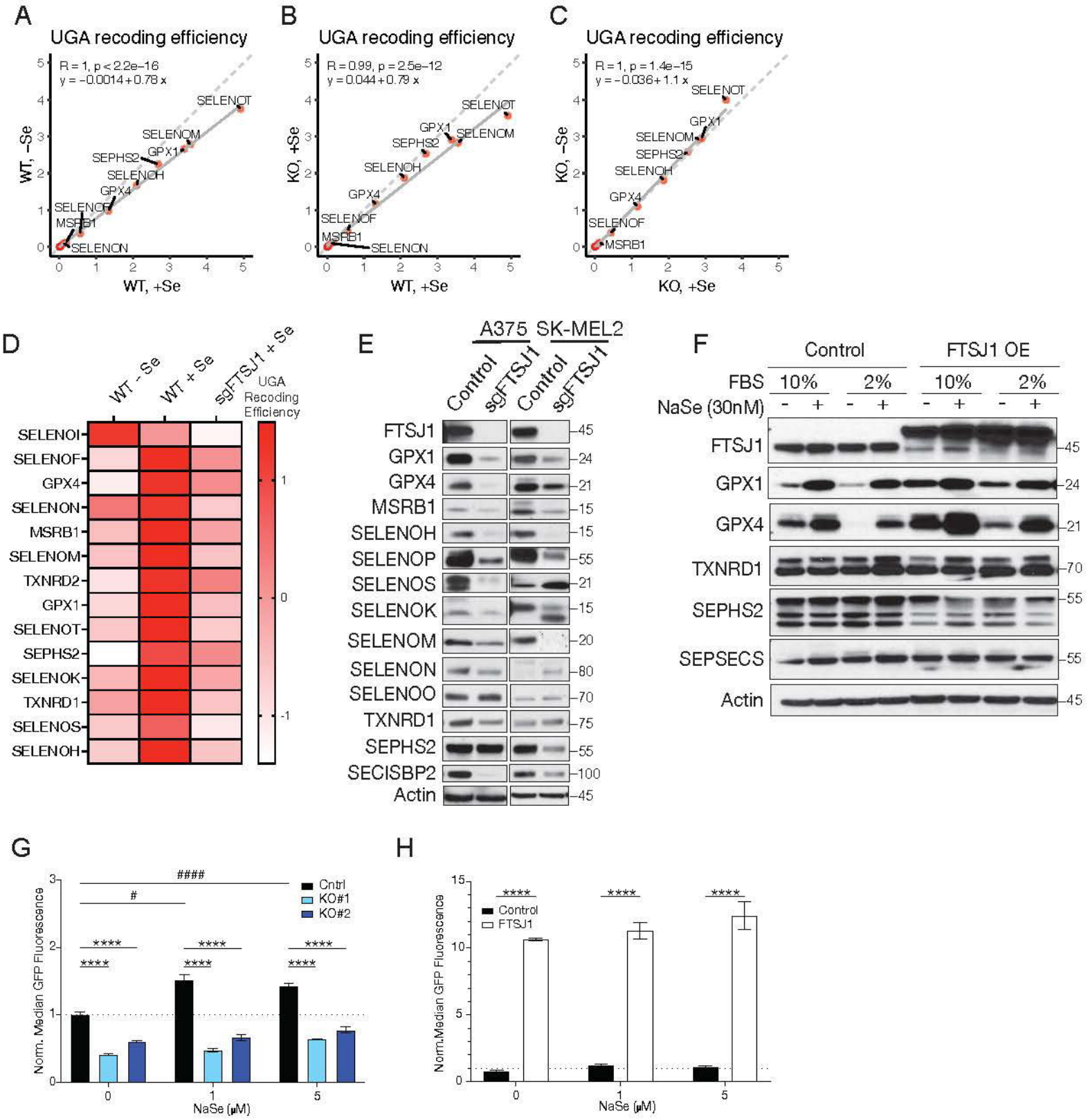
A
UGA recoding efficiency
R = 1, p < 2.2e−16
y = −0.0014 + 0.78 x
WT, −Se
WT, +Se
SELENOT
SELENOM
GPX1
SEPHS2
SELENOH
GPX4
SELENOF
MSRB1
SELENON
B
UGA recoding efficiency
R = 0.99, p = 2.5e−12
y = 0.044 + 0.79 x
KO, +Se
WT, +Se
C
UGA recoding efficiency
R = 1, p = 1.4e−15
y = −0.036 + 1.1 x
KO, −Se
KO, +Se
D
WT - Se
WT + Se
sgFTSJ1 + Se
UGA Recoding Efficiency
SELENOI
SELENOF
GPX4
SELENON
MSRB1
SELENOM
TXNRD2
GPX1
SELENOT
SEPHS2
SELENOK
TXNRD1
SELENOS
SELENOH
E
A375
SK-MEL2
Control
sgFTSJ1
Control
sgFTSJ1
FTSJ1
GPX1
GPX4
MSRB1
SELENOH
SELENOP
SELENOS
SELENOK
SELENOM
SELENON
SELENOO
TXNRD1
SEPHS2
SECISBP2
Actin
F
Control
FTSJ1 OE
FBS
10%
2%
10%
2%
NaSe (30nM)
FTSJ1
GPX1
GPX4
TXNRD1
SEPHS2
SEPSECS
Actin
G
Norm. Median GFP Fluorescence
Cntrl
KO#1
KO#2
NaSe (μM)
H
Norm.Median GFP Fluorescence
Control
FTSJ1
NaSe (μM)

**Figure 3: Um34 regulates UGA recoding efficiency in a subset of selenoproteins involved in oxidative stress**

(A) UGA Recoding Efficiency (Ratio of RPF 3' to Sec UGA/RPF 5' to Sec UGA) of selenoproteins in WT A375 melanoma cells with and without selenium (30nM NasSe).
(B) UGA Recoding Efficiency (Ratio of RPF 3' to Sec UGA/RPF 5' to Sec UGA) of selenoproteins in Control and FTSJ1 KO A375 melanoma cells in the presence of selenium (30nM NaSe).
(C) UGA Recoding Efficiency (Ratio of RPF 3' to Sec UGA/RPF 5' to Sec UGA) of selenoproteins in FTSJ1 KO A375 melanoma cells with and without selenium (30nM NaSe).
(D) Z-score values of UGA Recoding efficiency comparing WT A375 melanoma cells without selenium, WT A375 melanoma cells with selenium (30nM NaSe) and FTSJ1 KO A375 melanoma cells with selenium (30nM NaSe).
(E) Western blot analysis of selenoprotein levels in Control and FTSJ1-KO A375 and SK-MEL-2 melanoma cells grown in normal (10% FBS) media.
(F) Western blot analysis of selenoproteins in normal (10% FBS), selenium-depleted (2% FBS) and supplemented conditions (10% + 30nM NaSe and 2% + 30nM NaSe) in A375 melanoma cell line overexpressing either control Renilla or FTSJ1.
(G) Flow cytometry analysis of seleno-GFP reporter (gROSI) expression in control and FTSJ1 knockout A375 melanoma cells with and without selenium (30nM). Mean +/- SD of 3 independent replicates; representative experiment shown; One-way analysis of variance (ANOVA) followed by Dunnett's tests for multiple comparisons. $^{**}p<0.005$, $^{****}p<0.00005$.
(H) Flow cytometry analysis of seleno-GFP reporter (gROSI) expression in control Renilla-overexpressing or FTSJ1-overexpressing A375 melanoma cells. Mean +/- SD of 3 independent replicates; representative experiment shown; One-way analysis of variance (ANOVA) followed by Dunnett's tests for multiple comparisons. $^{****}p<0.00005$.

# Figure 4

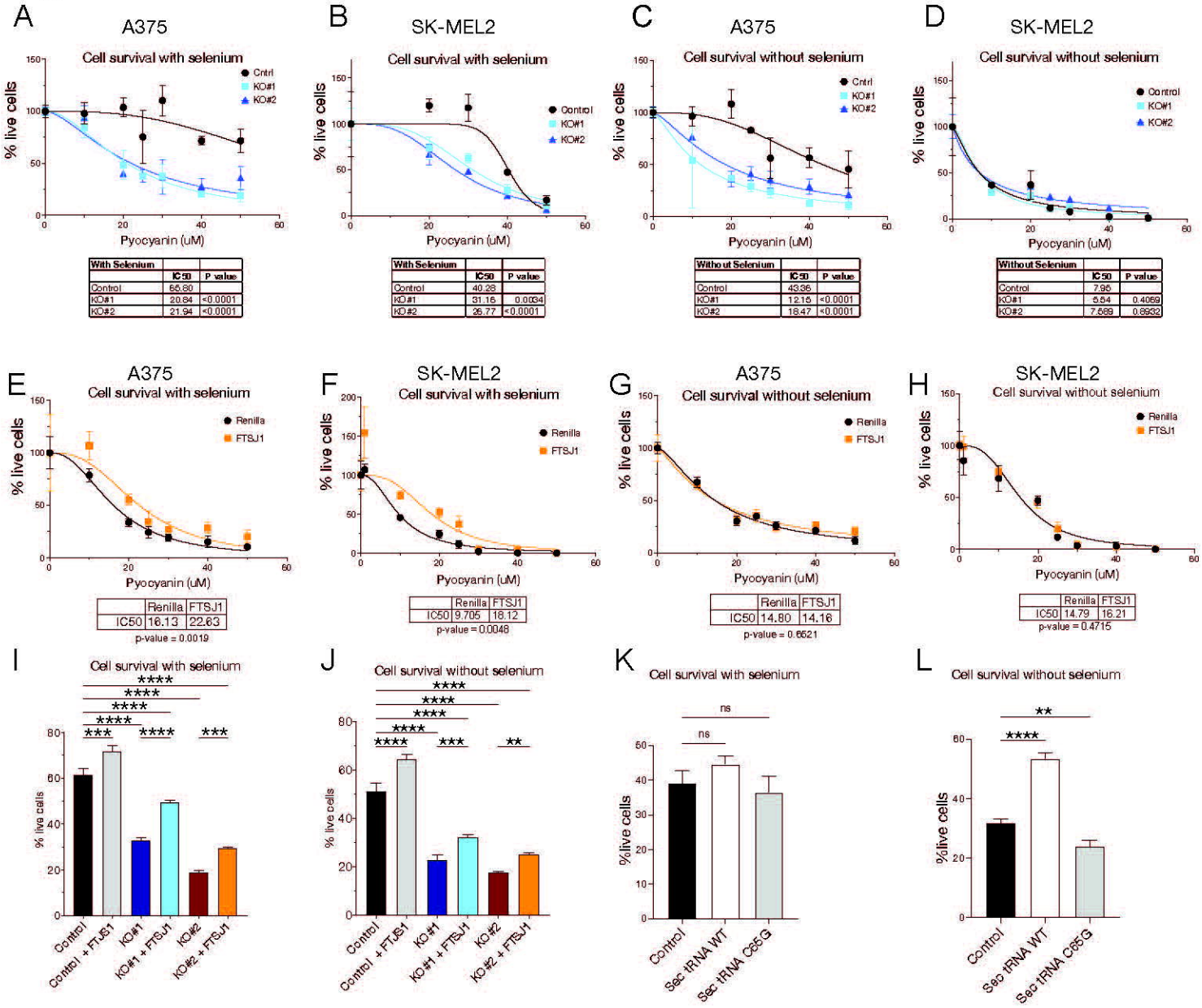


| With Selenium | | |
|---|---|---|
| | IC50 | P value |
| Control | 55.80 | |
| KO#1 | 20.84 | <0.0001 |
| KO#2 | 21.94 | <0.0001 |

| With Selenium | | |
|---|---|---|
| | IC50 | P value |
| Control | 40.28 | |
| KO#1 | 31.16 | 0.0034 |
| KO#2 | 26.77 | <0.0001 |

| Without Selenium | | |
|---|---|---|
| | IC50 | P value |
| Control | 43.36 | |
| KO#1 | 12.15 | <0.0001 |
| KO#2 | 18.47 | <0.0001 |

| Without Selenium | | |
|---|---|---|
| | IC50 | P value |
| Control | 7.95 | |
| KO#1 | 5.54 | 0.4069 |
| KO#2 | 7.569 | 0.8932 |

| | Renilla | FTSJ1 |
|---|---|---|
| IC50 | 16.13 | 22.63 |

p-value = 0.0019

| | Renilla | FTSJ1 |
|---|---|---|
| IC50 | 9.705 | 18.12 |

p-value = 0.0048

| | Renilla | FTSJ1 |
|---|---|---|
| IC50 | 14.80 | 14.16 |

p-value = 0.6521

| | Renilla | FTSJ1 |
|---|---|---|
| IC50 | 14.79 | 16.21 |

p-value = 0.4715

**Figure 4: Um34 modification protects cancer cells from oxidative stress**

(A) Cell survival of Control and FTSJ1-KO A375 melanoma cells under pyocyanin treatment in selenium-supplemented conditions (30nM NaSe) as measured by Cell Titer Glo. n=3. Representative of 4 independent experiments. Statistical difference between IC50 values analyzed by Extra-Sum-of-Squares F-Test.
(B) Cell survival of Control and FTSJ1-KO SK-MEL-2 melanoma cells under pyocyanin treatment in selenium-supplemented conditions (30nM NaSe) as measured by Cell Titer Glo. n=3. Representative of 3 independent experiments. Statistical difference between IC50 values analyzed by Extra-Sum-of-Squares F-Test.
(C) Cell survival of Control and FTSJ1-KO A375 melanoma cells under pyocyanin treatment in selenium-depleted conditions as measured by Cell Titer Glo. n=3. Representative of 4 independent experiments. Statistical difference between IC50 values analyzed by Extra-Sum-of-Squares F-Test.
(D) Cell survival of Control and FTSJ1-KO SK-MEL-2 melanoma cells under pyocyanin treatment in selenium-depleted conditions as measured by Cell Titer Glo. n=3. Representative of 3 independent experiments. Statistical difference between IC50 values analyzed by Extra-Sum-of-Squares F-Test.
(E) Cell survival of Control and FTSJ1 overexpressing A375 melanoma cells under pyocyanin treatment in selenium-supplemented conditions (30nM NaSe) as measured by Cell Titer Glo. n=3. Representative of 4 independent experiments. Statistical difference between IC50 values analyzed by Extra-Sum-of-Squares F-Test.
(F) Cell survival of Control and FTSJ1 overexpressing SK-MEL-2 melanoma cells under pyocyanin treatment in selenium-supplemented conditions (30nM NaSe) as measured by Cell Titer Glo. n=3. Representative of 3 independent experiments. Statistical difference between IC50 values analyzed by Extra-Sum-of-Squares F-Test.
(G) Cell survival of Control and FTSJ1 overexpressing A375 melanoma cells under pyocyanin treatment in selenium-depleted conditions as measured by Cell Titer Glo. n=3. Representative of 4 independent experiments. Statistical difference between IC50 values analyzed by Extra-Sum-of-Squares F-Test.
(H) Cell survival of Control and FTSJ1 overexpressing SK-MEL-2 melanoma cells under pyocyanin treatment in selenium-depleted conditions as measured by Cell Titer Glo. n=3. Representative of 3 independent experiments. Statistical difference between IC50 values analyzed by Extra-Sum-of-Squares F-Test.
(I) Cell survival of Control and FTSJ1-KO A375 melanoma cells with and without FTSJ1-overexpression treated with 25 uM Pyocyanin in the presence of selenium (30nM NaSe) as measured by Cell Titer Glo. n=3. Representative of 3 independent experiments. One-way ANOVA followed by Tukey test for multiple comparisons.
(J) Cell survival of Control and FTSJ1-KO A375 melanoma cells with and without FTSJ1-overexpression treated with 25 uM of Pyocyanin in the absence of selenium as measured by Cell Titer Glo. n=3. Representative of 3 independent experiments. One-way ANOVA followed by Tukey test for multiple comparisons.
(K) Cell survival of Control, WT tRNASec and C65G-mutant tRNASec overexpressing A375 melanoma cells treated with 25uM of Pyocyanin in the presence of selenium (30nM NaSe) as measured by Cell Titer Glo. n=3. Representative of 3 independent experiments. One-way ANOVA followed by Dunnett test for multiple comparisons.
(L) Cell survival of Control, WT tRNASec and C65G-mutant tRNASec overexpressing A375 melanoma cells treated with 25uM of Pyocyanin in the absence of selenium as measured by Cell Titer Glo. n=3. Representative of 3 independent experiments. One-way ANOVA followed by Dunnett test for multiple comparisons.

# Figure 5

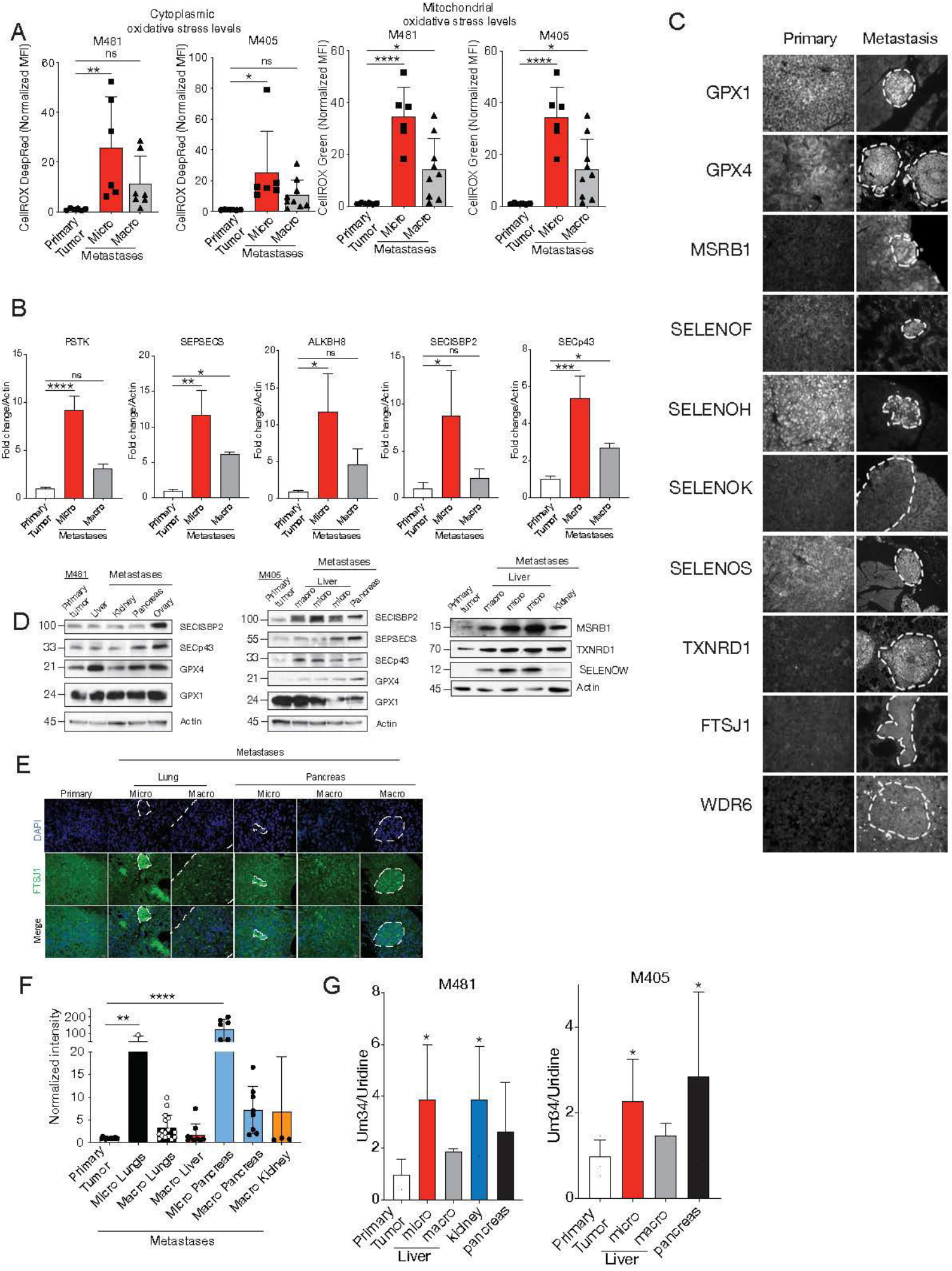
A
Cytoplasmic oxidative stress levels
Mitochondrial oxidative stress levels
M481
M405
CellROX DeepRed (Normalized MFI)
CellROX Green (Normalized MFI)
Primary Tumor
Micro
Macro
Metastases
B
PSTK
SEPSECS
ALKBH8
SECISBP2
SECp43
Fold change/Actin
C
Primary
Metastasis
GPX1
GPX4
MSRB1
SELENOF
SELENOH
SELENOK
SELENOS
TXNRD1
FTSJ1
WDR6
D
M481
M405
Primary tumor
Liver
Kidney
Pancreas
Ovary
SECISBP2
SECp43
GPX4
GPX1
Actin
SEPSECS
MSRB1
TXNRD1
SELENOW
E
Lung
Pancreas
DAPI
FTSJ1
Merge
F
Normalized intensity
Primary Tumor
Micro Lungs
Macro Lungs
Macro Liver
Micro Pancreas
Macro Pancreas
Macro Kidney
G
Um34/Uridine
Primary Tumor
micro
macro
kidney
pancreas

**Figure 5: Micrometastases experience high levels of stress and increase selenocysteine biosynthesis.**

(A) Levels of reactive oxygen species (ROS) in subcutaneous tumors vs micro and macrometastatic nodules from NSG mice transplanted with two different patient melanomas, M481 and M405, measured by flow cytometry with fluorescent dyes. CellROX DeepRed was used measure cytoplasmic oxidative stress and CellROX Green was used to measure mitochondrial oxidative stress levels. n = 6 - 9 mice from 2 - 3 independent experiments). Statistical significance assessed by one-way analysis of variance (ANOVAs) followed by Dunnett's tests for multiple comparisons. $^{*}p<0.05$, $^{**}p<0.005$, $^{***}p<0.0005$, $^{****}p<0.00005$.

(B) Transcript levels of selenocysteine biosynthesis machinery in subcutaneous tumors vs micro and macrometastatic nodules from NSG mice transplanted with patient-derived melanoma, M481, measured by qRT-PCR. Mean +/- SD of 3 independent replicates; One-way analysis of variance (ANOVAs) followed by Dunnett's tests for multiple comparisons. $^{*}p<0.05$, $^{**}p<0.005$, $^{***}p<0.0005$, $^{****}p<0.00005$.

(C) Levels of selenoproteins, FTSJ1 and WDR6 in metastases compared to primary tumor tissues from NSG mice transplanted with patient-derived melanoma, M405, measured by immunofluorescent staining.

(D) Levels of selenoproteins and components of selenocysteine biosynthesis machinery in metastases compared to primary tumor from NSG mice transplanted with patient-derived melanomas, M405 and M481, as measured by western blotting.

(E) Levels of FTSJ1 in subcutaneous vs micro vs macrometastatic nodules from NSG mice transplanted with Mewo melanoma cell lines, measured by immunofluorescence.

(F) Quantification of data shown in (H). Two-tailed one sample t-test. $^{**}p<0.005$, $^{****}p<0.00005$

(G) Levels of Um34 modification in subcutaneous tumors vs metastatic nodules from NSG mice transplanted with two different patient-derived melanomas, M405 and M481, measured by LC-MS/MS analysis of modified tRNASec nucleosides. n=3 mice for each patient-derived melanoma. One-way ANOVA (Kruskal-Wallis test) followed by Dunn's test for multiple comparisons. $^{*}p<0.05$.

# Figure 6

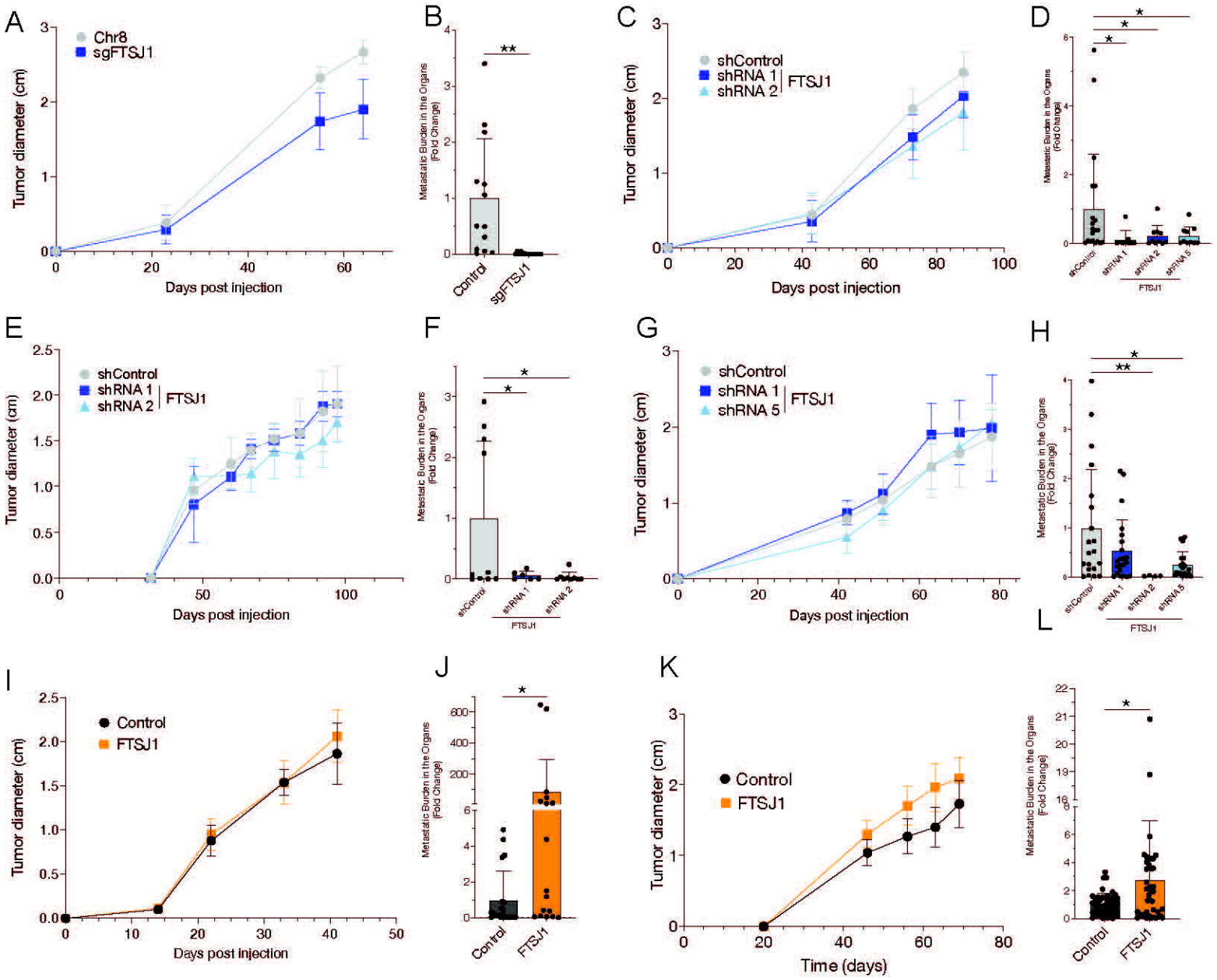


**Figure 6: tRNASec Um34 modification is necessary and sufficient for metastasis in vivo**

(A) Subcutaneous tumor growth in mice transplanted with either Control or FTSJ1 KO A375 melanoma cells. Data reflect 3 independent experiments but only one representative experiment is shown.
(B) Total metastatic burden in the visceral organs of mice subcutaneously transplanted with either Control of FTSJ1 KO A375 melanoma cells measured by bioluminescence after 7 weeks. n= 13-15 mice from 3 independent experiments. Mann-Whitney t-test **p <0.005
(C) Subcutaneous tumor growth in mice transplanted with either Control or FTSJ1 KD MeWo melanoma cells. Data reflect 3 independent experiments but only one representative experiment is shown.
(D) Total metastatic burden in the visceral organs of mice subcutaneously transplanted with either Control of FTSJ1 KD MeWo melanoma cells measured by bioluminescence. n= 13-15 mice from 3 independent experiments. One-way analysis of variance (ANOVA) followed by unpaired t with Welch's correction. *p<0.05
(E) Growth of subcutaneous tumors in mice transplanted with a patient-derived melanoma, M405, expressing either control shRNA or FTSJ1-targeting shRNAs. n=10 mice One-way analysis of variance (ANOVA) followed by unpaired t with Welch's correction. *p<0.05
(F) Total metastatic burden in visceral organs of mice transplanted with a patient-derived melanoma, M405, expressing either control shRNA or FTSJ1-targeting shRNAs. n=10 mice. One-way analysis of variance (ANOVA) followed by unpaired t with Welch's correction. *p<0.05
(G) Growth of subcutaneous tumors in mice transplanted from patient-derived melanoma, M481, expressing either Control shRNA or FTSJ1 targeting shRNAs.
(H) Total metastatic burden in visceral organs of mice transplanted with patient-derived melanoma, M481, expressing either Control shRNA or FTSJ1 targeting shRNAs. n = 20 mice. One-way analysis of variance (ANOVA) followed by unpaired t with Welch's correction. *p<0.05, **p<0.005
(I) Subcutaneous tumor growth in mice transplanted with either Control or FTSJ1 overexpressing A375 melanoma cells. Data reflect 3 independent experiments but only on representative experiment is shown.
(J) Total metastatic burden in the visceral organs of mice subcutaneously transplanted with either Control or FTSJ1 overexpressing A375 melanoma cells measured by bioluminescence after 7 weeks. n= 13-15 mice from 3 independent experiments. Mann-Whitney t-test. *p <0.05
(K) Growth of subcutaneous tumors in mice transplanted from patient-derived melanoma, M481, overexpressing either Renilla luciferase or FTSJ1 ORF.
(L) Total metastatic burden in visceral organs of mice transplanted with patient-derived melanoma, M481, overexpressing either Renilla luciferase or FTSJ1 ORF. n = 20 mice. Mann-Whitney t-test. *p <0.05

# Extended Figure 1

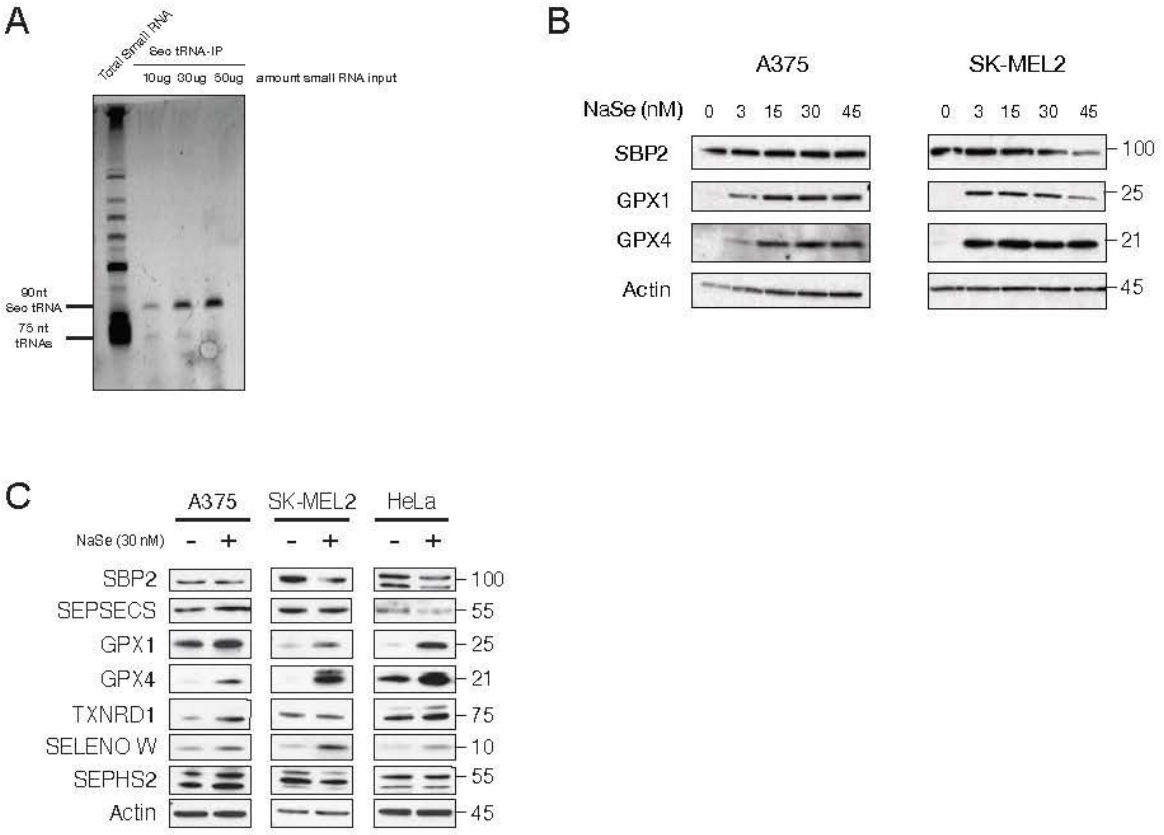


**Extended Figure 1: Extracellular selenium drives translation of selenoproteins**

(A) Levels and purity of tRNASec analyzed by SDS-PAGE gel after biotinylated pull-down from increasing amounts of small RNA input fraction.
(B) Western blot analysis of selenocysteine proteins GPX1 and GPX4 in DMEM/F12 media (0nM Se) with increasing amounts of selenium in A375 and SK-MEL2 cells.
(C) Western blot analysis of selenocysteine proteins TXNRD1, GPX1, GPX4, and SELENO W in DMEM/F12 media (0nM Se) with or without selenium supplementation (30nM NaSe) in A375, SK-MEL2 and HeLa cells.

# Extended Figure 2

A

| Gene Symbol | Description | Ren IP PSMs | EEPSEC IP PSMs | TOTAL PSMs |
|---|---|---|---|---|
| NSUN2 | tRNA (cytosine(34)-C(5))-methyltransferase | 53 | 80 | 133 |
| FTSJ3 | pre-rRNA 2'-O-ribose RNA methyltransferase FTSJ3 | 15 | 39 | 54 |
| NOP2 | Probable 28S rRNA (cytosine(4447)-C(5))-methyltransferase | 12 | 33 | 45 |
| TRMT2A | tRNA (uracil-5-)-methyltransferase homolog A | 9 | 29 | 38 |
| EMG1 | Ribosomal RNA small subunit methyltransferase NEP1 | 17 | 23 | 40 |
| FBL | rRNA 2'-O-methyltransferase fibrillarin | 14 | 19 | 33 |
| MRM3 | rRNA methyltransferase 3, mitochondrial | 10 | 17 | 27 |
| CMTR1 | Cap-specific mRNA (nucleoside-2'-O-)-methyltransferase 1 | 4 | 16 | 19 |
| NSUN5 | Probable 28S rRNA (cytosine-C(5))-methyltransferase | 8 | 15 | 23 |
| TRMT6 | tRNA (adenine(58)-N(1))-methyltransferase non-catalytic subunit TRM6 | 1 | 12 | 13 |
| BUD23 | Probable 18S rRNA (guanine-N(7))-methyltransferase | 11 | 12 | 23 |
| METTL16 | RNA N6-adenosine-methyltransferase METTL16 | 7 | 10 | 17 |
| FTSJ1 | Pulsive rRNA (cytosine(32)-2'-O-)-methyltransferase | 4 | 9 | 13 |
| TRMT1 | tRNA (guanine(26)-N(2))-dimethyltransferase | 10 | 9 | 19 |
| RNMT | mRNA cap guanine-N7 methyltransferase | 5 | 7 | 12 |
| ZCCHC4 | rRNA N6-adenosine-methyltransferase ZCCHC4 | 2 | 6 | 8 |
| TRMT61A | tRNA (adenine(58)-N(1))-methyltransferase catalytic subunit TRMT61A | 0 | 5 | 5 |
| NSUN4 | 5-methylcytosine rRNA methyltransferase | 4 | 2 | 6 |
| TRMT10C | tRNA methyltransferase 10 homolog C | 3 | 0 | 3 |

B

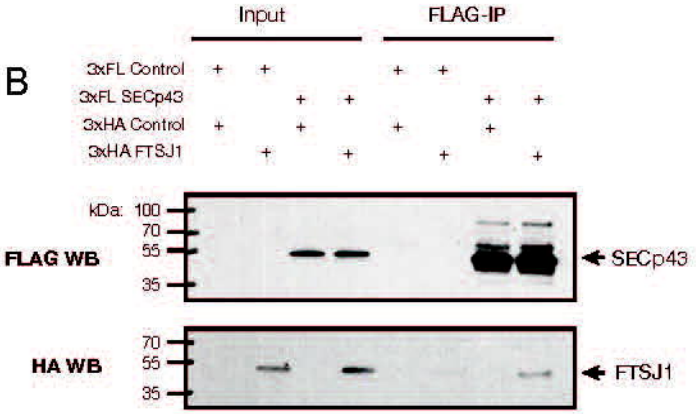


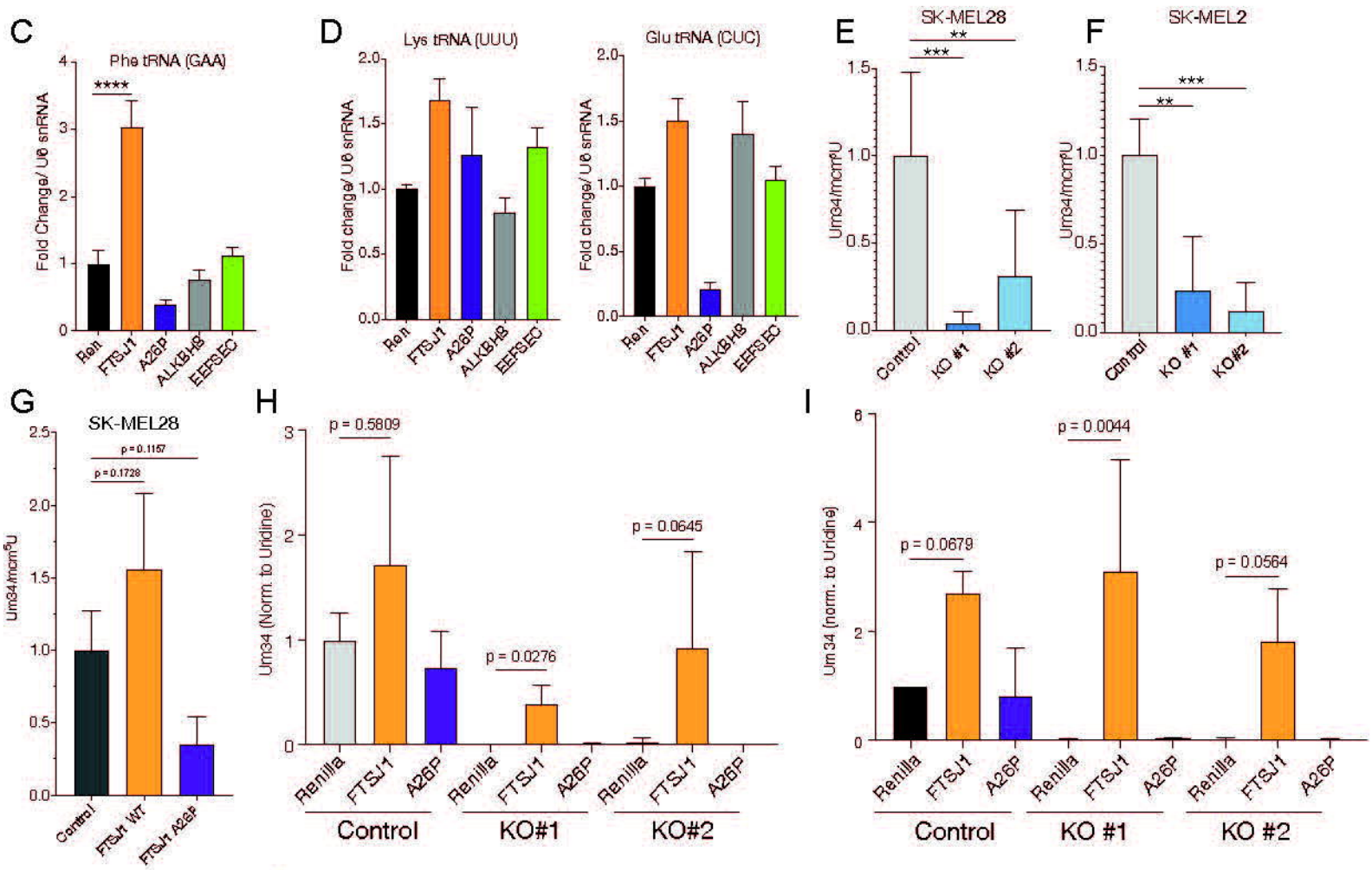


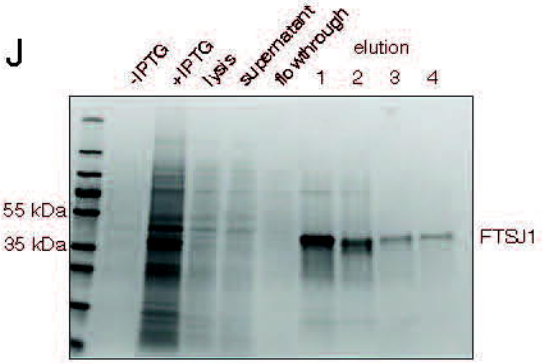


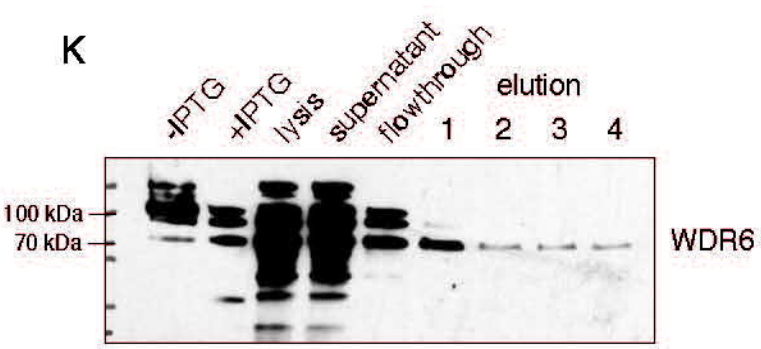

**Extended Figure 2: FTSJ1 is necessary and sufficient for Um34 modification on tRNASec**

(A) Summary of proteomic analysis of EEFSEC-interacting proteins with RNA-modifying activity in A375 melanoma cells. PSM – peptide spectrum matches.
(B) Co-immunoprecipitation assay of the interaction between HA-tagged FTSJ1 and FLAG-tagged component of selenocysteine machinery, SECp43, compared to empty vector control co-expressed in A375 melanoma cells. Representative experiment shown.
(C) Levels of Phe tRNA bound to FLAG-tagged Renilla, wild type or A26P-mutant FTSJ1, ALKBH8 and EEFSEC measured by qRT-PCR. n = 3. Mean +/- SD of 3 independent replicates. Two-sided unpaired t-test. $^{**}p<0.005$, $^{****}p<0.00005$
(D) Lys UUU and Glu CUC tRNA levels bound to FLAG-tagged Renilla, wild type and A26P FTSJ1, ALKBH8 and EEFSEC by qRT-PCR. n = 3. Mean +/- SD of 3 independent replicates.
(E) Quantification of Um34 levels on tRNASec in FTSJ1-KO SK-MEL-28 melanoma cells measured by LC-MS/MS. n=6 from two independent experiments, One-way analysis of variance (ANOVA) followed by Dunnett's tests for multiple comparisons. $^{**}p<0.005$, $^{***}p<0.0005$
(F) Quantification of Um34 levels on tRNASec in FTSJ1-KO SK-MEL-2 melanoma cells measured by LC-MS/MS. n=4 from two independent experimentd, One-way analysis of variance (ANOVA) followed by Dunnett's tests for multiple comparisons. $^{**}p<0.005$, $^{***}p<0.0005$
(G) Quantification of Um34 levels in SK-MEL-28 melanoma cells overexpressing wild-type FTSJ1 or A26P-mutant. n=3. One-way analysis of variance (ANOVA) followed by Dunnett's tests for multiple comparisons.
(H) Quantification of Um34 modification levels on tRNASec in Control and FTSJ1 knockout A375 melanoma cells overexpressing either Renilla luciferase, WT FTSJ1 or mutant A26P FTSJ1 measured by LC-MS/MS. n = 3. Two-tailed one sample t-test.
(I) Quantification of Um34 modification levels on tRNASec in Control and FTSJ1 knockout HeLa cells overexpressing Renilla luciferase, WT FTSJ1 or mutant A26P FTSJ1 measured by LC-MS/MS. n = 3. Two-tailed one sample t-test.
(J) Levels of recombinant FTSJ1 from a His- tag purification assessed by Coomassie staining.
(K) Levels of recombinant WDR6 from a His-tag purification assessed by Western blotting for WDR6.

# Extended Figure 3

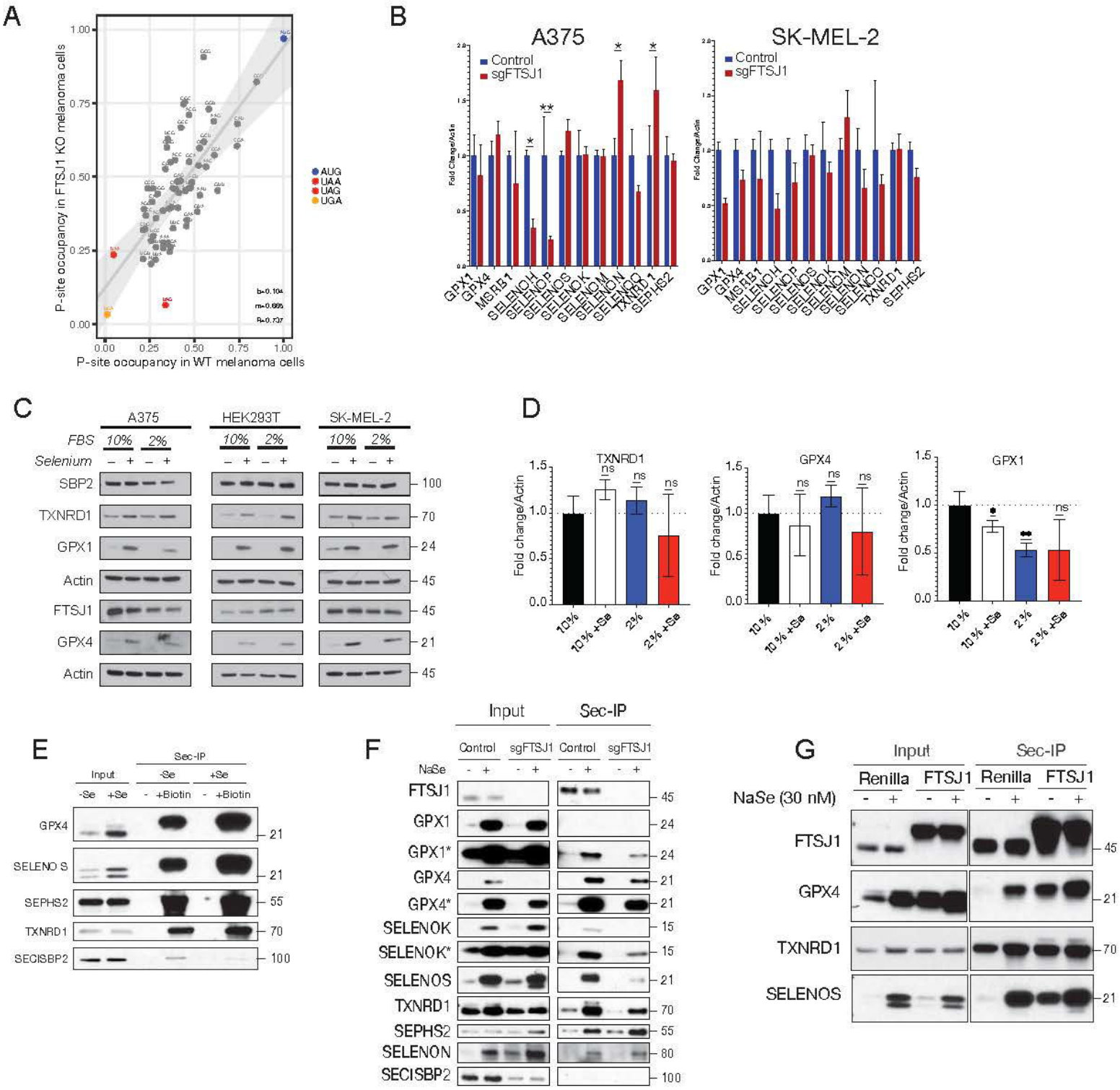


**Extended Figure 3: FTSJ1 regulates recoding of UGA as a selenocysteine**

(A) Global analysis of codon readthrough in FTSJ1 KO A375 melanoma cells compared to WT A375 melanoma cells in the presence of selenium (30nM).
(B) Levels of selenoprotein transcripts in Control and FTSJ1-KO A375 and SK-MEL-2 melanoma cell lines as measured by qRT-PCR. Mean +/- SD from 3 independent replicates. Two-way ANOVA followed by Fisher LSD test for multiple comparisons. *$p<0.05$, **$p<0.005$.
(C) Western blot analysis of selenocysteine proteins TXNRD1, GPX1 and GPX4, in normal (10% FBS), selenium-depleted (2%) and supplemented conditions ( 10% + 30nM NaSe and 2% + 30nM NaSe) in A375 melanoma cell line, HEK293Ts and SK-MEL-2 melanoma cell line.
(D) Transcript levels of TXNRD1, GPX4 and GPX1 in normal (10% FBS), selenium-depleted (2%) and supplemented conditions (10% + 30nM NaSe and 2% + 30nM NaSe) in A375 melanoma cell line by qRT-PCR. Mean +/- SD of 3 independent replicates; two-sided unpaired t-test.
(E) Western blot analysis of selenocysteine-containing proteins immunoprecipitated with selenocysteine-specific pulldown. SECISBP2 was used as a non-selenocysteine control protein. 1% of total protein input was run.
(F) Western blot analysis of selenocysteine-containing proteins immunoprecipitated with selenocysteine-specific pulldown from Control and FTSJ1-KO A375 melanoma cells. 1% of total protein input was run. (* = longer exposure of film)
(G) Western blot analysis of selenocysteine-containing proteins immunoprecipitated with selenocysteine-specific pulldown from A375 melanoma cells overexpressing Renilla or FTSJ1. 1% of total protein input was run.

# Extended Figure 4

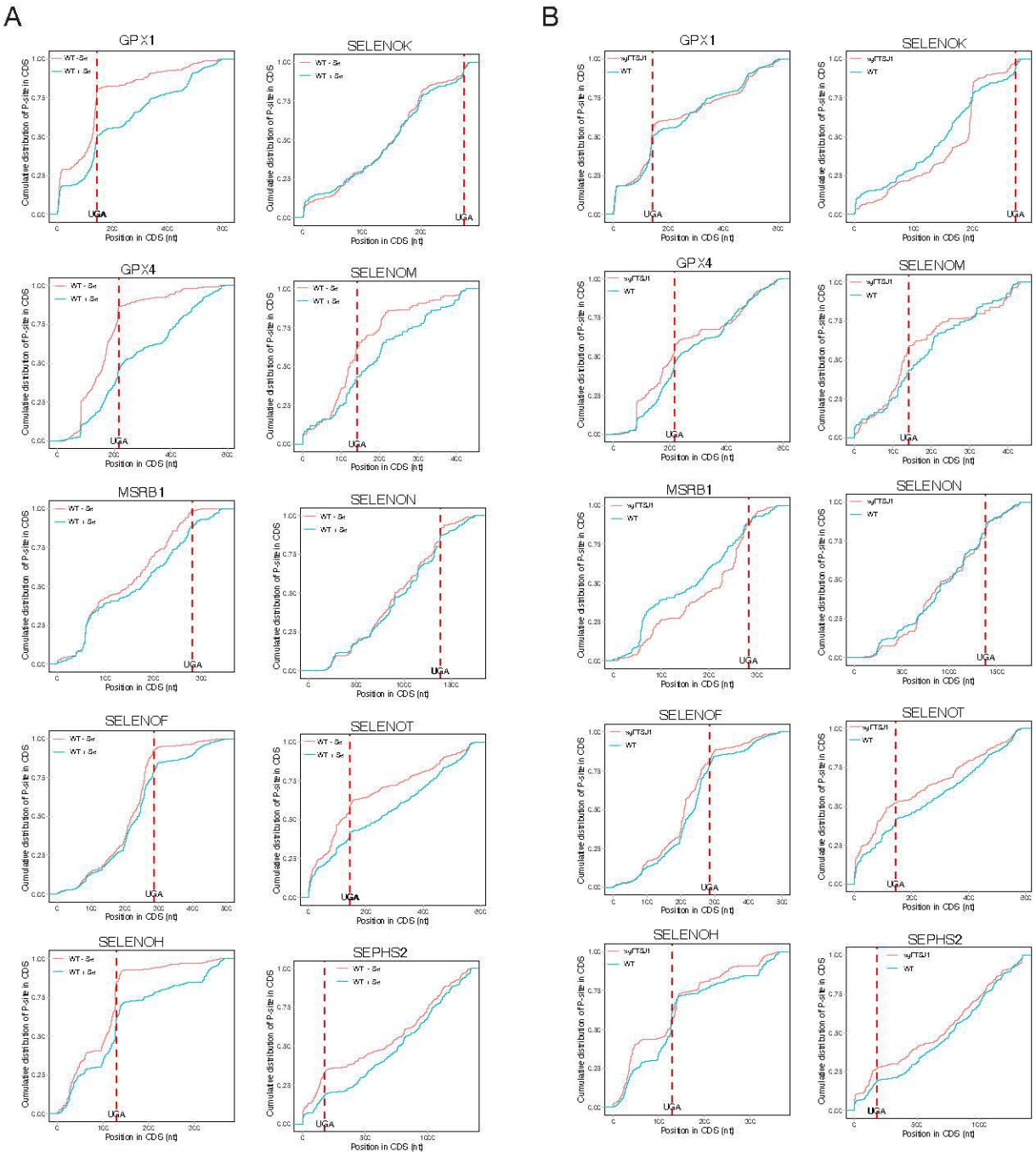


**Extended Figure 4: Loss of FTSJ1 causes ribosomal stalling around Sec UGA in a subset of selenoproteins**

(A) Cumulative RPF plots for affected selenoproteins in WT A375 melanoma cells in the asbsence and presence of selenium (30nM NaSe).
(B) Cumulative RPF plots for affected selenoproteins in WT and FTSJ1 KO melanoma cells in the presence of selenium (30nM NaSe).

# Extended Figure 5

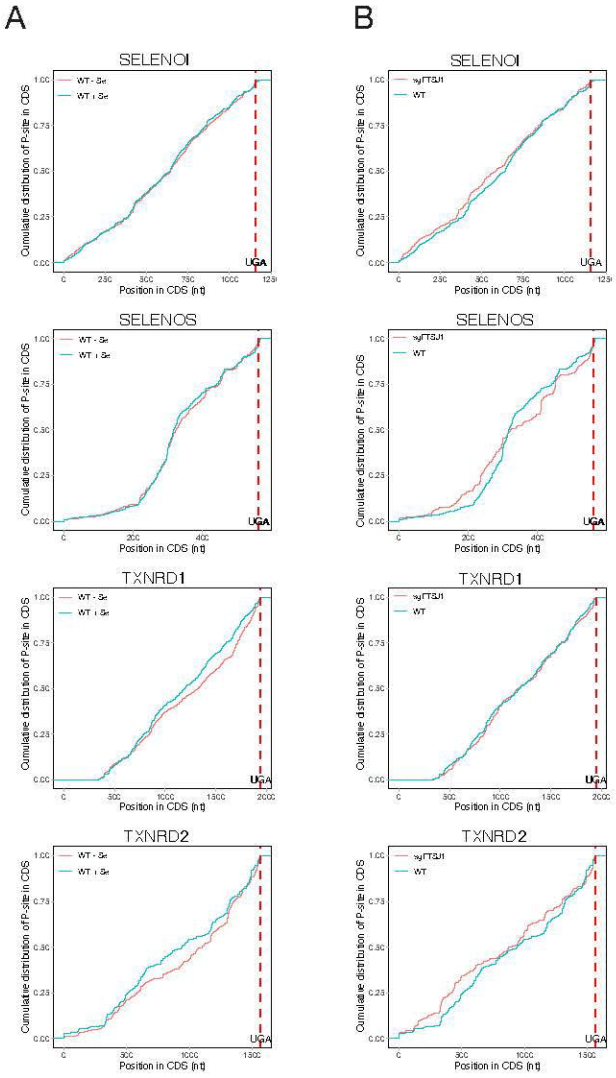


**Extended Figure 5: Loss of FTSJ1 has no additional effect on selenoprotein translation in the absence of selenium**

(A) Cumulative RPF plots for unaffected selenoproteins in WT A375 melanoma cells in the asbsence and presence of selenium (30nM NaSe).
(B) Cumulative RPF plots for unaffected selenoproteins in WT and FTSJ1 KO melanoma cells in the presence of selenium (30nM NaSe).

# Extended Figure 6

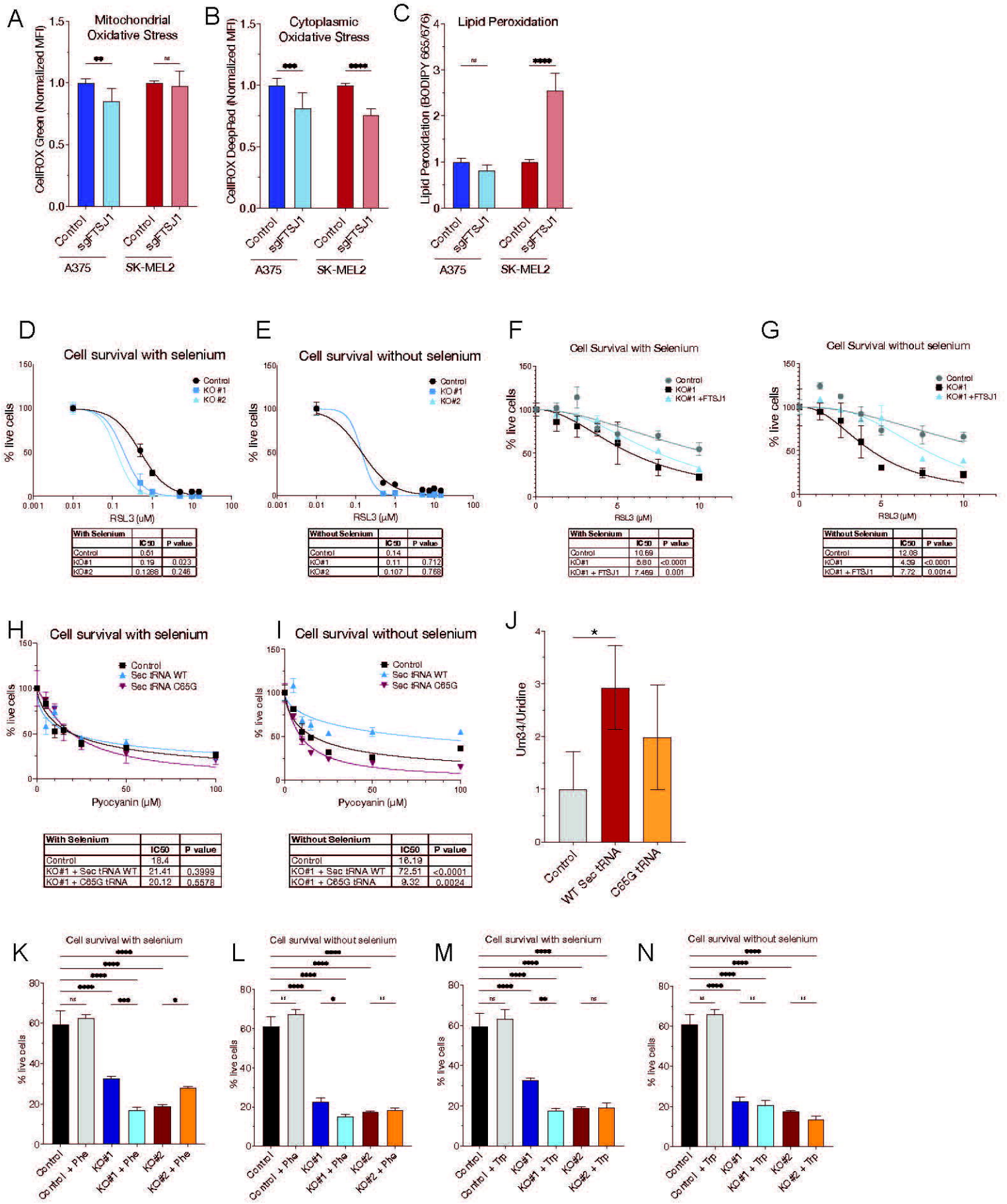


| With Selenium | IC50 | P value |
|---|---|---|
| Control | 0.51 | |
| KO#1 | 0.19 | 0.023 |
| KO#2 | 0.1268 | 0.246 |

| Without Selenium | IC50 | P value |
|---|---|---|
| Control | 0.14 | |
| KO#1 | 0.11 | 0.712 |
| KO#2 | 0.107 | 0.768 |

| With Selenium | IC50 | P value |
|---|---|---|
| Control | 10.69 | |
| KO#1 | 5.80 | <0.0001 |
| KO#1 + FTSJ1 | 7.469 | 0.001 |

| Without Selenium | IC50 | P value |
|---|---|---|
| Control | 12.08 | |
| KO#1 | 4.39 | <0.0001 |
| KO#1 + FTSJ1 | 7.72 | 0.0014 |

| With Selenium | IC50 | P value |
|---|---|---|
| Control | 18.4 | |
| KO#1 + Sec tRNA WT | 21.41 | 0.3999 |
| KO#1 + C65G tRNA | 20.12 | 0.5578 |

| Without Selenium | IC50 | P value |
|---|---|---|
| Control | 16.19 | |
| KO#1 + Sec tRNA WT | 72.51 | <0.0001 |
| KO#1 + C65G tRNA | 9.32 | 0.0024 |

**Extended Figure 6: Sensitivity to oxidative stress can not be rescued by overexpression of other FTSJ1 tRNA targets**

(A) Mitochondrial ROS levels measured by flow cytometry using CellROXGreen dye in Control and A375 melanoma cells in the presence of selenium (30nM). n=3. Representative of 2 independent experiments. Two-way ANOVA followed by Sidak's multiple comparison test. **$p<0.005$

(B) (B) Cytoplasmic ROS levels measured by flow cytometry using CellROX DeepRed in Control and A375 melanoma cells in the presence of selenium (30nM). n=3. Representative of 2 independent experiments. Two-way ANOVA followed by Sidak's multiple comparison test.***$p<0.0005$, ****$p<0.00005$

(C) Lipid peroxidation levels measured by flow cytometry using BODIPY665/676 in Control and A375 melanoma cells in the presence of selenium (30nM). n=3. Representative of 2 independent experiments. Two-way ANOVA followed by Sidak's multiple comparison test. ****$p<0.00005$

(D) Cell survival of Control vs FTSJ1-KO A375 melanoma cells under increasing concentrations of RSL3 in the presence of selenium. n=3. Representative of 3 independent experiments. Statistical difference between IC50 values analyzed by Extra-Sum-of-Squares F-Test.

(E) Cell survival of Control vs FTSJ1-KO A375 melanoma cells under increasing concentrations of RSL3 in the absence of selenium. n=3. Representative of 3 independent experiments. Statistical difference between IC50 values analyzed by Extra-Sum-of-Squares F-Test.

(F) Cell survival of Control or FTSJ1-KO A375 melanoma cells with or without FTSJ1 overexpression under increasing concentrations of RSL3 in the presence of selenium. n=3. Representative of 2 independent experiments. Statistical difference between IC50 values analyzed by Extra-Sum-of-Squares F-Test.

(G) Cell survival of Control or FTSJ1-KO A375 melanoma cells with or without FTSJ1 overexpression under increasing concentrations of RSL3 in the absence of selenium. n=3. Representative of 2 independent experiments. Statistical difference between IC50 values analyzed by Extra-Sum-of-Squares F-Test.

(H) Cell survival of Control, WT tRNASec or C65G mutant tRNASec overexpressing A375 melanoma cells under increasing concentrations of pyocyanin in the presence of selenium. n=3. Representative of 3 independent experiments. Statistical difference between IC50 values analyzed by Extra-Sum-of-Squares F-Test.

(I) Cell survival of Control, WT tRNASec or C65G mutant tRNASec overexpressing A375 melanoma cells under increasing concentrations of pyocyanin in the absence of selenium. n=3. Representative of 3 independent experiments. Statistical difference between IC50 values analyzed by Extra-Sum-of-Squares F-Test.

(J) Quantification of Um34 modification levels on tRNASec in Control, WT tRNASec or C65G mutant tRNASec overexpressing A375 melanoma cells. n=3 individual replicates

(K) Cell survival of Control or FTSJ1-KO A375 melanoma cells with or without overexpression of Phe tRNA with 25uM of pyocyanin in the presence of selenium (30nM NaSe). n=3. Representative of 3 independent experiments. One-way ANOVA followed by Tukey test for multiple comparisons.

(L) Cell survival of Control or FTSJ1-KO A375 melanoma cells with or without overexpression of Phe tRNA with 25uM of pyocyanin in the absence of selenium. n=3. Representative of 3 independent experiments. One-way ANOVA followed by Tukey test for multiple comparisons.

(M) Cell survival of Control or FTSJ1-KO A375 melanoma cells with or without overexpression of Trp tRNA with 25uM of pyocyanin in the presence of selenium (30nM NaSe). n=3. Representative of 3 independent experiments. One-way ANOVA followed by Tukey test for multiple comparisons.

(N) Cell survival of Control or FTSJ1-KO A375 melanoma cells with or without overexpression of Trp tRNA with 25uM of pyocyanin in the absence of selenium. n=3. Representative of 3 independent experiments. One-way ANOVA followed by Tukey test for multiple comparisons.

# Extended Figure 7

A

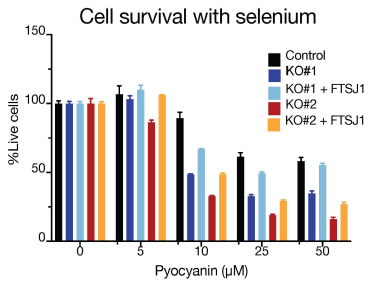


| With Selenium | | |
|---|---|---|
| | IC50 | P value |
| Control | 53.90 | |
| KO#1 | 17.30 | 0.0103 |
| KO#1 + FTSJ1 | 40.54 | |
| KO#2 | 9.05 | 0.0119 |
| KO#2 + FTSJ1 | 15.25 | |

B

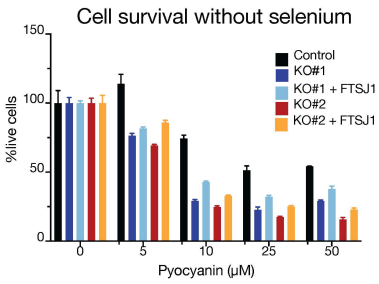


| Without Selenium | | |
|---|---|---|
| | IC50 | P value |
| Control | 41.12 | |
| KO#1 | 8.586 | 0.0794 |
| KO#1 + FTSJ1 | 13.94 | |
| KO#2 | 6.912 | 0.038 |
| KO#2 + FTSJ1 | 10.13 | |

C

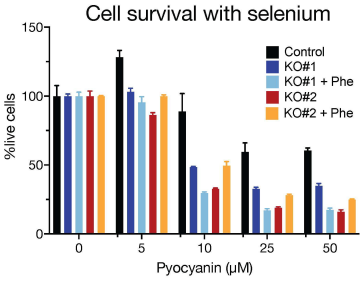


| With Selenium | | |
|---|---|---|
| | IC50 | P value |
| Control | 52.29 | |
| KO#1 | 17.30 | 0.0012 |
| KO#1 + Phe | 8.51 | |
| KO#2 | 9.05 | 0.0108 |
| KO#2 + Phe | 14.42 | |

D

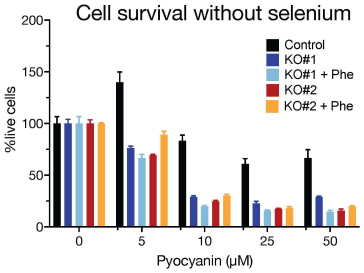


| Without Selenium | | |
|---|---|---|
| | IC50 | P value |
| Control | 62.65 | |
| KO#1 | 8.59 | 0.1698 |
| KO#1 + Phe | 6.35 | |
| KO#2 | 6.91 | 0.2023 |
| KO#2 + Phe | 8.29 | |

E

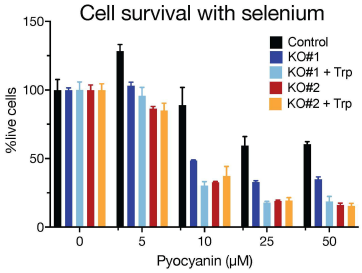


| With Selenium | | |
|---|---|---|
| | IC50 | P value |
| Control | 52.29 | |
| KO#1 | 17.30 | 0.0025 |
| KO#1 + Trp | 8.57 | |
| KO#2 | 9.05 | 0.6895 |
| KO#2 + Trp | 9.59 | |

F

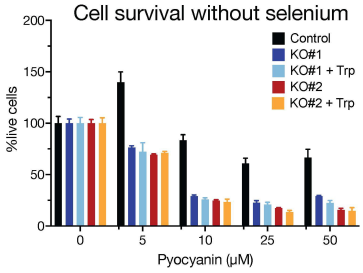


| Without Selenium | | |
|---|---|---|
| | IC50 | P value |
| Control | 62.65 | |
| KO#1 | 8.59 | 0.5782 |
| KO#1 + Trp | 7.46 | |
| KO#2 | 6.91 | 0.9906 |
| KO#2 + Trp | 6.90 | |

**Extended Figure 7: FTSJ1 overexpression can partially rescue sensitivity to oxidative stress while other tRNA targets of FTSJ1 can not**

(A) Cell survival of Control and FTSJ1-KO A375 melanoma cells with and without FTSJ1-overexpression under increasing concentrations of pyocyanin in the presence of selenium (30nM NaSe) as measured by Cell Titer Glo. n=3. Representative of 3 independent experiments. Statistical difference between IC50 values analyzed by Extra-Sum-of-Squares F-Test.

(B) Cell survival of Control and FTSJ1-KO A375 melanoma cells with and without FTSJ1-overexpression under increasing concentrations of pyocyanin in the absence of selenium as measured by Cell Titer Glo. n=3. Representative of 3 independent experiments. Statistical difference between IC50 values analyzed by Extra-Sum-of-Squares F-Test.

(C) Cell survival of Control or FTSJ1-KO A375 melanoma cells with or without overexpression Phe tRNA under increasing concentrations of pyocyanin in the presence of selenium (30nM NaSe). n=3. Representative of 3 independent experiments. Statistical difference between IC50 values analyzed by Extra-Sum-of-Squares F-Test.

(D) Cell survival of Control or FTSJ1-KO A375 melanoma cells with or without overexpression Phe tRNA under increasing concentrations of pyocyanin in the absence of selenium. n=3. Representative of 3 independent experiments. Statistical difference between IC50 values analyzed by Extra-Sum-of-Squares F-Test.

(E) Cell survival of Control or FTSJ1-KO A375 melanoma cells with or without overexpression Trp tRNA under increasing concentrations of pyocyanin in the presence of selenium(30nM NaSe). n=3. Representative of 3 independent experiments. Statistical difference between IC50 values analyzed by Extra-Sum-of-Squares F-Test.

(F) Cell survival of Control or FTSJ1-KO A375 melanoma cells with or without overexpression Trp tRNA under increasing concentrations of pyocyanin in the absence of selenium. n=3. Representative of 3 independent experiments. Statistical difference between IC50 values analyzed by Extra-Sum-of-Squares F-Test.

# Extended Figure 8

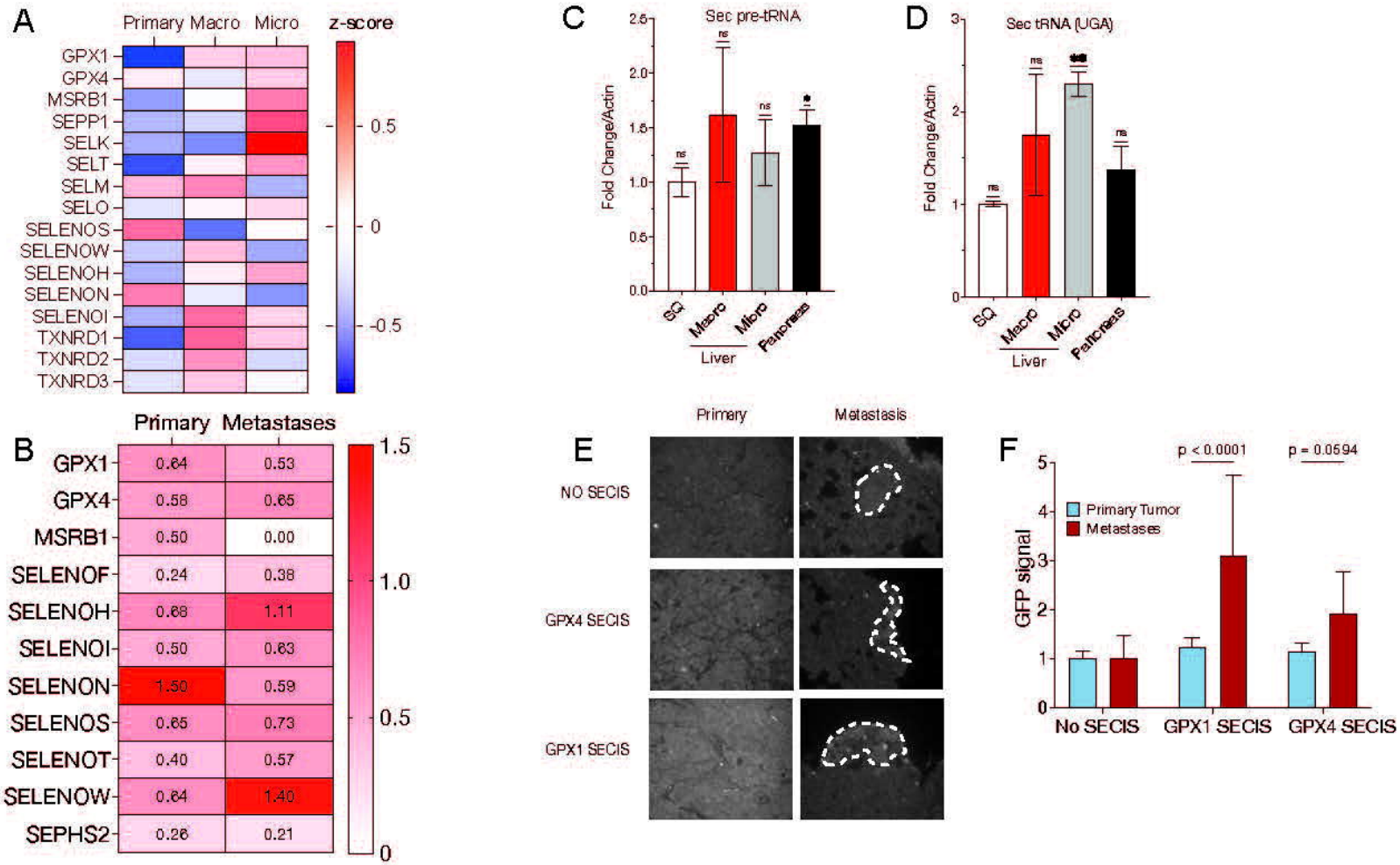


**Extended Figure 8: Metastases show translational upregulation of selenoproteins**

(A) Transcript levels of selenoproteins in primary tumors compared to macro and micro metastatic nodules, isolated from NSG mice transplanted with patient-derived melanomas M481 and M405, as measured by RNA-sequencing, quantified as a z-score.
(B) UGA recoding efficiency of different selenoproteins in primary tumors compared to metastatic nodules from NSG mice transplanted with patient-derived melanoma, M405, as measured by ribosomal profiling.
(C) Levels of precursor tRNASec in Primary, macro and micrometastatic nodules from patient-derived M405 melanoma measured by qRT-PCR. Mean +/- SD from 3 independent replicates. One-way analysis of variance (ANOVAs) followed by Dunnett's tests for multiple comparisons. *$p<0.05$
(D) Levels of mature tRNASec in Primary, macro and micrometastatic nodules from patient-derived M405 melanoma measured by qRT-PCR. Mean +/- SD from 3 independent replicates. One-way analysis of variance (ANOVAs) followed by Dunnett's tests for multiple comparisons. *$p<0.05$
(E) Levels of gROSI variant levels with No UTR, GPX1 SECIS or GPX4 SECIS in primary and metastatic nodules, formed by A375 melanoma cells transplanted into NSG mice, as measured by immunofluorescence staining for GFP expression.
(F) Quantification of the GFP signal from gROSI variants shown in (E). Two-Way ANOVA followed by Fisher's LSD Test

# Extended Figure 9

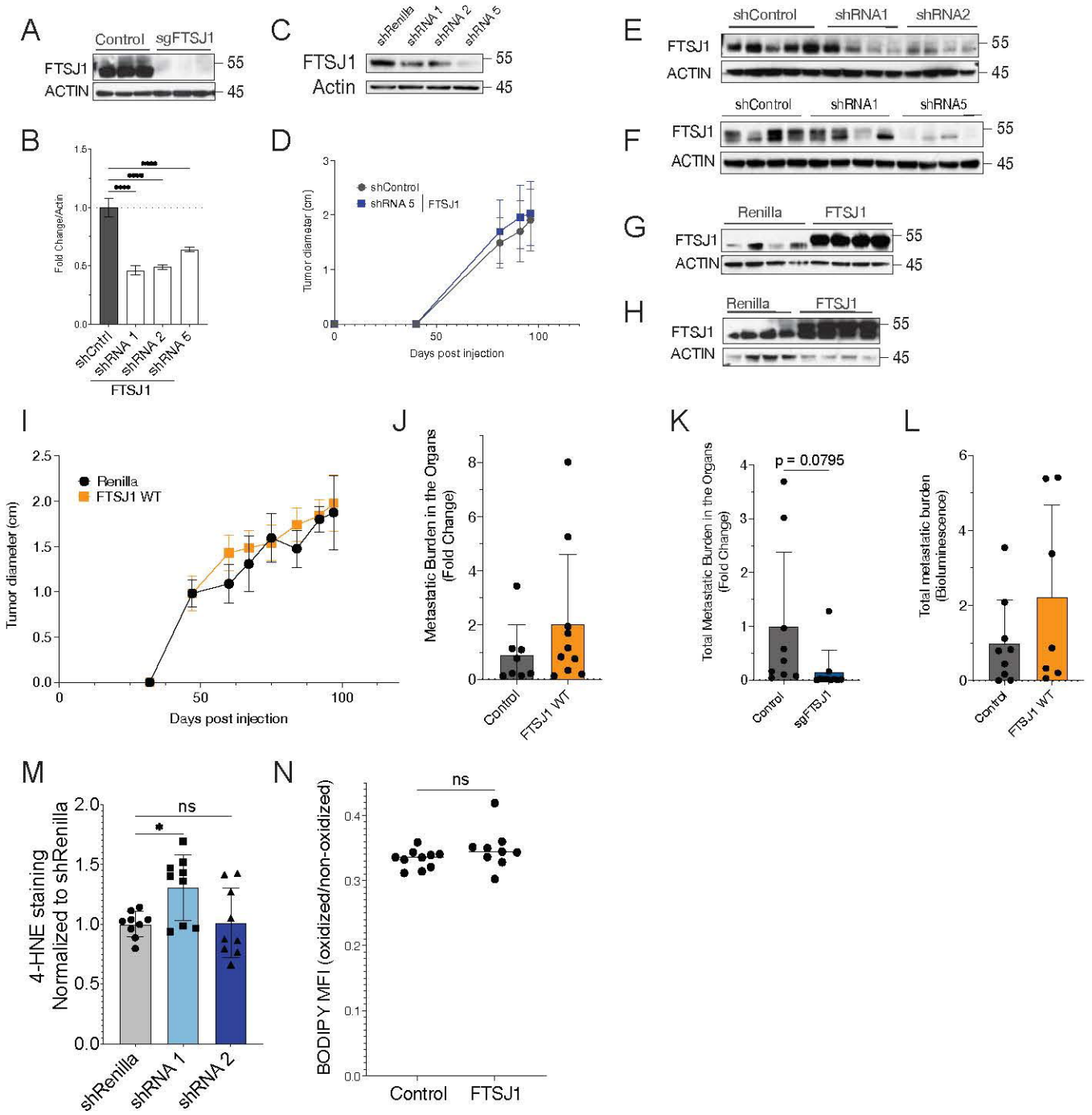

**Extended Figure 9: Loss of FTSJ1 affects metastatic colonization but does not effect lipid peroxidation levels**

(A) Western blot analysis of control and FTSJ1 KO A375 melanoma primary tumors.
(B) qRT-PCR analysis of FTSJ1 targeting shRNAs in A375 melanoma cells. Mean +/- SD from 3 independent replicates. One-way analysis of variance (ANOVAs) followed by Dunnett's tests for multiple comparisons. *$p<0.05$
(C) Western blot analysis of FTSJ1 targeting shRNAs in MeWo melanoma cells.
(D) Subcutaneous tumor growth of MeWo cells transplanted into mice expressing Control or shRNA5 targeting FTSJ1. n=5 mice. Representative of 3 independent experiments.
(E) Western blot analysis of M405 tumors with either control or FTSJ1-targeting shRNAs.
(F) Western blot analysis of M481 tumors with either control or FTSJ1-taregting shRNAs.
(G) Western blot analysis of A375 melanoma tumors overexpressing Control Renilla luciferase or FTSJ1.
(H) Western blot analysis of M481 melanoma tumors overexpressing Control Renilla luciferase or FTSJ1.
(I) Growth of subcutaneous tumors in mice transplanted from patient-derived melanoma, M405, overexpressing either Renilla luciferase or FTSJ1 ORF. n=5. Representative of 2 independent experiments.
(J) Total metastatic burden in visceral organs of mice transplanted with patient-derived melanoma, M405, overexpressing either Renilla luciferase or FTSJ1 ORF. n = 10 mice from 2 independent experiments. Statistical significance assessed by one-way analysis of variance (ANOVAs) followed by Dunnett's tests for multiple comparisons.
(K) Total metastatic burden in visceral organs of mice transplanted intravenously with either Control or FTSJ1 KO A375 melanoma cells. n=9-10 mice.
(L) Total metastatic burden in visceral organs of mice transplanted intravenously with either Control or FTSJ1 overexpressing A375 melanoma cells. n=7-10 mice.
(M) Quantification of 4-HNE immunofluorescent staining of subcutaneous tumors expressing either control shRNA or FTSJ1-targeting shRNAs. n=3 mice.
(N) Flow cytometry analysis of lipid peroxidation levels in subcutaneous tumors overexpressing Control Renilla luciferase or FTSJ1, using BODIPY dye. n=10 mice.